Black hole production and graviton emission in models with large extra dimensions

Dissertation
zur Erlangung des Doktorgrades
der Naturwissenschaften

vorgelegt beim Fachbereich Physik
der Johann Wolfgang Goethe–Universität
in Frankfurt am Main

von
Benjamin Koch
aus Nördlingen

Frankfurt am Main 2007
(D 30)

vom Fachbereich Physik der Johann Wolfgang Goethe–Universität
als Dissertation angenommen

Dekan .....

Gutachter .....

Datum der Disputation .....

Zusammenfassung

In dieser Arbeit wird die mögliche Produktion von mikroskopisch kleinen Schwarzen Löchern und die Emission von Gravitationsstrahlung in Modellen mit großen Extra-Dimensionen untersucht.
Zunächst werden der theoretisch-physikalische Hintergrund und die speziellen Modelle des behandelten Themas skizziert. Anschließend wird auf die durchgeführten Untersuchungen zur Erzeugung und zum Zerfall mikroskopisch kleiner Schwarzer Löcher in modernen Beschleunigerexperimenten eingegangen und die wichtigsten Ergebnisse zusammengefasst. Im Anschluss daran wird die Produktion von Gravitationsstrahlung durch Teilchenkollisionen diskutiert. Die daraus resultierenden analytischen Ergebnisse werden auf hochenergetische kosmische Strahlung angewandt.

Die Suche nach einer einheitlichen Theorie der Naturkräfte

Eines der großen Ziele der theoretischen Physik seit Einstein ist es, eine einheitliche und möglichst einfache Theorie zu entwickeln, die alle bekannten Naturkräfte beschreibt. Als großer Erfolg auf diesem Wege kann es angesehen werden, dass es gelang, drei [1] der vier bekannten Kräfte mittels eines einzigen Modells, des Standardmodells (SM), zu beschreiben.
Das Standardmodell der Elementarteilchenphysik ist eine Quantenfeldtheorie. In Quantenfeldtheorien werden Invarianten unter lokalen Symmetrietransformationen betrachtet. Die Symmetriegruppen, die man für das Standardmodell gefunden hat, sind die $U(1)$, $SU(2)_L$ und die $SU(3)$. Die Vorhersagen des Standardmodells wurden durch eine Vielzahl von Experimenten mit höchster Genauigkeit bestätigt. Dennoch fehlt diesem Modell mit der Gravitation ein wichtiger Baustein auf dem Weg zu einer vereinheitlichten Theorie.
Die Gravitation wird durch die allgemeine Relativitätstheorie (ART) beschrieben. In der geometrischen Formulierung der ART wird angenommen, dass die vierdimensionale Raumzeit durch Energie, Masse oder Impulse ge-

[1] Diese sind die ektromagnetische, die schwache und die starke Kraft.

krümmt wird. Des Weiteren wird angenommen, dass sich Massenpunkte in der verformten Raumzeit auf so genannten Geodäten (den kürzesten Verbindungen zwischen zwei Punkten) bewegen. Diese geometrische Theorie beinhaltet keinerlei Quanteneffekte.
Bei dem Versuch die ART in Analogie zu Quantentheorien umzuformulieren, stößt man auf konzeptionelle Probleme. Ein erster Schritt in diese Richtung ist die Formulierung von Quantentheorien auf dem Hintergrund einer gekrümmten Raumzeit. Ein solches Vorgehen führt zum Beispiel im Fall eines Schwarzen Lochs auf die berühmte Hawkingstrahlung.

Das Hierarchieproblem und große Extra-Dimensionen

Bei der Betrachtung der Kopplungen der bekannten Naturkräfte fällt auf, dass die gravitative Kopplung $\sim 10^{34}$ mal schwächer ist als die nächststärkere Kopplung ($g_{U(1)} \sim 1/60$). Bei dem Versuch, alle Kräfte in einer einheitlichen Theorie zu beschreiben, müsste auch dieses so genannte Hierarchieproblem gelöst werden. Als eine mögliche Erklärung dieser Hierarchie wurden zusätzliche Raumdimensionen, die in sich aufgerollt sind, vorgeschlagen. Mit Hilfe der Zusatzbedingung, dass nur die Gravitation in die Extra-Dimensionen propagiert und alle anderen Kräfte auf die dreidimensionale Untermannigfaltigkeit (brane) beschränkt bleiben, kann das Hierarchieproblem gelöst (oder zumindest stark abgeschwächt) werden. Ein Vergleich des höherdimensionalen Kraftgesetzes mit dem dreidimensionalen Kraftgesetz führt zu einem Zusammenhang zwischen der Planckmasse M_p, der neuen fundamentalen Masse M_f, dem Kompaktifizierungsradius R und der Anzahl der Extra-Dimensionen d,

$$M_p^2 = M_f^{2+d} R^d \quad . \tag{1}$$

Für einen Kompaktifizierungsradius von $R \sim 10$ nm und drei Extra-Dimensionen kann eine fundamentale Skala von $M_f \sim 1000$ GeV das für große Abstände vermessene Newton'sche Gesetz für $r > R$ mit seiner schwachen Kopplung $G \sim 1/M_p^2$ reproduzieren. Bei einem noch kleineren Abstand von $r_q \sim 1/M_f$ (bei dem Quantenkorrekturen zum klassischen Kraftgesetz zu erwarten sind) erreicht die gravitative Kopplung ungefähr die Größenordnung der anderen Kopplungen, also $m^2/(M_f^{2+d} r_q^d) \sim 1/137$. Eine andere Art diese Lösung des Hierarchieproblems auszudrücken, ist die Feststellung, dass die neue Gravitationsskala ($M_f \sim 1000$ GeV) von vergleichbarer Größenordnung wie die elektroschwache Skala ($M_Z \sim 100$ GeV) ist. Bei solchen Modellen spricht man auch von großen Extra-Dimensionen, da der Kompaktifizierungsradius R viel größer als die Planckmasse M_p ist. Eines der konkreten Modelle, das solche kompaktifizierten Dimensionen enthält, ist das

so genannte ADD-Modell. Das von Arkani-Hammed, Dimopoulos und Dvali vorgeschlagene Modell dient als Grundlage dieser Arbeit.

Erzeugung mikroskopisch kleiner Schwarzer Löcher im Beschleuniger

Die Lösung des Hierarchieproblems in der beschriebenen Weise bedeutet, dass gravitative Wechselwirkungen auf kleinen Abstandsskalen sehr viel stärker sind als von der Newton'schen Kopplung $G \sim 1/M_p^2$ suggeriert wird. Falls dies zuträfe, hätte es bedeutsame experimentelle Konsequenzen. So wurde bereits 1999 vermutet, dass im Fall von großen Extra-Dimensionen die in zukünftigen Beschleunigerexperimenten erreichbaren Energiedichten ausreichen könnten, um mikroskopisch kleine Schwarze Löcher zu erzeugen. In der Folgezeit wurde diese Vermutung durch detailliertere Abschätzungen untermauert.
Die Grundstrategie der experimentellen Elementarteilchenphysik ist es, unter Ausnutzung der Beziehung $\lambda = 1/p$, die Zusammenhänge bei immer kleineren Längenskalen (λ) mit immer größeren Impulsen (p) zu untersuchen. Die Erzeugung von Schwarzen Löchern ab einer Impulsskala $p_s \sim$TeV würde dieser Philosophie ein abruptes Ende bereiten, da man von diesem Punkt an keine kleineren Abstände mehr untersuchen könnte, sondern immer in der „Sackgasse"eines Schwarzen Loches landen würde.
Es wird im Allgemeinen angenommen, dass ein Schwarzes Loch unmittelbar nach seiner Erzeugung wieder zerstrahlt. Ein Großteil dieser Strahlungsenergie wird vermutlich durch die bereits erwähnte Hawkingstrahlung abgegeben. Die Temperatur dieser Strahlung ist umso größer, je kleiner die Masse des Schwarzen Loches ist. Im Fall von kleinen Schwarzen Löchern in Extra-Dimensionen kann diese Temperatur bis zu mehreren 100 GeV erreichen. Es ist jedoch bisher nicht klar, ob ein Schwarzes Loch komplett zerstrahlt oder sich aufgrund quantengravitativer Effekte abkühlt, um am Ende seiner aktiven Phase einen massiven so genannten Remnant zu bilden. Sowohl ein vollständiges Zerstrahlen als auch die Bildung eines stabilen Remnants wird als mögliches Szenario in der Literatur diskutiert.
In dieser Arbeit wird die Frage untersucht, inwieweit man diese beiden Szenarien experimentell, anhand der im Detektor messbaren Teilchen, von einander unterscheiden könnte. Es werden mehrere Beobachtungsgrößen ausgewählt und mit Hilfe numerischer Simulationen mit einander verglichen. Dabei zeigt sich, dass neben der Unterdrückung von Jets mit hohen Transversalimpulsen eine Reihe anderer Beobachtungsgrößen als Signal für die Erzeugung Schwarzer Löcher geeignet sind. Auch die Suche nach Spuren, die auf ein ungewöhnlich hohes Masse/Ladungsverhältnis hinweisen, kann als eine viel

versprechende Observable für Remants vorgeschlagen werden. Ebenso zeigt sich, dass ein Signal mit hohem fehlendem Transversalimpuls p_T auf ein neutrales Remnant hindeuten könnte. Es stellt sich auch heraus, dass die Form der p_T-Spektren und der Multiplizitäten der Sekundärteilchen charakteristisch für die unterschiedlichen Szenarien ist.

Gravitationsstrahlung in Extra-Dimensionen

Die große gravitative Kopplung und der große Phasenraum durch die zusätzlichen Dimensionen erhöht auch die Wahrscheinlichkeit der Emission von Gravitationswellen. Dieses generelle Argument wird im zweiten Teil dieser Arbeit, durch die Herleitung einer Formel für die (durch Teilchenstöße induzierte) Emission von Gravitationswellen, quantifiziert. Diese Formel verallgemeinert die ursprünglich vierdimensionale Herleitung von Weinberg auf den Fall von $3 + d$ räumlichen Dimensionen wie sie im ADD-Modell gegeben sind. Als Anwendung für die Formel wird die Stärke der Gravitationsstrahlung im Fall von hochenergetischer kosmischer Strahlung untersucht. Dies geschieht durch die Implementierung der analytischen Wirkungsquerschnitte in ein numerisches Modell zur Simulation von kosmischer Höhenstrahlung. Es stellt sich heraus, dass im Fall der Existenz von großen Extra-Dimensionen ($M_f \leq 2$ TeV, $d \geq 4$), die Stärke des kosmischen Flusses im Energiebereich $E > 5 \cdot 10^{18}$ eV um 20% bis 45% höher interpretiert werden müsste, als vom Standardmodell vorhergesagt. Dieses Ergebnis zeigt einerseits, dass Gravitationsstrahlung im Fall der Existenz von großen Extra-Dimensionen zu einem nicht vernachlässigbarem Effekt führt, es widerlegt andererseits frühere Abschätzungen, bei denen Gravitationsstrahlung als mögliche Erklärung für das so genannte Knie (bei $10^{15.5}$ eV) im Spektrum der hochenergetischen kosmischen Höhenstrahlung herangezogen wird.

Contents

List of Figures

ADD	model by Arkani-Hamed, Dimopoulos, and Dvali
BH	black hole
BHR	black hole remnant
CKM	mass matrix for quarks by Cabibbo-Kobayashi-Maskawa
CR	cosmic rays
GR	general relativity
GZK	maximum energy condition for cosmic rays by Greisen, Zatsepin, and Kuzmin
KK	Kaluza-Klein
LHC	large hadron collider
LXD	large extra dimensions
QCD	quantum-chromo-dynamics
QED	quantum-electro-dynamics
RS	model by Randall and Sundrum
SM	standard model
TOF	time of flight
TPC	time projection chamber
UHECR	ultra high energetic cosmic rays
UXD	universal extra dimensions
XD	extra dimensions

Table 1: Abbreviations

Chapter 1

Introduction

The search for a theory that describes the physically measurable world within one elegant framework is an ongoing challenge for physicists since Einstein formulated his dream of such a theory. The incompatibility of the standard model of particle physics (SM) and the theory of general relativity (GR) is considered one major problem on this way. The most apparent difference between gravity (described by GR) and all other interactions (like the electromagnetic-, weak-, or strong-force, described by the SM), is that gravity is much smaller (by a factor of $\sim 10^{-30}$) than all the other known forces. Theories with large extra dimensions offer an elegant and intuitive way to explain this huge difference. Therefore the confirmation or falsification of such theories could offer an important hint on how to proceed in the search for a unified theory. In this theses the rich phenomenology of such models is studied. Predictions are made for the observability of black holes and black hole remnants at the large hadron collider (LHC) and for the production of gravitational radiation from high energetic cosmic rays. Those predictions aim to support or exclude specific models of large extra dimensions and their parameter space.

The second chapter introduces the main properties of the SM as a quantum field theory, and gives the contributions of the SM Lagrangian from matter fields, interaction fields and the Higgs field. Achievements and drawbacks of this theory are mentioned. In the third chapter GR as geometrical theory, based on Rieman's mathematical description of curved spaces is introduced. Einstein's field equations are derived and a short excursion to quantum field theory on curved spacetimes is made, which leads to effects like Unruh in accelerated reference frames or Hawking radiation from the surface of black holes. In the end of this section achievements and drawbacks of GR are also mentioned.

In the fourth chapter effective physical theories that have additional spatial dimensions are introduced. In the first section the elegant idea of Kaluza-Klein theories is drafted. Furthermore, in the second section volume compactifications and the ADD model as their most prominent representative are introduced. For such models it is shown how one can explain the apparent weakness of gravity, how tree level Feynman rules can be derived, and how black holes could be produced in high energetic collisions. In the last section of that chapter a model with extra dimensions is mentioned which represents an alternative to the previous volume compactification (Randall Sundrum model).

In the fifth and sixth chapter, it is argued why the standard Hawking law for black hole evaporation does not hold as soon as the mass of the black hole approaches the Planck mass. It is further argued that a sensible modification of this spectrum could lead to stable non radiating black hole remnants with a mass of the order of the Planck mass. In theories with large extra dimensions this Planck mass can be as low as a $\sim$ TeV. Then the direct and indirect collider signals of such microscopic black holes and black hole remnants, which might be produced a the next generation of proton proton collider, are numerically studied. It is found that large extra dimensions would provide clear collider signatures through the production and decay of these microscopic black holes. It is also found that it might even be possible to disentangle the production of completely decaying black holes from the production of black holes that have a stable remnant as final state.

In the seventh chapter, the classical cross section for energy loss due to gravitational radiation in elastic N- particle scattering is derived. The result is extended to an effective cross section which is not only valid in the high energy regime, but also gives the correct low energy limit. The obtained cross section is then applied in the eighth to elastic two particle scattering. The integrated forms of those cross sections are applied to a numerical model for the simulation of cosmic ray air showers. From those simulations it is found that the estimation of the flux of highest energetic cosmic rays would be modified by up to 50%, by the existence of large extra dimensions.

In the nineth chapter a summary over the result of the previous chapters is given.

Finally, in the appendix additional analytical calculations that are useful for the understanding of the concepts of curved spacetime, and the energy loss in different reference frames, are given.

Chapter 2

The standard model of particle physics

The standard model of particle physics is a theory that describes three fundamental forces of nature within a single framework. It is formulated in the mathematical language of quantum field theory.

2.1 Fundamental concepts and achievements of the standard model

It is far beyond the scope of this work to discuss all the features and mathematical techniques that come with the standard model of particle physics; these can be found in standard text books [1, 2]. Here a short sketch of the content of the standard model will be provided.

2.1.1 Fermions

The fundamental building blocks of matter are fermions, which have spin $\frac{1}{2}$. Among these one further distinguishes between leptons and quarks. As shown below the leptons consist of left handed duplets and a right handed singlets

$$\begin{pmatrix}\nu_e\\ e\end{pmatrix}_L, \begin{pmatrix}\nu_\mu\\ \mu\end{pmatrix}_L, \begin{pmatrix}\nu_\tau\\ \tau\end{pmatrix}_L, e_R, \mu_R, \tau_R \quad .$$

Each generation (electron, muon, tau) of the left handed leptons has a partner called the electron neutrino ν_e, muon neutrino ν_μ and tauon neutrino ν_τ [1].

[1] After several experiments confirmed the oscillation of neutrinos [3, 4, 5], it is generally believed that one has to introduce right handed neutrinos or some other mass generating

The non leptonic part of fermionic matter are the quarks. Quarks have electrical charges of $\pm\frac{1}{2}$ or $\pm\frac{2}{3}$, they carry a nonzero color charge, and they can be categorized in the same duplet-singlet structure as the leptons

$$\begin{pmatrix} u \\ d \end{pmatrix}_L, \begin{pmatrix} c \\ s \end{pmatrix}_L, \begin{pmatrix} t \\ b \end{pmatrix}_L, u_R, d_R, s_R, c_R, b_R, t_R \quad .$$

For all these fermionic fields the kinetic term of the Lagrangian $\mathcal{L}_{FK}$ reads

$$\mathcal{L}_{FK} = i\bar{\psi}\gamma_\mu\partial^\mu\psi \quad . \tag{2.1}$$

2.1.2 Gauge bosons and local symmetries

Interactions between the fermions are mediated by gauge particles. Those particles have spin one and they are called gauge bosons. To every known force in nature one can assign a corresponding local symmetry and one type of gauge boson. The local symmetry groups of the standard model are

$$U(1) \times SU(2)_L \times SU(3)_c \quad , \tag{2.2}$$

with the couplings g_1, g_2 and g_3. The fermions transform under the fundamental representation of the corresponding gauge group with generators λ^a like

$$\psi \to \psi e^{i\lambda^a\phi_a(x)} \quad . \tag{2.3}$$

The gauge bosons transform under the adjoint representation of their group

$$G^a_\mu\frac{\lambda_a}{2} \to G^a_\mu\frac{\lambda_a}{2} + \frac{1}{g}(\partial_\mu\phi_a)\frac{\lambda^a}{2} + i\left[\phi_a\frac{\lambda^a}{2}, G^b_\mu\frac{\lambda_b}{2}\right] \quad , \tag{2.4}$$

where g is the coupling constant of the theory. Since gauge bosons are propagating particles, one has to include their kinetic term, $\mathcal{L}_{GK}$, into the Lagrangian

$$\begin{aligned} \mathcal{L}_{GK} = \; & -\tfrac{1}{4}\left(\partial_\mu G^a_\nu - \partial_\nu G^a_\mu + g f^{abc} G^b_\mu G^c_\nu\right)\left(\partial^\mu G^\nu_a - \partial^\nu G^\mu_a + g f^{ade} G^{\mu\,d} G^{\nu\,e}\right) \\ & + \mathcal{O}(g^2) \; , \end{aligned} \tag{2.5}$$

where the structure constants f^{abc} are defined by

$$\left[\lambda^a, \lambda^b\right] = 2i f^{abc}\lambda^c \quad . \tag{2.6}$$

This gauge theory is composed of two main parts:

terms in the standard model [6].

- **The electroweak sector of the standard model**
  For the generator of the $U(1)$ symmetry group one introduces the four vector field $B_\mu(x)$ and for the three generators τ^i of the $SU(2)_L$ symmetry group one introduces three different vector fields W_1, W_2 and W_3. Experimental results show that not all of those fields correspond directly to physical gauge bosons [7, 8]. It turns out that the $U(1)$ gauge sector is coupled to the neutral sector of the $SU(2)_L$ gauge group by the electroweak mixing matrix

$$\begin{pmatrix} Z^0_\mu \\ A_\mu \end{pmatrix} = \begin{pmatrix} \cos\theta_\mathrm{W} & \sin\theta_\mathrm{W} \\ -\sin\theta_\mathrm{W} & \cos\theta_\mathrm{W} \end{pmatrix} \begin{pmatrix} W^3_\mu \\ B_\mu \end{pmatrix} \quad , \tag{2.7}$$

  where θ_W is called the weak mixing angle. The vector field A_μ is the photon field known from quantum electrodynamics (QED) and Z^0_μ is the mediator of the electrically uncharged interactions of the weak force. This mixing explains why the QED coupling can be as small as $\sim \frac{1}{137}$ although the coupling of the $U(1)$ group is $\sim \frac{1}{60}$ and the coupling of the $U(2)_L$ group is with $\sim \frac{1}{27}$ even bigger.

- **The strong sector of the standard model**
  This sector of the standard model describes quantum chromo dynamics (QCD). It is called strong because its coupling constant g_3 at nuclear distances, is more than 300 times larger than the coupling of QED (at the ~ 100 GeV scale). As the fundamental representation of $SU(3)$ is three-dimensional, it couples to three different charges, so called color charges (red, green, blue). According to the eight different generators of the $SU(3)$, QCD has 8 gauge bosons, which are called gluons.

If one wants the total Lagrangian to be independent of the transformations (2.3, 2.4) one has to replace the partial derivatives in eq. (2.1) by covariant derivatives D_μ. For the left-handed leptons this is

$$\partial_\mu \rightarrow D_\mu = \partial_\mu - ig_1\frac{Y}{2}B_\mu - ig_2\frac{\tau^i}{2}W^i_\mu \quad , \tag{2.8}$$

for the right handed leptons

$$\partial_\mu \rightarrow D_\mu = \partial_\mu - ig_1\frac{Y}{2}B_\mu \quad , \tag{2.9}$$

for the left-handed quarks

$$\partial_\mu \rightarrow D_\mu = \partial_\mu - ig_1\frac{Y}{2}B_\mu - ig_2\frac{\tau^i}{2}W^i_\mu - ig_3\frac{\lambda^a}{2}G^a_\mu \quad , \tag{2.10}$$

and for the right handed quarks

$$\partial_\mu \rightarrow D_\mu = \partial_\mu - ig_1 \frac{Y}{2} B_\mu - ig_3 \frac{\lambda^a}{2} G^a_\mu \quad . \tag{2.11}$$

At this point the standard model would be readily defined if all known particles would be massless. This is obviously not the case, thus one needs a mass generating but symmetry preserving mechanism.

2.1.3 Mass sector for the gauge bosons

Straight forward mass terms for gauge bosons do not preserve the symmetries which were the guiding principle for the construction of the SM Lagrangian. Therefore, observation of the massive gauge bosons W^+, W^- and Z^0 meant serious trouble for theorists. Conveniently, the Higgs mechanism pointed a way out of this dilemma. It manages to incorporate masses in a gauge invariant way into the standard model by introducing a duplet scalar field Φ composed of four scalar fields (Higgs fields): H, ϕ^0, ϕ^1, and ϕ^2 where,

$$\Phi = \frac{1}{\sqrt{2}} \begin{pmatrix} v + H + i\phi^0 \\ i\phi^1 - \phi^2 \end{pmatrix} = \begin{pmatrix} \frac{v+H+i\phi^0}{\sqrt{2}} \\ i\phi^- \end{pmatrix} \quad . \tag{2.12}$$

The quantum numbers for the Higgs fields are shown in table (2.1.3). The fields ϕ^0 and $\phi^\pm = (\phi^1 \mp i\phi^2)/\sqrt{2}$ are unphysical "would-be" Goldstone bosons associated with spontaneous symmetry breaking. The only physical field that remains is the Higgs field H. The vacuum expectation value of this field

$$< 0|\Phi|0 >= \begin{pmatrix} \frac{v}{\sqrt{2}} \\ 0 \end{pmatrix} \quad , \tag{2.13}$$

is given by the constant v and its value determines the scale of the symmetry breaking. The Lagrangian for the Higgs sector is

$$\mathcal{L}_\Phi = (D_\mu \Phi)^\dagger (D_\mu \Phi) - \mu^2 \frac{\lambda}{2} (\Phi^\dagger \Phi) - \frac{\lambda}{2} (\Phi^\dagger \Phi)^2 \tag{2.14}$$

	Q	T^3_W	Y	C
$\frac{v+H+i\phi^0}{\sqrt{2}}$	0	$\frac{1}{2}$	-1	0
$i\phi^-$	-1	$\frac{1}{2}$	-1	0

Table 2.1: Quantum numbers for the components of the Higgs duplet

with

$$D_\mu \Phi = \left[\partial_\mu - i g_1 \frac{Y}{2} B_\mu - i g_2 \frac{\tau^j}{2} W_\mu^j \right] \Phi \quad , \tag{2.15}$$

as in eq. (2.8). The last two terms of eq. (2.14) represent the potential of the Higgs Lagrangian whose form is determined by the values of the factors μ and λ. If $\mu < 0$ and $\lambda > 0$ the potential has a minimum at

$$v = \sqrt{\frac{-2\mu}{\lambda}} \quad . \tag{2.16}$$

The Goldstone bosons $\phi^\pm$ and ϕ^0 are "eaten" by the vector bosons $W^\pm$ and Z^0, which therefore acquire their mass according to

$$M_W = \frac{1}{2} g_2 v \ \text{ and } \ \mathrm{M_Z} = \frac{\mathrm{M_W}}{\cos\theta_\mathrm{W}} \quad . \tag{2.17}$$

The mass of the Higgs field is given by expanding eq. (2.14) around the minimum (2.16),

$$m_H = v\sqrt{\lambda} \quad . \tag{2.18}$$

2.1.4 Mass sector for the fermions

To formulate fermion masses in a gauge invariant way one uses the very same Higgs field combined with Yukawa coupling interactions. For the first generation

$$\begin{array}{c} \mathcal{L}_{Yukawa} = \frac{\sqrt{2} m_u}{v} \left(\bar{u}_L \bar{d}_L \right) \Phi u_R + \frac{\sqrt{2} m_d}{v} \left(\bar{u}_L \bar{d}_L \right) (-i\tau_2 \Phi^*) d_R \\ + \frac{\sqrt{2} m_e}{v} \left(\bar{\nu}_L \bar{e}_L \right) (-i\tau_2 \Phi^*) e_R + \text{Hermitian conjugate} \end{array} \quad , \tag{2.19}$$

where m_u, m_d and m_e are up quark, down quark and electron masses, respectively (neutrinos are assumed to be massless), and the Higgs douplet is turned around by one of the generators of $SU(2)$, τ_2, via

$$-i\tau_2 \Phi^* = \begin{pmatrix} i\phi^+ \\ \frac{v + H + i\phi^0}{\sqrt{2}} \end{pmatrix} \quad . \tag{2.20}$$

It is important to note that the quarks in eq. (2.19) are given in their mass representation. From experiment one knows with high precision that electrically neutral couplings with γ, Z^0 and G do not change flavor [9]. Only the charged currents coupled to $W^\pm$ are observed to change flavor. There is a chance that an up quark can change to a down, a strange or even a bottom

quark. This is called mixing, which is due to the fact that the weak eigenstates of quarks are not simultaneously the mass eigenstates. By convention, the quarks with charge $+2/3$ are defined to be unmixed:

$$\begin{pmatrix} u \\ c \\ t \end{pmatrix}_{\text{Weak}} = \begin{pmatrix} u \\ c \\ t \end{pmatrix}_{\text{Mass}} \quad . \tag{2.21}$$

The quark mass mixings can then be expressed in the three-dimensional space of the quarks with charge $-1/3$ d, s and b:

$$\begin{aligned} \begin{pmatrix} d \\ s \\ b \end{pmatrix}_{\text{Weak}} &= \begin{pmatrix} V_{ud} & V_{us} & V_{ub} \\ V_{cd} & V_{cs} & V_{cb} \\ V_{td} & V_{ts} & V_{tb} \end{pmatrix} \begin{pmatrix} d \\ s \\ b \end{pmatrix}_{\text{Mass}} \\ \approx \begin{pmatrix} 1-\lambda^2/2 & \lambda & A\lambda^3(\rho - i\eta) \\ -\lambda & 1-\lambda^2/2 & A\lambda^2 \\ A\lambda^3(1-\rho-i\eta) & -A\lambda^2 & 1 \end{pmatrix} &\begin{pmatrix} d \\ s \\ b \end{pmatrix}_{\text{Mass}} \quad . \end{aligned} \tag{2.22}$$

V is known as the Cabibbo-Kobayashi-Maskawa (CKM) matrix, which can be parametrised by three mixing angles and one phase. The parametrisation shown in the second line of eq. (2.22) is due to Wolfenstein [10], where $\lambda \sim 0.22$, $A \sim 1$, $\eta \sim 0.5$ and $-0.4 \leq \rho \leq 0.2$. Up to now the only part of the standard model where violation of the combined symmetries of charge conjugation $\mathcal{C}$ and parity transformation $\mathcal{P}$ occurs in the CKM matrix and is parametrisable by the so called $\mathcal{CP}$ violating phase in $\rho - i\eta$.

2.2 The total Lagrangian of the standard model

We complete this short review on the gauge invariant construction of the standard model by summing up the equations to obtain the total Lagrangian

$$\mathcal{L}_{SM} = \sum_{\text{fermions and gauge bosons}} (\mathcal{L}_{FK} + \mathcal{L}_{GK} + \mathcal{L}_{\Phi} + \mathcal{L}_{Yukawa}) \quad . \tag{2.23}$$

In its general form it is invariant under the local symmetry transformation (2.2) and a global $SU(2)$ symmetry for the Higgs sector $\mathcal{L}_{\Phi}$. The transition of the Higgs to its vacuum state breaks the second symmetry spontaneously and makes the weak gauge bosons and the fermions massive.

2.3 Global symmetries

The main guiding principles in the construction of the SM Lagrangian have been symmetries. In addition to the local symmetries (2.2), which give the types of interactions and forces in the theory, there are global symmetries as well. Global symmetries can have two possible physical consequences:

- If they are exact symmetries, they give rise to conserved currents, and quantum numbers, by the virtue of Noether's theorem.
- If they are spontaneously broken, they give rise to a Nambu-Goldstone boson for every broken generator of this symmetry.

The lepton sector of the SM Lagrangian has global $SU(2)_L \times U(1)_{EM} \times U(1)_{Lep}$ symmetries. The quantum number corresponding to global $SU(2)_L$ is the weak isospin T^3. The quantum number corresponding to the global $U(1)_{EM}$ is the weak hypercharge Y, where the electric charge is related to T^3 and Y by $Q = T^3 + Y/2$ for left handed leptons and by $Q = Y$ for right handed lepton. The quantum number corresponding to the global $U(1)_{Lep}$ is the lepton number L.
The quark sector of the SM Lagrangian for N flavors in the limit of vanishing quark masses $m_q \to 0$ has , in addition to the electro-weak $SU(2)_L \times U(1)_{EM}$, a large global symmetry $U(N)_L \times U(N)_R = U(N)_V \times U(N)_A$. Since $m_u \approx m_d \ll 1$ GeV, one knows that at least for these quarks, the limit of sending the quark masses to zero is sensible. Thus one can expect the strong interactions to be approximately $U(2)_V \times U(2)_A$ invariant. Experimentally, one finds that, indeed, the vector symmetry corresponds to the strong isospin I times baryon number B: $U(2)_V = SU(2)_I \times U(1)_B$. The global axial symmetry can be split of in the same way: $U(2)_A = SU(2)_A \times U(1)_A$. The $SU(2)_A$ turns out to be spontaneously broken in a quark condensate $\langle \bar{u}u \rangle = \langle \bar{u}u \rangle \neq 0$, giving the three light pion states π^+, π^-, and π^0. Only the remaining $U(1)_A$ causes some trouble, as it neither could be identified with an other conserved quantum number nor with a light Goldstone boson. This issue is the seed of one of the naturalness problems of the SM and will be discussed in the following section.

2.4 Problems of the standard model

The only measured and settled discrepancy of standard model predictions in particle physics comes from neutrino physics, but one can hope that mass terms for neutrinos can be introduced into the standard model without the

definition of fundamentally new and unknown mechanisms (e.g. by an additional see-saw mass term could do the job). In addition to the experimental success, the standard model succeeded in largely unifying the theory landscape by describing three of the four known fundamental interactions within one single framework. This success encouraged theoretical physicists all over the world to go even further and search for a theory that could describe all known fundamental interactions within one single framework. Because of three reasons, the standard model is considered an important but not final step on the way to such a theory:

2.4.1 Problem of large number of parameters

The standard model has 18 parameters at the level of its fundamental Lagrangian, which all have to be determined by experiment. Those parameters are

- nine fermion masses: $m_e,\ m_\mu,\ m_\tau,\ m_u,\ m_d,\ m_c,\ m_s,\ m_b,\ m_t$ (actually three more due to neutrino masses $m_{\nu e},\ m_{\nu\mu},\ m_{\nu\tau}$)
- four CKM parameters: $\lambda,\ A,\ \eta,\ \rho$,
- four electro-weak parameters: $e,\ \theta_W,\ M_W,\ m_H$,
- the strong coupling constant: α_S.

Not counting the so called "natural constants" like h, and c and also not counting the experimentally fitted parton distribution functions of protons and neutrons [2].

2.4.2 The weak hierarchy problem

The mass scales of the electro-weak [3] gauge bosons and their matter fields (leptons, quarks) show strong hierarchies like

$$\frac{m_\nu}{m_H} \sim 10^{-17}, \quad \frac{m_e}{m_H} \sim 10^{-8} \quad , \tag{2.24}$$

which can not be explained by the SM.

But there are more complications concerning m_H: If the mass of the Higgs boson is around 170 GeV the running couplings and interactions of the SM

[2] Still one has to admit that there exists no objective measure of how many parameters are " too many" and all one is left with, is a gut instinct telling that one might be able to do better than 18.

[3] Therefore the name " weak" hierarchy problem.

can be described up to energy scales of 10^{19} GeV. But such a small Higgs mass can only be achieved for the price of extreme fine tuning. As the Higgs sector of the SM still lacks direct confirmation there are several serious attempts to describe the masses of fermions and the electro-weak gauge bosons. Such attempts are e.g. quantum condensation of fields, compositeness, indirect symmetry breaking or extra dimensions.

2.4.3 The strong hierarchy problem

In section (2.3) it was mentioned that the lack of experimental confirmation of the $U(1)_A$ symmetry (broken or not) was a worry for particle physicists. The solution was pointed out by 't Hooft [11], realizing that the quantum QCD vacuum has a more complicated structure, which makes $U(1)_A$ not a true symmetry of QCD. Even though $U(1)_A$ is a symmetry of the classical QCD Lagrangian, a loop calculation shows that the axial current $J^\mu_{\gamma 5}$ corresponding to this symmetry is not conserved on quantum level:

$$\partial_\mu J^\mu_{\gamma 5} = \frac{g^2 N}{32\pi^2} F^{\mu\nu}_a \tilde{F}_{a\mu\nu}, \tag{2.25}$$

where $\tilde{F}_{a\mu\nu} = \frac{1}{2}\epsilon_{\mu\nu\alpha\beta}F^{\alpha\beta}_a$. This effect is known as the axial anomaly of QCD. As often, the solution to one problem raised another problem. This term would violate CP symmetry in strong interactions and cause e.g. a magnetic dipole-moment of neutrons which is 10^{12} times bigger than experimental bounds [12]. In order to explain this discrepancy, an additonal parameter θ (axionic field) had to be introduced, which couples to the term (2.25) and suppresses it [13]. The fact that this parameter has to be fine tuned to such an extremely tiny value ($\theta \sim 10^{-12}$) is called the strong hierarchy problem.

2.4.4 Missing gravity

The most obvious reason for the SM not being truly fundamental is the fact that it does not explain gravitational forces. If one assumes that GR and the SM have their origin in one single unified field theory X with one unified mass scale M_X it is not understood why the mass scales of GR (M_{Pl}) and the SM (m_H) have such a huge hierarchy:

$$\frac{m_H}{M_{Pl}} \sim 10^{-19} \quad . \tag{2.26}$$

As the coupling of gravity is $G_N \sim 1/M^2_{Pl}$, this question is equivalent to the question: " Why is gravity so weak as compared to the other forces in

nature". The hierarchy (2.26) could either be resolved by a Higgs mass which is of the order of 10^{19} GeV rather than the expected 170 GeV or by lowering the Planck mass down to the $\sim$TeV region. As an increased Higgs mass would aggravate the hierarchies (2.24), this attempt is not useful. Therefore the lowering of the Planck scale would be much more desirable. A possible scenario that could explain such a lowered Planck scale [4] and solve (2.26) can be given in the context of theories with extra dimensions, which will be discussed in chapter 4.

[4]Explaining the hierarchy does not mean that the unified theory X is already found, it only might give a hint in which direction to proceed the search.

Chapter 3

The theory of general relativity

General relativity describes gravity in the mathematical language of geometry. In this theory, Einstein found an extremely elegant way to derive a well motivated set of equations which not only reproduced Newtons law and special relativity, but also allowed for exiting new predictions and interpretations.

It is part of the beauty of the theory of general relativity that all classical predictions and solution of this theory can be found by starting from one single set of equations

$$R_{\mu\nu} - \frac{1}{2} g_{\mu\nu} R = -8\pi G T_{\mu\nu} \quad , \tag{3.1}$$

the Einstein equations. The left side of eq. (3.1) reflects the curvature (and therefore, the equations of motion) of a given spacetime via the Riemann tensor $R_{\mu\nu}$. The right side reflects the energy and momentum distribution of a given amount of matter which by, virtue of (3.1), determines the curvature of space and time. The gravitational coupling, G, which determines how much a certain mass distribution curves the spacetime, can be obtained by matching eq. (3.1) to Newton's law.

3.1 Riemannian geometry

It is useful to study the concepts and notation of Riemannian geometry (the geometry of curved spaces) before going into the details of (3.1).

3.1.1 Parallel transport and covariant derivative

A vector X on a manifold N can be seen as a dirctional derivative acting on a function $f : N \to \Re$, which means in components $X : f \to X[f] = X^\mu \frac{\partial f}{\partial x^\mu}$.

Now the question arises how such a vector, which was calculated at a certain point x of the manifold, can be compared to other vectors on other points x'. As usual, one would hope that such a comparison applied for infinitesimal displacements $x - x' = \triangle x$ allows the definition of a derivative on the vector component V^μ

$$\frac{\partial V^\mu}{\partial x^\nu} = \lim_{\triangle \mathrm{x} \to 0} \frac{\mathrm{V}^\mu(..., \mathrm{x}^\nu + \triangle \mathrm{x}^\nu, ...) - \mathrm{V}^\mu(..., \mathrm{x}^\nu, ...)}{\triangle \mathrm{x}^\nu} \quad . \tag{3.2}$$

This naive comparison might fail because it is not even guaranteed that the unit vectors in x and x' can be compared directly. Therefore, one should not directly compare two vectors which are defined on different points.
The solution to this problem is to define an operation that provides a parallel transport of one of the vectors to the point where the other vector is defined. The vector coefficient $V^\mu(x)$ is now parallel transported from the point x to the infenitesimally displaced point $x + \triangle x$

$$V^\mu_x \parallel (x + \triangle x) = V^\mu(x) - V^\lambda(x) \Gamma^\mu_{\ \nu\lambda} \triangle x^\nu \quad , \tag{3.3}$$

where $\Gamma^\mu_{\ \nu\lambda}$ are called **connection coefficients**. With this one can now define the so called covariant derivative of $V^\mu e_\mu$ with respect to x^ν

$$\nabla_\nu V^\mu(x) e_\mu = \lim_{\triangle x^\nu \to 0} \frac{V^\mu(x + \triangle x) - V^\mu_x \parallel (x + \triangle x)}{\triangle x^\nu} e_\mu \quad , \tag{3.4}$$

which gives according to eq. (3.2, 3.3)

$$\nabla_\nu V^\mu(x) e_\mu = \frac{\partial V^\mu}{\partial x^\nu} e_\mu + V^\lambda(x) \Gamma^\mu_{\ \nu\lambda} e_\mu \quad . \tag{3.5}$$

In order to make the result (3.5) compatible with the mathematical requirement on a derivative (see appendix A) like the chain rule for functions f and vectors X ($\nabla_\nu(fX) = (\partial_\nu f)X + f \nabla_\nu X$) we take X^μ as f and e_μ as X and find

$$\nabla_\nu V^\mu(x) e_\mu = (\partial_\nu V^\mu) e_\mu + V^\mu \nabla_\nu e_\mu \quad . \tag{3.6}$$

Comparing eq. (3.6) to (3.5) we obtain a transformation rule for the covariant derivative of unit vectors e_ν

$$\nabla_\mu e_\nu = \Gamma^\lambda_{\ \mu\nu} e_\lambda \quad . \tag{3.7}$$

This reflects the fact that unit vectors might change when going from one point on a manifold to another point. The covariant derivative (3.5) with respect to single components of elements of $T_p M$ can of course be generalized

to the covariant derivative with respect to a complete tangent vector $\epsilon\, T_pM$. The covariant derivative of a tangent vector $V = V^\mu e_\mu = \partial V^\mu/\partial x^\mu$ with respect to another tangent vector $W = W^\mu e_\mu = \partial W^\mu/\partial x^\mu$ is

$$\nabla_W V(x) = W^\nu \nabla_\nu (V^\mu e_\mu) = W^\nu \left(\frac{\partial V^\mu}{\partial x^\nu} + V^\lambda(x) \Gamma^\mu_{\ \nu\lambda} \right) \frac{\partial}{\partial x^\mu} \quad . \tag{3.8}$$

Note that the ad hoc definition of the covariant derivative (3.5) has to be made sure that it fulfills certain mathematical conditions (see Appendix A) and that the connection coefficients are not determined uniquely yet (apart from these conditions).

3.1.2 Parallel transport and geodesics

For the definition of the covariant derivative (3.5) we used some ansatz (3.3) for the infinitesimal parallel transport of a vector $X\, \epsilon\, T_pM$. Now we want to specify the parallel transport of a vector along a curve. Let $c : (a, b) \to M$ be a curve in M. For simplicity, we assume the image of the m-dimensional manifold M to be covered by one single chart $(U,\ \phi)$ $(\phi : \tilde{U}\epsilon\ \mathrm{M} \to \mathrm{U}\epsilon\ \Re^{\mathrm{m}})$ whose coordinate is $x = \phi(p)$. Let X be a vector field defined along the curve $c(t)$,

$$X|_{c(t)} = X^\mu(c(t)) e_\mu\ |_{c(t)} \quad . \tag{3.9}$$

If the vector field is defined at every point along $c(t)$ in such a way that the infinitesimal parallel transported vector (from x to $x + \triangle x$) equals the element of the vector field at the point $x + \triangle x$, it is said to be **parallel transported**. For the covariant derivative at the point x we find by using eq. (3.3) and (3.4)

$$\begin{aligned} \nabla_\nu X^\mu(x) &= \lim_{\triangle x^\nu \to 0} \frac{X^\mu(x+\triangle x) - X^\mu_x \| (x+\triangle x)}{\triangle x^\nu} \\ &= \lim_{\triangle x^\nu \to 0} \frac{X^\mu(x+\triangle x) - X^\mu(x+\triangle x)}{\triangle x^\nu} = 0 \quad . \end{aligned} \tag{3.10}$$

As this is true for any point on $c(t)$ and independent of the specific component of X, the statement of eq. (3.10) can be generalised: If X satisfies the condition

$$\nabla_V X = 0 \quad \text{for any t } \ \epsilon(a,\ b) \quad , \tag{3.11}$$

X is said to be parallel transported along $c(t)$ where $V = d(c(t))/dt = (dx^\mu(c(t))/dt)\ e_\mu|_{c(t)}$. This condition in terms of the coordinates X^μ is obtained from eq. (3.10) by using $V^\mu = dx^\mu(c(t))/dt$,

$$\begin{aligned} \nabla_V X^\mu &= V^\nu \left(\partial_\nu X^\mu + \Gamma^\mu_{\ \nu\beta} x^\beta \right) \\ &= \tfrac{\mathrm{dX}^\mu}{\mathrm{dt}} + \Gamma^\mu_{\ \nu\beta} \tfrac{\mathrm{dx}^\nu(\mathrm{c(t)})}{\mathrm{dt}} X^\beta = 0 \quad . \end{aligned} \tag{3.12}$$

If X^μ is the component of the tangent vector V of the curve $c(t)$ this special curve is called a **geodesic** and we find

$$\nabla_V V = 0 \quad , \tag{3.13}$$

or for the coordinates $\{x^\mu\}$ on $c(t)$

$$\frac{\mathrm{d}^2\mathrm{x}^\mu}{\mathrm{dt}^2} + \Gamma^\mu_{\nu\beta}\frac{\mathrm{dx}^\nu(\mathrm{c(t)})}{\mathrm{dt}}\frac{\mathrm{dx}^\beta(\mathrm{c(t)})}{\mathrm{dt}} = 0 \quad . \tag{3.14}$$

From this definition of derivative and parallel transport one can interpret curves that fulfill condition (3.13) as the straightest possible curve on the manifold M. But (3.13) might be too strong a condition and not allow solutions on a general topology. Then one can use the argument that as long as the change of V is parallel to V, $c(t)$ will still be a straight line (although stretched). This would only require

$$\nabla_V V = fV \quad , \tag{3.15}$$

where $f : M \to \Re$, which is the same as condition (3.13) in the reparameterised coordinate system

$$\frac{\mathrm{dx}^\mu}{\mathrm{dt}} \to \frac{\mathrm{dt}}{\mathrm{d\tilde{t}}}\frac{\mathrm{dx}^\mu}{\mathrm{dt}} \quad , \tag{3.16}$$

if $\tilde{t}$ satisfies

$$\frac{\mathrm{d}^2\tilde{\mathrm{t}}}{\mathrm{dt}^2} = f\frac{\mathrm{d\tilde{t}}}{\mathrm{dt}} \quad . \tag{3.17}$$

Thus it is always possible to give a parameterisation in which the geodesic follows condition (3.13).

3.1.3 Covariant derivative of tensor fields

We defined ∇_V in such a way that it can be interpreted as a derivative as well for functions $\nabla_V f = V[f]$ as for vectors (3.5), where f is $\epsilon\, \mathcal{F}(M)$ which are the real functions on M $f: M \to \Re$. The product rule holds and

$$\nabla_V(fX) = (V[f])X + f\nabla_V X \quad . \tag{3.18}$$

Now we require that the analog should hold for arbitrary tensors (T_i) and products of tensors,

$$\nabla_X(T_1 \otimes T2) = (\nabla_X T_1) \otimes T_2 + T_1 \otimes (\nabla_X T_2) \quad . \tag{3.19}$$

Let $X,\ Y$ be vectors in T_pM and $\omega = \omega_\alpha \mathrm{dx}^\alpha$ be a one-form, for which the unit vector dx^α obeys

$$\langle \mathrm{dx}^\alpha, \partial_\beta \rangle = \delta^\alpha_\beta \text{ and } \langle \omega, Y \rangle \ \epsilon \ \mathcal{F}(M) \quad . \tag{3.20}$$

For the covariant derivative of the one-form ω it is assumed that

$$\nabla_X \omega = (\nabla_X \omega_\nu)\mathrm{dx}^\nu + \omega_\nu \nabla_\mathrm{X} \mathrm{dx}^\nu \quad , \tag{3.21}$$

where $\omega_\nu \ \epsilon \ \mathcal{F}(M)$. It is instructive to look at the scalar product $[\langle \omega, Y \rangle]$, finding

$$X\left[\langle \omega, Y \rangle\right] = \nabla_X \left[\langle \omega, Y \rangle\right] = \langle \nabla_X \omega, Y \rangle + \langle \omega, \nabla_X Y \rangle \quad . \tag{3.22}$$

Written in components, and by using eq. (3.20) this is,

$$\begin{aligned} X^\nu \partial_\nu (\left\langle \omega_\alpha \mathrm{dx}^\alpha,\ \mathrm{Y}^\beta \partial_\beta \right\rangle) \ &= X^\nu \partial_\nu (\omega_\alpha Y^\alpha) = X^\nu \left((\partial_\nu \omega_\alpha) Y^\alpha + \omega_\alpha (\partial_\nu Y^\alpha) \right) \\ &= X^\nu \left((\partial_\nu \omega_\alpha) Y^\beta \delta^\alpha_\beta + \omega_\alpha Y^\beta \langle \nabla_\nu \mathrm{dx}^\alpha, \partial_\beta \rangle \right. \\ &\quad \left. + \omega_\alpha (\partial_\nu Y^\beta) \delta^\alpha_\beta + \omega_\alpha Y^\beta \langle \mathrm{dx}^\alpha, \nabla_\nu \partial_\beta \rangle \ \right) \end{aligned} \quad . \tag{3.23}$$

If we now take $X = 1\partial_\mu$ and compare the last part of eq. (3.23) to the last part of the first line of eq. (3.23) we find

$$\langle \nabla_\nu \mathrm{dx}^\alpha, \partial_\beta \rangle = \langle \mathrm{dx}^\alpha, \nabla_\nu \partial_\beta \rangle \quad . \tag{3.24}$$

By using eq. (3.7) on this equation, it turns out that the covariant derivative of $\mathrm{d}x^\nu$ gives,

$$\nabla_\mu \mathrm{dx}^\nu = -\Gamma^\nu_{\ \mu\lambda} \mathrm{dx}^\lambda \tag{3.25}$$

and the covariant derivativ of ω gives

$$\nabla_\mu \omega = (\partial_\mu \omega_\nu)\mathrm{dx}^\nu - \omega_\lambda \Gamma^\lambda_{\ \mu\nu} \mathrm{dx}^\nu \quad . \tag{3.26}$$

It can be easily generalised that the connection coefficient for p-form tensors is the negative of the connection coefficient for q-tensors. As the chain rule has to hold for all coefficients of a $(q,\ p)$ tensor t, its covariant derivative is

$$\begin{aligned} \nabla_\nu t^{\lambda_1 \ldots \lambda_q}_{\mu_1 \ldots \mu_p} \ \ &\mathrm{dx}^1 \otimes \ldots \mathrm{dx}^\mathrm{p} \otimes \partial_1 \otimes \ldots \partial_\mathrm{q} = \partial_\nu \mathrm{t}^{\lambda_1 \ldots \lambda_\mathrm{q}}_{\mu_1 \ldots \mu_\mathrm{p}} \mathrm{dx}^1 \otimes \ldots \mathrm{dx}^\mathrm{p} \otimes \partial_1 \otimes \ldots \partial_\mathrm{q} \\ &+ (\Gamma^{\lambda_1}_{\nu\kappa} t^{\kappa \ldots \lambda_q}_{\mu_1 \ldots \mu_p} + \Gamma^{\lambda_q}_{\nu\kappa} t^{\lambda_1 \ldots \lambda_{q-1} \kappa}_{\mu_1 \ldots \mu_p}) \mathrm{dx}^1 \otimes \ldots \mathrm{dx}^\mathrm{p} \otimes \partial_1 \otimes \ldots \partial_\mathrm{q} \\ &- (\Gamma^\kappa_{\nu\mu_1} t^{\lambda_1 \ldots \lambda_q}_{\kappa \ldots \mu_p} + \Gamma^{\lambda_1}_{\nu\mu_p} t^{\lambda_1 \ldots \lambda_q}_{\mu_1 \ldots \kappa}) \mathrm{dx}^1 \otimes \ldots \mathrm{dx}^\mathrm{p} \otimes \partial_1 \otimes \ldots \partial_\mathrm{q} \quad . \end{aligned} \tag{3.27}$$

For tensors the unit vectors $\mathrm{d}x^\mu$ and ∂_ν are often not explicitly written down. This saves time and effort but one has to keep in mind that the connection coefficients would also not be there without them. In this sloppy notation the covariant derivative of the metric tensor is

$$(\nabla_\nu g)_{\lambda\mu} = \partial_\nu g_{\lambda\mu} - \Gamma^\kappa_{\ \nu\lambda} g_{\kappa\mu} - \Gamma^\kappa_{\ \nu\mu} g_{\lambda\kappa} \quad . \tag{3.28}$$

3.1.4 The metric connection

As shown in subsection (A.4), the connection is still arbitrary to some extent and has to be fixed by further restrictions. For manifolds, that are endowed with a metric, a reasonable restriction would be that the scalar product of two vectors should not change under parallel transport. This should hold true for any vectors X and Y along any curve on the manifold and therefore in any direction V along the curve. Expressed mathematically,

$$\begin{aligned} 0 = \nabla_V(g(X,Y)) \quad &= V^\kappa \left[(\partial_\kappa g)(X,Y)\right. \\ &\quad \left. + \partial_Z(g(Z,Y))|_{Z=X} \underbrace{\nabla_\kappa X}_{0} + \partial_Z(g(X,Z))|_{Z=Y} \underbrace{\nabla_\kappa Y}_{0}\right] \\ &= V^\kappa X^\alpha Y^\beta (\nabla_\kappa g)_{\alpha\beta} \quad , \end{aligned} \tag{3.29}$$

where we have used the condition for parallel transport of vectors (3.12). Since eq. (3.29) is supposed to hold true for arbitrary vectores, we have a condition for every single component

$$(\nabla_\kappa g)_{\alpha\beta} = 0 \quad , \tag{3.30}$$

which gives according to eq. (3.28)

$$\partial_\lambda g_{\alpha\beta} - \Gamma^\kappa_{\lambda\alpha} g_{\kappa\beta} - \Gamma^\kappa_{\lambda\beta} g_{\kappa\alpha} = 0 \quad . \tag{3.31}$$

Subtracting the two other cyclic permutations of the indices in eq. (3.31) yields

$$-\partial_\lambda g_{\alpha\beta} + \partial_\alpha g_{\beta\lambda} + \partial_\beta g_{\lambda\alpha} + \Gamma^\kappa_{[\lambda\alpha]} g_{\kappa\beta} + \Gamma^\kappa_{[\lambda\beta]} g_{\kappa\alpha} - 2\Gamma^\kappa_{(\alpha\beta)} g_{\kappa\lambda} = 0 \quad , \tag{3.32}$$

where we split up the connection coefficients $\Gamma^\kappa_{(\alpha\beta)}$ into their symmetric $\Gamma^\kappa_{(\alpha\beta)} = 1/2(\Gamma^\kappa_{\alpha\beta} + \Gamma^\kappa_{\beta\alpha})$ and their antisymmetric $\Gamma^\kappa_{[\alpha\beta]} = 1/2(\Gamma^\kappa_{\alpha\beta} - \Gamma^\kappa_{\beta\alpha})$ part with respect to the 2^{nd} and 3^{rd} indices

$$\Gamma^\kappa_{\alpha\beta} = \Gamma^\kappa_{(\alpha\beta)} + \Gamma^\kappa_{[\alpha\beta]} \quad . \tag{3.33}$$

Plugging the solution for $\Gamma^\kappa_{(\alpha\beta)}$ of eq. (3.32) into eq. (3.33) the connection coefficient is found to be

$$\Gamma^\kappa_{\alpha\beta} = \frac{g^{\kappa\lambda}}{2}\left(\partial_\alpha g_{\beta\kappa} + \partial_\beta g_{\alpha\kappa} - \partial_\lambda g_{\alpha\beta}\right) + \frac{1}{2}(\Gamma_\beta \left[{}^{\kappa}_{\alpha}\right] + \frac{1}{2}(\Gamma_\alpha \left[{}^{\kappa}_{\beta}\right] + \Gamma^\kappa_{[\alpha\beta]}) \quad . \tag{3.34}$$

The second part of eq. (3.33) is called contorsion and denoted by $K^\kappa_{\alpha\beta} = \frac{1}{2}(\Gamma_\beta \left[{}^{\kappa}_{\alpha}\right] + \frac{1}{2}(\Gamma_\alpha \left[{}^{\kappa}_{\beta}\right] + \Gamma^\kappa_{[\alpha\beta]})$. It is easy to show that the contorsion $K^\kappa_{\alpha\beta}$ is a tensor under coordinate transformations. Under certain circumstances the

contorsion vanishes and the symmetric connection coefficients $\Gamma^{\kappa}_{(\alpha\beta)}$ equal the total connection coefficients

$$\Gamma^{\kappa}_{\alpha\beta} = \frac{1}{2} g^{\kappa\lambda} \left(\partial_\alpha g_{\beta\kappa} + \partial_\beta g_{\alpha\kappa} - \partial_\lambda g_{\alpha\beta} \right) \tag{3.35}$$

and are called **Christoffel symbols**. In this case, the connection ∇ is called **Levi-Civita connection**. For such a connection, the Christoffel symbols are determined as soon as the metric of a certain space is defined. It is important to notice that at a single point p in a manifold with a Levi-Civita connection it is always possible to choose the coordinates in such a way (see the transformation properties of $\Gamma(p)$ in subsection (A.4)) that the Christoffel symbols $\Gamma^{\mu}_{\alpha\beta}(p)$ vanish. This does not mean that derivatives of $\Gamma(p)$ vanish as well.

3.1.5 Curvature

With the definition of the covariant derivative we have now a tool at hand with which we can formulate mathematical objects which uncover geometrical properties of a given manifold M. For a given M, first one would like to find out whether it is flat and allows the application of euclidian geometry. The first guess for a mathematical object that is sensitive to the curvature would be the connection symbols Γ, as they are zero for euclidian coordinates in flat spaces. But they do not necessarily vanish in flat space because they might be non zero as soon as one chooses non euclidian coordinates such as spherical coordinates. So $\Gamma = 0$ for all $x \,\epsilon\, M$ allows to conclude that M is not curved but not vice versa. To get a feeling for the interplay between curvature and parallel transport it will be useful to look at the specific example of a S^2 sphere in 3 dimensions which is given in subsection (A.5). The general approach to this example is to study the infinitesimal parallel transport of a vector V at the point x^μ along two different paths (1: $x^\mu \to x^\mu + \epsilon^\mu \to x^\mu + \epsilon^\mu + \delta^\mu$ and 2: $x^\mu \to x^\mu + \delta^\mu \to x^\mu + \delta^\mu + \epsilon^\mu$), as shown in figure (3.1). The difference of the two final vectors ($V1(x^\mu + \epsilon^\mu + \delta^\mu)$ and $V2(x^\mu + \delta^\mu + \epsilon^\mu)$) will then provide a measure of the curvature at the point x^μ. Written down in components $V1^\mu(r)$ gives with eq. (3.4)

$$\begin{aligned} V1^\mu(r) &= V1^\mu(q) - V1^\kappa(q)\Gamma^{\mu}_{\kappa\tau}\delta^\tau \\ &= V^\mu(p) - V^\nu(p)\Gamma^{\mu}_{\nu\rho}\epsilon^\rho - \left[V^\kappa(p) - V^\nu(p)\Gamma^{\kappa}_{\nu\rho}\epsilon^\rho\right] \\ &\quad \times \left[\Gamma^{\mu}_{\tau\kappa}(p) + \partial_\lambda \Gamma^{\mu}_{\tau\kappa}\epsilon^\lambda\right]\delta^\tau \\ &\simeq V^\mu(p) - V^\nu(p)\Gamma^{\mu}_{\nu\rho}\epsilon^\rho - V^\kappa(p)\Gamma^{\mu}_{\tau\kappa}(p)\delta^\tau \\ &\quad -V^\kappa(p)\left[\partial_\lambda\Gamma^{\mu}_{\tau\kappa} - \Gamma^{\rho}_{\lambda\kappa}\Gamma^{\mu}_{\tau\rho}(p)\right]\epsilon^\lambda\delta^\tau + \mathcal{O}(\epsilon^i\delta^{3-i} \wedge\ i\,\epsilon\,\{0,1,2,3\}), \end{aligned} \tag{3.36}$$

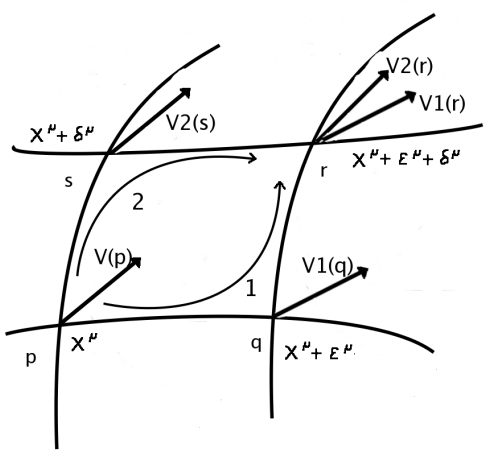

Figure 3.1: If a vector $V1(r)$, which is $V(p)$ parallel transported along the path 1, differs from the $V2(r)$, which is $V(p)$ parallel transported along the path 2, the underlying manifold is curved.

where we dropped higher order terms in the infinitesimal displacements ϵ and μ. The procedure for parallel transport along path 2 gives

$$\begin{aligned} V2^{\mu}(r) \; &\simeq V^{\mu}(p) - V^{\nu}(p)\Gamma^{\mu}_{\ \nu\rho}\delta^{\rho} - V^{\kappa}(p)\Gamma^{\mu}_{\ \tau\kappa}(p)\epsilon^{\tau} \\ &\quad -V^{\kappa}(p)\left[\partial_{\tau}\Gamma^{\mu}_{\ \lambda\kappa} - \Gamma^{\rho}_{\ \tau\kappa}\Gamma^{\mu}_{\ \lambda\rho}(p)\right]\epsilon^{\lambda}\delta^{\tau} + \mathcal{O}(\epsilon^{i}\delta^{3-i} \wedge \; i \,\epsilon\, \{0,1,2,3\})\,. \end{aligned} \tag{3.37}$$

In the difference between those two vectors the terms that are linear in ϵ and δ drop out and one finds in lowest order of ϵ and δ

$$\begin{aligned} V2^{\mu}(r) - V1^{\mu}(r) \; &= V^{\kappa}(p)\left[\partial_{\lambda}\Gamma^{\mu}_{\ \tau\kappa} - \partial_{\tau}\Gamma^{\mu}_{\ \lambda\kappa}\right. \\ &\quad \left. +\Gamma^{\rho}_{\ \tau\kappa}\Gamma^{\mu}_{\ \lambda\rho}(p) - \Gamma^{\rho}_{\ \lambda\kappa}\Gamma^{\mu}_{\ \tau\rho}(p)\right]\epsilon^{\lambda}\delta^{\tau} \\ &= V^{\kappa}(p)R^{\mu}_{\ \kappa\lambda\tau}\epsilon^{\lambda}\delta^{\tau} \quad . \end{aligned} \tag{3.38}$$

Where we defined the **Riemann tensor** as

$$R^{\mu}_{\ \kappa\lambda\tau} = \partial_{\lambda}\Gamma^{\mu}_{\ \tau\kappa} - \partial_{\tau}\Gamma^{\mu}_{\ \lambda\kappa} + \Gamma^{\rho}_{\ \tau\kappa}\Gamma^{\mu}_{\ \lambda\rho}(p) - \Gamma^{\rho}_{\ \lambda\kappa}\Gamma^{\mu}_{\ \tau\rho}(p) \quad . \tag{3.39}$$

This tensor has certain symmetries and obeys certain conservation laws which will be discussed in the appendix (A.5).

3.2 Einstein's field equations

There exist several derivations [14, 15] of Einstein's equation (3.1) based on the **strong principle of equivalence** and the **principle of general**

covariance.

- Strong principle of equivalence:
  In a freely falling, non-rotating, laboratory the local laws of physics take on standard form, including a standard numerical content, independent of the position of the laboratory in space.

- Principle of general covariance:
  The equations of physics should have the same tensorial form in all coordinate systems.

Because of these principles Einstein's theory is frequently called the theory of general relativity. In the following we want to derive Einstein's equations from a variational principle where we implicitly (by the choice of our ansatz) make use of the strong principle of equivalence and the principle of general covariance. We start from the action integral,

$$\mathcal{S} = \int \sqrt{-g}\, \mathrm{d}^4x (L_G - 2\kappa L_F) \quad , \tag{3.40}$$

and demand its variation to be zero ($\delta S = 0$). Here g is the determinant of the metric, $\sqrt{-g}\, \mathrm{d}^4x$ is the invariant volume measure of the four-dimensional pseudo-Riemannian spacetime, L_G and L_F are the Lagrangians for the gravitational and matter, respectively. From the assumption that freely falling laboratories are just propagating along a geodesic trajectory in curved spacetime and from subsection (A.5) we know that the Riemann curvature tensor and its contracted form must play an important role in the equations we are trying to find. Therefore, the first and most simple guess for L_G is the only non trivial scalar of Riemannian geometry $R = R_{\mu\nu} g^{\mu\nu}$. Using this, the variation of the first part of the integral (3.40) gives

$$\delta \int \sqrt{-g}\, \mathrm{d}^4x R = \int \sqrt{-g}\, \mathrm{d}^4x g^{\mu\nu} \delta R_{\mu\nu} + \int \mathrm{d}^4x \delta(\sqrt{-g} g^{\mu\nu}) R_{\mu\nu} \quad . \tag{3.41}$$

To find $\delta R_{\mu\nu}$ the definition (A.18) turns out to be a useful starting point

$$\begin{aligned} \delta R^{\kappa}_{\ \mu\kappa\nu} &= \delta(< dx^\kappa, \nabla_\kappa \Gamma^\eta_{\mu\nu} e_\eta > - < dx^\kappa, \nabla_\nu \Gamma^\eta_{\mu\kappa} e_\eta >) \\ &= \nabla_\kappa < dx^\kappa, \delta\Gamma^\eta_{\mu\nu} e_\eta > - \nabla_\nu < dx^\kappa, \delta\Gamma^\eta_{\mu\kappa} e_\eta > \quad . \end{aligned} \tag{3.42}$$

Relabeling and exploiting the invariance of the metric $g_{\mu\nu}$ and of the relation $\nabla_\mu V^\mu = \frac{1}{\sqrt{-g}} \partial_\mu (\sqrt{-g} V^\mu)$ gives

$$\begin{aligned} g^{\mu\nu} \delta R_{\,\mu\nu} &= g^{\mu\nu} (\nabla_\kappa < dx^\kappa, \delta\Gamma^\eta_{\mu\nu} e_\eta > - \nabla_\nu < dx^\kappa, \delta\Gamma^\eta_{\mu\kappa} e_\eta >) \\ &= \nabla_\kappa g^{\mu\nu} < dx^\kappa, \delta\Gamma^\eta_{\mu\nu} e_\eta > - \nabla_\kappa g^{\mu\kappa} < dx^\tau, \delta\Gamma^\eta_{\mu\tau} e_\eta > \\ &= \nabla_\kappa (g^{\mu\nu} < dx^\kappa, \delta\Gamma^\eta_{\mu\nu} e_\eta > - g^{\mu\kappa} < dx^\tau, \delta\Gamma^\eta_{\mu\tau} e_\eta >) \\ &= \tfrac{1}{\sqrt{-g}} \partial_\kappa \left(\sqrt{-g} (g^{\mu\nu} < dx^\kappa, \delta\Gamma^\eta_{\mu\nu} e_\eta > - g^{\mu\kappa} < dx^\tau, \delta\Gamma^\eta_{\mu\tau} e_\eta > \right) \quad . \end{aligned} \tag{3.43}$$

The integral over this term vanishes by Gauss' theorem if we choose vanishing variation on the boundary. Therefore, only the second summand of eq. (3.41) needs to be computed. By using

$$\delta g = g g^{\mu\nu}\delta g_{\mu\nu} = -g g_{\mu\nu}\delta g^{\mu\nu} \tag{3.44}$$

we find

$$\int \mathrm{d}^4x \delta(\sqrt{-g}g^{\mu\nu})R_{\mu\nu} = \int \mathrm{d}^4x\sqrt{-g}(R_{\mu\nu} - \frac{1}{2}g_{\mu\nu}R)\delta g^{\mu\nu} \quad . \tag{3.45}$$

The second part of the integral (3.40) leads to

$$\delta \int \mathrm{d}^4x\sqrt{-g}L_F = \frac{1}{2}\int \mathrm{d}^4x\sqrt{-g}T_{\mu\nu}\delta g^{\mu\nu} \quad , \tag{3.46}$$

where $T_{\mu\nu}$ is the energy momentum tensor and is given by

$$T_{\mu\nu} = \frac{-2}{\sqrt{-g}}\left[\partial_\alpha\left(\frac{\partial(\sqrt{-g}L_F)}{\partial(\partial_\alpha g^{\mu\nu})}\right) - \frac{\partial(\sqrt{-g}L_F)}{\partial(g^{\mu\nu})}\right] \quad . \tag{3.47}$$

Combining equations (3.47),(3.45) and (3.41) leads to the well known form of Einstein's field equations

$$R_{\mu\nu} - \frac{1}{2}g_{\mu\nu}R = \kappa T_{\mu\nu} \quad . \tag{3.48}$$

This shows us that the ansatz $\mathbf{L_G} = \mathbf{R}_{\mu\nu}\mathbf{g}^{\mu\nu}$ was just the right choice for obtaining the form of Einstein's equations of motion. Now only the constant κ needs to be determined by matching eq. (3.48) to the Newtonian limit (see appendix B.1), which then finally gives $\kappa = -8\pi G$ and therefore eq. (3.1).

3.3 The first solution of Einstein's equations

After Einstein derived his equations of motion, it was mostly believed that it is not possible to derive an exact solution for this system of highly coupled differential equations. Nevertheless in 1915 the first exact solution of Einstein's equations was found by Karl Schwarzschild [16]. As starting point for this solution we will take the standard form of a static and isotropic metric. The corresponding line element to this metric in spherical coordinates is

$$\mathrm{d}\tau^2 = g_{\mu\nu}\mathrm{d}x^\mu\mathrm{d}x^\nu = B(r)\mathrm{d}t^2 - A(r)\mathrm{d}r^2 - r^2(\mathrm{d}\theta^2\sin^2\theta\mathrm{d}\phi^2), \tag{3.49}$$

where A and B are arbitrary functions of r. Static means that the invariant proper time $\mathrm{d}\tau$ does not depend on the coordinate dependent time t and

isotropic means that eq. (3.49) respects spherical symmetry. Eq. (3.49) can be derived from a more general ansatz, as off diagonal elements like $X(r)\mathrm{d}t\mathrm{d}r$ or non standard spherical elements like $Y(r)r^2\mathrm{d}r^2$ can be removed by appropriate coordinate transformations. In the outside region of a spherically symmetric static mass distribution, Einstein's field equations simply read in the spherical coordinates r, θ, and ϕ

$$R_{\mu\nu} = 0 \quad . \tag{3.50}$$

It is laborious work to calculate all components of the Ricci tensor for the metric (3.49) resulting in

$$\begin{aligned} R_{tt} &= \tfrac{-B^{''}(r)}{2B(r)} + \tfrac{B^{'}(r)}{4B(r)}\left(\tfrac{A^{'}(r)}{A(r)} + \tfrac{B^{'}(r)}{B(r)}\right) - \tfrac{B^{'}(r)}{rA(r)}, \\ R_{rr} &= \tfrac{B^{''}(r)}{2B(r)} - \tfrac{B^{'}(r)}{4B(r)}\left(\tfrac{A^{'}(r)}{A(r)} + \tfrac{B^{'}(r)}{B(r)}\right) - \tfrac{A^{'}(r)}{rA(r)}, \\ R_{\theta\theta} &= -1 + \tfrac{r}{2A(r)}\left(\tfrac{-A^{'}(r)}{A(r)} + \tfrac{B^{'}(r)}{B(r)}\right) - \tfrac{1}{A(r)}, \\ R_{\phi\phi} &= \sin^2\theta R_{\theta\theta} \quad , \\ R_{\mu\nu} &= 0 \quad \text{for} \quad \mu \neq \nu \quad , \end{aligned} \tag{3.51}$$

where $A^{'}$ stands for a derivative of A with respect to r. Now the functions $A(r)$ and $B(r)$ have to be determined from eq. (3.50) by the use of eq. (3.51). From the first two eqations of eq. (3.51) we see that

$$\frac{R_{rr}}{A(r)} + \frac{R_{tt}}{B(r)} = \frac{1}{rA(r)}\left(\frac{A^{'}(r)}{A(r)} + \frac{B^{'}(r)}{B(r)}\right) \quad , \tag{3.52}$$

giving

$$A(r)B(r) = \text{constant} \quad . \tag{3.53}$$

Apart from that it is sensible to impose the boundary conditions that in large enough distance r from any gravitational source the spacetime is supposed to be Minkowskian, which determines the constant in eq. (3.53):

$$\lim_{r\to\infty} = 1 \implies \text{constant} = 1 \implies A(r) = \frac{1}{B(r)} \quad . \tag{3.54}$$

Replacing $A(r)$ in the Ricci tensor conditions (3.50) gives

$$\begin{aligned} R_{\theta\theta} &= -1 + B^{'}(r)r + B(r) \\ R_{rr} &= \tfrac{B^{''}(r)}{2B(r)} + \tfrac{B^{'}(r)}{rB(r)} = \tfrac{R^{'}_{\theta\theta}}{2rB(r)} \quad . \end{aligned} \tag{3.55}$$

The integral of the differential equation in the first line of eq. (3.55) is

$$B(r) = 1 + \frac{k}{r} \quad , \tag{3.56}$$

where the constant $k(r)$ can again be determined from the Newtonian limit (see B.1) $g_{tt} = B \to 1 - 2\phi(x)$, where ϕ is the Newtonian potential MG/r. Therefore we end up with

$$\begin{array}{rcl} B(r) & = & \left[1 - \frac{2MG}{r}\right] \\ A(r) & = & \left[1 - \frac{2MG}{r}\right]^{-1} \end{array} \quad , \tag{3.57}$$

which determines the Schwarzschild metric to

$$g_{\mu\nu} = \begin{pmatrix} 1 - \frac{2MG}{r} & 0 & 0 & 0 \\ 0 & -(1 - \frac{2MG}{r})^{-1} & 0 & 0 \\ 0 & 0 & -r^2 & 0 \\ 0 & 0 & 0 & -r^2 \sin^2\theta \end{pmatrix} \quad . \tag{3.58}$$

At the so called Schwarzschild radius $r = 2MG$ the g_{00} component becomes zero and the g_{rr} component becomes infinite. This infinity does not reflect a singularity of spacetime, as it is not there under a different choice of coordinate system. But it reflects the fact that there is an event horizon, which does not allow light or matter to leave from inside of the Schwarzschild radius. This is the reason why such an object is called black hole. The second infinity of this solution exists at $r = 0$. This is a true singularity, which can not be cured by a different choice of coordinates. Fortunately it is shielded by the event horizon, so that an outside observer is not bothered with a singularity in its observable spacetime. Apart from the Schwarzschild solution of eq. (3.1) there exist further solutions like the Kerr solution, the Reissner Nordstrom solution or the Robertson Walker solution, which we will not discuss here further.

3.4 Quantum fields in curved spacetime

The generalization of quantum field theory to curved spacetimes was considered to be the first step towards a unified theory of gravity and quantum field theory. Here gravity is not quantised itself but considered as classical background for the relativistic quantum field equations. This means that the quantum fields do not have any effect on the spacetime metric. This assumption is reasonable as long as the energy scale of quantum fluctuations is much smaller than the expected energy scale of quantum gravity effects. As it is a long way to go from the energy scale of the electro-weak theory ($\sim$ 90 GeV) to the energy scale where quantum gravity is supposed to become important ($\sim 10^{19}$ GeV), this approach is supposed to have a vast region of applicability. Most subtleties in this approach arise from the

definition and interpretation of what we are used to know as particles, because this concept looses its uniqueness as soon as there is no inertial global observer any more, who could decide what is a particle and what not. Therefore it depends upon the individual coordinate frame of an observer whether he sees a bunch of particles or just the "empty" vacuum. To quantify this statement we will start out from the standard formulation of particles in flat spacetime and give the straight forward generalization of this concept to a curved spacetime background. The translation between states in different coordinate systems is done with the help of Bogolubov coefficients.

3.4.1 Bogolubov coefficients

The field quantization procedure in curved spacetime is formally in close analogy to the case in Minkowski space. The simplest Lagrangian density for a complex **scalar field** ϕ coupled to gravity is

$$\sqrt{-g}\mathcal{L} = \sqrt{-g}\left(\nabla_\mu\phi^*(x)\frac{1}{2\sqrt{-g}}g^{\mu\nu}\nabla_\nu\phi(x) - m^2\phi^2(x)\right) \quad , \tag{3.59}$$

where $g = g(x) = det(g_{\mu\nu}(x))$ is the determinant of the metric, m is the mass of the scalar particle and ∇_μ is the covariant derivative from the previous section. For a scalar object like ϕ one knows that $\nabla_\mu\phi = \partial_\phi$ and therefore eq.3.59 reads after partial integration as

$$\mathcal{L} = \phi^*(x)\left(\frac{1}{2\sqrt{-g}}\partial_\mu\sqrt{-g}g^{\mu\nu}\partial_\nu - m^2\right)\phi(x) \quad . \tag{3.60}$$

First we notice that for a flat Minkowski metric eq. (3.60) turns into the well known Klein Gordon Lagrangian

$$\begin{aligned}\mathcal{L}_{KG} &= \phi^*(x)(\tfrac{1}{2}\partial_\mu\partial^\mu - m^2)\phi(x) \\ &= \tfrac{1}{2}\left(\tfrac{1}{2}\partial_\mu\phi^*(x)\partial^\mu\phi(x) - m^2\phi^*(x)\phi(x) + c.c.\right) \quad ,\end{aligned} \tag{3.61}$$

where partial integration was used in the second line. This is the simplest possible case, the Dirac field in curved spacetime is given in the appendix B.3 and higher spin fields can be found in [17]. Without any further interaction the Lagrangian (3.61) is invariant under the global $U(1)$ transformations

$$\phi \to \phi' = e^{i\alpha}\phi \simeq (1 + i\alpha)\phi \;, \quad \phi^* \to \phi^{*\prime} = e^{-i\alpha}\phi^* \simeq (1 - i\alpha)\phi^* \quad . \tag{3.62}$$

The conserved current J^μ for this transformation is

$$J_\mu \sim \frac{1}{2}((\partial_\mu\phi^*)\phi - (\partial_\mu\phi)\phi^*) \quad , \tag{3.63}$$

which leads with $\lim_{r\to\infty}\phi(t,r)=0$ to the conserved charge $\partial^0\int \mathrm{d^3x J_0}=0$, which is interpreted as conservation of (charge)-probability and expressed with the time invariant integral

$$N(\phi,\ \phi)=\int \mathrm{d^3x}\frac{1}{2}((\partial_0\phi^*)\phi-(\partial_0\phi)\phi^*) \quad . \tag{3.64}$$

This is the motivation to define the time invariant scalar product of two Klein Gordon fields ϕ_1 and ϕ_2

$$(\phi_1,\ \phi_2)=-i\int \mathrm{d^3x}((\partial_0\phi_2^*)\phi_1-(\partial_0\phi_1)\phi_2^*) \quad . \tag{3.65}$$

For the generalization of eq. (3.65) to the case with curved spacetime background (3.60) one has to redefine the meaning of ∂_0 first. This is done by defining a space-like hypersurface Σ with a volume element $\mathrm{d}\Sigma$ and a future-directed unit vector n^μ orthogonal to Σ. With the induced metric g_Σ on the hypersurface eq. (3.65) is generalized to

$$(\phi_1,\phi_2)=-i\int_\Sigma \mathrm{d}\Sigma\, \mathrm{n^\mu}((\partial_\mu\phi_2^*)\phi_1-(\partial_\mu\phi_1)\phi_2^*)\sqrt{-\mathrm{g_\Sigma(x)}} \quad . \tag{3.66}$$

The value of $(\phi_1,\ \phi_2)$ does not depend on the actual choice of Σ (at least as long it is a Cauchy surface on a globally hyperbolic spacetime [18]).
There also exists a complete set of mode solutions $u_i(x)$ of the equation of motion that come with the Lagrangian (3.60) which are orthonormal in the products (3.65)

$$(u_i,\ u_j)=\delta_{ij},\quad (u_i^*,\ u_j^*)=-\delta_{ij},\ \text{and}\ \ (u_i,\ u_j^*)=0 \quad . \tag{3.67}$$

Therefore, an arbitrary field $\phi(x)$ can be expanded in a coordinate system C into those modes

$$\phi(x)=\sum_i\left[a_iu_i(x)+a_i^\dagger u_i^*(x)\right] \quad . \tag{3.68}$$

The index i represents schematically the set of all indices that are necessary to label the modes $u_i(x)$. Remember that in the case of a flat spacetime the $u_i(x)$ are simply plane waves labeled by the three-dimensional momentum vector $i\leftrightarrow\boldsymbol{k}$

$$u_{(KG)\,\boldsymbol{k}}=\frac{\exp(i\boldsymbol{kx}-i\omega t)}{\sqrt{2\omega(2\pi)^3}} \quad . \tag{3.69}$$

This theory is covariantlely quantized introducing the equal time commutation relations [1] in momentum space

$$\begin{array}{rcl} [\, a_i,\, a_j \,] & = & 0 \quad , \\ [\, a_i,\, a_j^\dagger \,] & = & \delta_{ij} \quad , \\ [\, a_i^\dagger,\, a_j^\dagger \,] & = & 0 \quad . \end{array} \tag{3.70}$$

The vacuum for the creation and annihilation operators is definded as

$$a_i^\dagger \,|0\rangle = |a_i\rangle \;\; , \quad a_i \,|0\rangle = 0 \;\; \forall i \quad . \tag{3.71}$$

The eigenmodes in Minkowski space (3.68) are uniquely determined from the Lagrangian (3.61). However, in curved spacetime this is not the case, since a different choice of coordinate system $\bar{C}$ with the metric $\bar{g}_{\mu\nu}$ might as well mean that there is a different set of eigenmodes $\bar{u}_i$ corresponding to this specific coordinate system. The field ϕ may then be as well expanded in this new set of eigenmodes $\{\bar{u}_i\}$ with the coefficients $\bar{a}_i$ and $\bar{a}_i^\dagger$

$$\phi(x) = \sum_i \left[\bar{a}_i \bar{u}_i(x) + \bar{a}_i^\dagger \bar{u}_i^*(x) \right] \quad . \tag{3.72}$$

Both decompositions (3.68) and (3.72) are supposed to describe the same physical state, but the new modes define a new Fock space with a new vacuum state $|\bar{0}\rangle$ by

$$\bar{a}_i^\dagger \,|\bar{0}\rangle = |\bar{a}_i\rangle \;\; , \quad \bar{a}_i \,|\bar{0}\rangle = 0 \;\; \forall i \quad . \tag{3.73}$$

As both sets ($\bar{u}_i^\dagger$ and $u_i^\dagger$) are complete they can be expanded each with the other

$$\begin{array}{rcl} \bar{u}_j & = & \sum\limits_i (\alpha_{ji} u_i + \beta_{ji} u_i^*) \;\; \text{and} \\ u_i & = & \sum\limits_j (\gamma_{ij} \bar{u}_j + \tau_{ij} \bar{u}_j^*) \quad . \end{array} \tag{3.74}$$

The coefficient matrices can be evaluated from the scalar product (3.66)

$$\begin{array}{lll} \alpha_{ij} = (\bar{u}_i,\, u_j) \quad , & \beta_{ij} = (\bar{u}_i,\, u_j^*) \\ \gamma_{ji} = (\bar{u}_j^*,\, u_i^*) \quad , & \tau_{ji} = -(\bar{u}_j,\, u_i^*) \quad , \end{array} \tag{3.75}$$

which leads to relations known as **Bogolubov transformations**

$$\begin{array}{rcl} \bar{u}_j & = & \sum\limits_i (\alpha_{ji} u_i + \beta_{ji} u_i^*) \;\; \text{and} \\ u_i & = & \sum\limits_j (\alpha_{ij}^* \bar{u}_j - \beta_{ij} \bar{u}_j^*) \quad . \end{array} \tag{3.76}$$

[1] In curved spacetime the expression "equal time" can be given a meaning by the definition of hyper surfaces Σ. If such a hyper surface is crossed by any time-like curve exactly once it is called a **Cauchy hyper surface**. Unfortunately this is not always the case, which aggravates the quantization procedure.

Analogous relations can be derived for the annihilation (and creation) operators in both coordinate systems

$$\begin{aligned} a_i &= \sum_j (\alpha_{ji}\bar{a}_j + \beta_{ji}\bar{a}_j^\dagger) \text{ and} \\ \bar{a}_j &= \sum_i (\alpha_{ji}^* a_i - \beta_{ji}^* a_i^\dagger) \quad . \end{aligned} \tag{3.77}$$

From the orthonormality relations one can see that the **Bogolubov coefficients** ($\alpha,\ \beta$) possess the following properties

$$\begin{aligned} \sum_k (\alpha_{ik}\alpha_{jk}^* - \beta_{ik}\beta_{kj}^*) &= \delta_{ij} \\ \sum_k (\alpha_{ik}\beta_{jk} - \beta_{ik}\alpha_{jk}) &= 0 \quad . \end{aligned} \tag{3.78}$$

These simple transformation properties have the dramatic consequence that observers in two different coordinate systems (for example in systems that are accelerated with respect to each other) do not agree on their definition a field theoretical vacuum. This can be seen when an observer in the coordinate system C applies his particle number operator $N_i = a_i^\dagger a_i$ on the vacuum of his college in the system $\bar{C}$

$$\begin{aligned} \langle\bar{0}|\, N_i\, |\bar{0}\rangle &= \langle\bar{0}|\, a_i^\dagger a_i\, |\bar{0}\rangle \\ &= \langle\bar{0}|\, a_i^\dagger \sum_j (\alpha_{ji}\bar{a}_j + \beta_{ji}\bar{a}_j^\dagger)\, |\bar{0}\rangle \\ &= \sum_j \langle 0|\, |\beta_{ji}|^2\, |0\rangle \neq 0\,! \end{aligned} \tag{3.79}$$

It means that the vacuum of observer $\bar{C}$ contains $\sum_j |\beta_{ji}|^2$ particles in the u_i mode as seen from observer C. Note that the coefficients β are zero as soon as $\bar{u}_j$ are linear combinations of the positive frequency modes u_i alone (not u_i^*) and therefore such two coordinate systems ($C,\ \bar{C}$) share the same vacuum states. The most prominent cases, where the observers do not agree an their definition of vacuum states were discovered by William Unruh and Stephen Hawking.

3.4.2 Unruh effect

In 1976, William Unruh pointed out that a permanently accelerated observer should, according to the described straight forward approach of quantum fields in curved spacetime, measure a thermal radiation from the surrounding Minkowski vacuum [19]. For finding this effect the vacua of two different observers C and $\bar{C}$ are studied. The observer $\bar{C}$ is assumed to move with

constant acceleration in the direction x through a flat spacetime. According to the principle of equivalence one expects to draw conclusions from this setup about the curvature in the equivalent scenario, where $\bar{C}$ is freely falling in a curved spacetime. The problem is now to find adequate **coordinates**, **eigenmodes** and **Bogolubov coefficients** for $\bar{C}$. On this way it is useful to note that in a rectangular coordinate system, the two other spacial coordinates y ad z are not altered in this setup and therefore will be neglected in the following discussion.

- Rindler coordinates:

To the observer C in a flat Lorentz frame with the coordinates t and x, his college with the coordinates $\bar{t}$ and $\bar{x}$ will not appear to be constantly accelerated, the more their respective velocity approaches the velocity of light c the less will $\bar{C}$ appear to be accelerated. Therefore, $\bar{C}$ who has the velocity of almost minus c in the past will appear to be more and more rapidly decelerated until he stands still for an instance before his less and less strong acceleration makes him approach the velocity plus c as shown in figure (3.2). In the Rindler coordinates $\bar{C}$ the spatial origin describes a movement of a constantly accelerated point as seen from the Minkowski coordinates. They are related to the Minowski coordinates according to

$$t = \frac{\bar{x}}{g}\sinh(g\bar{t}), \quad x = \frac{\bar{x}}{g}\cosh g\bar{t} \quad , \tag{3.80}$$

where g is a positive constant. The velocity $v(\bar{t})$ of the observer $\bar{C}$ who is sitting on a fixed point (for instance $\bar{x} = 1$) of his accelerated coordinate system, as measured by C will then be

$$v(\bar{t}) = \frac{\triangle x}{\triangle t}(\bar{t}) = \lim_{\delta\to 0}\frac{\cosh(g\bar{t}) - \cosh(g(\bar{t}-\delta))}{\sinh(g\bar{t}) - \sinh(g(\bar{t}-\delta))} = \tanh(g\bar{t}) \quad . \tag{3.81}$$

The acceleration $a(\bar{t})$ of the observer $\bar{C}$ who is sitting on a fixed point of his accelerated coordinate system, as measured by C will then be

$$a(\bar{t}) = \frac{\triangle v}{\triangle t}(\bar{t}) = \lim_{\delta\to 0} g\frac{\tanh(g\bar{t}) - \tanh(g(\bar{t}-\delta))}{\sinh(g\bar{t}) - \sinh(g(\bar{t}-\delta))} = g\frac{1}{\cosh(\bar{t})} \quad . \tag{3.82}$$

At the time $\bar{t} = 0$ the acceleration is therefore $a(\bar{t} = 0) = g$ and the positive constant g can therefore be interpreted as the maximal acceleration that can be measured by the observer C.
As $\bar{x}$ is constant, the equations (3.81, 3.82) do still hold, even if we would replace $\bar{x}$ in eq. (3.80) by any smooth function $f(\bar{x})$. This means that we

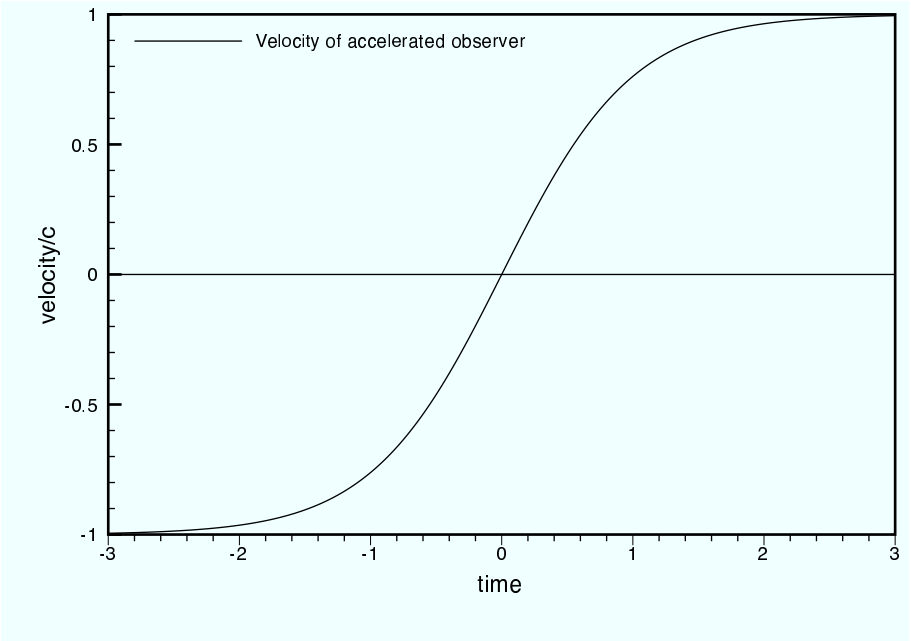

Figure 3.2: Velocity of an steadily accelerated observer $\bar{C}$, as seen from a resting observer C.

have determined the desired coordinate system by the generalized Rindler transformation

$$t = \frac{f(\bar{x})}{g}\sinh(g\bar{t}), \quad x = \frac{f(\bar{x})}{g}\cosh g\bar{t} \quad . \tag{3.83}$$

- Wave equation for observer in Rindler coordinates:

The metric of flat spacetime C induces the metric of the coordinate system $\bar{C}$ as given in eq. (3.83)

$$\bar{g}_{ab} = \begin{pmatrix} f^2 & 0 \\ 0 & -\frac{f'^2}{g^2} \end{pmatrix} \quad , \tag{3.84}$$

where $f' = \partial_{\bar{x}} f$. In these coordinates the kinetic term of the Lagrangian (3.61) for a complex scalar field ϕ is

$$\begin{aligned} \mathcal{L}_{kin} &= \frac{g}{2ff'}\phi^* \left(\partial_{\bar{t}} \frac{f'}{fg} \partial_{\bar{t}} - \partial_{\bar{x}} \frac{fg}{f'} \partial_{\bar{x}} \right) \phi \\ &= \frac{1}{2}\phi^* \left(\frac{1}{f^2}\partial_{\bar{t}}^2 - \frac{g^2}{ff'}(\partial_{\bar{x}} \frac{f}{f'})\partial_{\bar{x}} - \frac{g^2}{f'^2}\partial_{\bar{x}}^2 \right) \phi \quad . \end{aligned} \tag{3.85}$$

As we want to have harmonic solutions with positive energy modes to the resulting equations of motion we demand that the non harmonic term in eq. (3.85) vanishes and find

$$\partial_{\bar{x}}(\frac{f}{f'}) = 0 \text{ and therefore } f = \exp(k\bar{x}) \quad , \tag{3.86}$$

where k is an arbitrary constant. If we now plug the solution (3.86) into the Lagranian and choose $k = g$ we find

$$\mathcal{L}_{kin} = \frac{1}{2f^2}\phi^* \left(\partial_{\bar{t}}^2 - \partial_{\bar{x}}^2\right)\phi \quad . \tag{3.87}$$

The positive mode solutions for this Lagrangian on the hyperplane I:$\{\bar{x} > 0\}$ are

$${}^{I}v_k = \frac{1}{\sqrt{4\pi\omega}} e^{i(-\omega\bar{t}+k\bar{x})} \quad . \tag{3.88}$$

Now its time to remember that the second Rindler transformation (3.83) covers only the Minkowski wedge $|x| > |t| \Leftrightarrow \bar{x} > 0$ and therefore one has different positive mode solutions in the hyperplane $II : \{\bar{x} < 0\}$,

$${}^{II}v_k = \frac{1}{\sqrt{4\pi\omega}} e^{i(\omega\bar{t}+k\bar{x})} . \tag{3.89}$$

As the two spacetime sectors I and II are causally disconnected the solution (3.88) is zero in the sector II and the solution (3.89) is zero in the sector I. Those modes form a complete Fock space and it is possible to express a Minkowski mode of C in terms of the modes (3.88, 3.89)

$$u_k = \int \mathrm{dm} \left({}^{\mathrm{I}}\alpha_{\mathrm{km}}\ {}^{\mathrm{I}}\mathrm{v}_{\mathrm{m}} + {}^{\mathrm{II}}\alpha_{\mathrm{km}}\ {}^{\mathrm{II}}\mathrm{v}_{\mathrm{m}} + {}^{\mathrm{I}}\beta_{\mathrm{km}}\ {}^{\mathrm{I}}\mathrm{v}^*_{\mathrm{m}} + {}^{\mathrm{II}}\beta_{\mathrm{km}}\ {}^{\mathrm{II}}\mathrm{v}^*_{\mathrm{m}}\right) \quad . \tag{3.90}$$

The vacuum of the Minkowsi space shall be denoted as $|0_C\rangle$ and the vacuum of the future directed Rindlerspace as $\left|{}^{I}0_{\bar{C}}\right\rangle$.

- Bogolubov coefficients in Rindler coordinates and particle creation:

According to eq. (3.79) the difference of the two vacuum states of C and $\bar{C}$ is proportional to the square of their Bogolubov coefficient β. The particle content in the state i in the Rindler system $\bar{C}$, will not be zero when $\bar{C}$ tries to measure the Minkowski vacuum $\left|{}^{I}0_C\right\rangle$,

$$\left\langle {}^{I}0_C\right| \bar{a}_i^\dagger \bar{a}_i \left|{}^{I}0_C\right\rangle = \sum_j \left|{}^{I}\beta_{ij}\right|^2 \quad . \tag{3.91}$$

The β coefficient can be found from definiton (3.75) and (3.66) with the harmonic states (the analog to eq. 3.69 with only one spatial dimension) and (3.88)

$$\begin{aligned} {}^{I}\beta_{km} &= (u_k,\ {}^{I}v_m^*) \\ &= -i\int \mathrm{d}\Sigma\ {}^{-g_\Sigma}\sqrt{n}^{\mu}\left[(\partial_\mu\ {}^{\mathrm{I}}\mathrm{v_m})\mathrm{u_k} - (\partial_\mu \mathrm{u_k})\ {}^{\mathrm{I}}\mathrm{v_m}\right] \end{aligned} \tag{3.92}$$

The evaluation of this is a rather lengthy procedure which, was therefore put into appendix (B.4). One finds for the Bogolubov coefficients of mass-less modes

$${}^{I}\beta_{\omega\bar{\omega}} = \frac{-i}{2\pi g}\sqrt{\frac{\bar{\omega}}{\omega}}e^{\frac{-\bar{\omega}\pi}{2g}}\Gamma(\frac{-i\bar{\omega}}{g})\left(\frac{\omega}{g}\right)^{i\bar{\omega}/g} \quad . \tag{3.93}$$

By using the relation

$$\left|\Gamma(\frac{-i\bar{\omega}}{g})\right|^2 = \frac{\pi g}{\omega\sinh(\pi\frac{\bar{\omega}}{g})} \quad , \tag{3.94}$$

one finds for the squared of the Bogolubov coefficient

$$\left|{}^{I}\beta_{\omega\bar{\omega}}\right|^2 = \frac{1}{2\pi g\omega}\frac{1}{\exp(\frac{2\pi\bar{\omega}}{g})-1} \quad . \tag{3.95}$$

Therefore, the Rindler observer measures the Minkowski vacuum as

$$\left\langle {}^{I}0_{\bar{C}}\right| \bar{a}_{\bar{\omega}}^{\dagger}\bar{a}_{\bar{\omega}} \left|{}^{I}0_{\bar{C}}\right\rangle = \sum_{\omega}\frac{1}{2\pi g\omega}\frac{1}{\exp(\frac{2\pi\bar{\omega}}{g})-1} = A\ \frac{1}{\exp(\frac{2\pi\bar{\omega}}{g})-1} \quad , \tag{3.96}$$

where A is a (logarithmically diverging) constant, which comes from the summation (integration) over all ω states. The fact that A is infinite can be understood by noting that the Rindler observer was assumed to continue his acceleration for all times, and the steady flux of radiation will accumulate an infinite number of quanta per mode. This problem can be cured by a different normalization definition for the Rindler vacuum solutions (3.88, 3.89) as finite wave packets rather than plane wave modes and by considering the number of quanta per $\mathrm{d}\omega$ per unit time. Leaving this subtlety aside one can see that eq. (3.96) provides an exact Planck spectrum for the radiation observed by a constantly accelerated observer $\bar{C}$. The temperature of this spectrum (T) is directly proportional to the acceleration g

$$T = \frac{g}{2\pi k_B} \quad . \tag{3.97}$$

3.4.3 Hawking effect

In 1975, S.W. Hawking showed that quantum effects in the vicinity of a black hole lead to thermal radiation [20, 21, 22]. Like in the previous section the aim is to compare two different vacuum states. The physical setup will be a star that at a certain time collapses into a black hole. For this setup one tries to compare vacuum solutions of the star, that come from the infinite Past $\mathcal{J}_-$ to vacuum solutions of the (stable) black hole, that end up in the infinite future $\mathcal{J}_+$. Therefore, we consider a spherical symmetric matter distribution, which has the radius R_0 at $t = 0$ and then collapses into a black hole. In the outside region we will work in coordinates r^* that respect the redshift of due to the gravitating mass

$$\begin{aligned} r^* &= \int_{R_0}^{r_{max}} \frac{1}{C(r)} \mathrm{d}r \\ R_0^* &= \int \frac{1}{C(r)} \mathrm{d}r \quad . \end{aligned} \tag{3.98}$$

For a static and spherical symmetric mass distribution the function $C(r)$ would be given from the outer Scharzschild solution $\frac{1}{1-2MG/r}$. In the outside region one uses the redshifted radii for the definition of light cone coordinates

$$\begin{aligned} u &= t - r^* + R_0^* \quad , \\ u &= t + r^* - R_0^* \quad , \end{aligned} \tag{3.99}$$

with the induced metric

$$\mathrm{d}s^2 = C(r)\mathrm{d}u\mathrm{d}v \quad . \tag{3.100}$$

As the metric in eq. (3.58) seems to diverge at the Schwarzschild radius, we have to find different coordinates at this region and make the ansatz

$$\mathrm{ds}^2 = \mathrm{A(U,\ V)dUdV} \quad , \tag{3.101}$$

where

$$U = \tau - r + R_0 \ \text{ and } \ V = \tau + r - R_0 \tag{3.102}$$

are again light cone coordinates, τ is a time-like coordinate, and $A(U, V)$ as a arbitrary function which is still to determine. For a continuous description we have to match the inside coordinates $(U,\ V)$ to the outside coordinates $(u,\ v)$, which can only be done in the outside region as the metric of $(u,\ v)$ is nonsingular there. Because of this we have to find the matching functions α and β which provide the transformation

$$U = \alpha(u,\ v)\ , \ \ V = \beta(u,\ v) \quad . \tag{3.103}$$

Let the surface of the star run on the world line $R(\tau)$ and the coordinate origin be chosen in such a way that the collapse starts at $t = \tau = 0 = U = V = u = v$.
The original $|0_-\rangle$ vacuum is defined in such a way that it does not contain any particles in the origin of any light-like curve $\mathcal{J}_-$. For finding a solution of the Klein Gordon equation (3.85) in this asymptotic region we remember that for reasons of normalizability the amplitude of the wave function should decay at least with a factor $r^{-1}$and make the ansatz

$$\phi(x,t) \sim \frac{1}{r}\psi_l(r,t)Y_{lm}(\theta\phi) \quad , \tag{3.104}$$

where Y_{lm} are the spherical harmonic functions. With this ansatz the radial part has to fulfill the differential equation

$$\frac{\partial^2\psi_l(r,t)}{\partial u\partial v} = (1-\frac{2M}{r})\left(\frac{2M}{r^3}+\frac{l(l+1)}{r^2}\right)\psi_l(r,t) \quad . \tag{3.105}$$

Expressed in the coordinates $(t,\ r^*)$ this is

$$\left(\frac{\partial^2}{\partial t\partial t}-\frac{\partial^2}{\partial r^*\partial r^*}\right)\psi_l(r,t) = (1-\frac{2M}{r})\left(\frac{2M}{r^3}+\frac{l(l+1)}{r^2}\right)\psi_l(r,t) \quad . \tag{3.106}$$

This is a wave equation with a potential term on the right side. The potential has a maximum outside of the Scharzschild radius (e.g. for $l = 0$ at $r = \frac{8M}{3}$), which can lead to partial back scattering of modes that come from $\mathcal{J}_-$. By further taking an harmonic ansatz $\psi_l(r,t) \sim \psi_l(r)e^{i\omega' t}$ one finds in terms of r^*

$$\frac{\partial^2\psi_l(r)}{\partial r^*\partial r^*} = \left\{(1-\frac{2M}{r})\left(\frac{2M}{r^3}+\frac{l(l+1)}{r^2}\right)-\omega'^2\right\}\psi_l(r) \quad . \tag{3.107}$$

As long as one restricts to measurements in the asymptotic region ($r \to \infty$), it is not necessary to solve this equation. The potential drops off sufficiently rapid in the outside region and therefore the solutions of the free wave equations are

$$\frac{\partial^2\psi_l(r,t)}{\partial u\partial v} = 0, \text{ and } \frac{\partial^2\psi_l(r,t)}{\partial U\partial V} = 0 \quad . \tag{3.108}$$

For purely spherical waves ($l = 0$) the solution to the second equation is

$$\psi(r,t) \sim e^{i\omega V} - Be^{i\omega U} \quad , \tag{3.109}$$

where B is some constant. For an incoming wave of constant V we know that it will turn into an outgoing wave of constant U as soon as it reaches

the center (r=0) of the (non collapsed) star. This is achieved by imposing the boundary condition

$$\psi(0,t) = 0 \;\Rightarrow\; B = e^{i\omega(V-U)}\big|_{r=0} \quad . \tag{3.110}$$

By taking the definition of U and V at $r = 0$ one finds

$$V = U - 2R_0 \quad , \tag{3.111}$$

and therefore

$$\psi(r,t) \sim e^{i\omega V} - e^{i\omega(U-2R_0)} \quad . \tag{3.112}$$

Lets follow the trace of a single wave: A wave that starts at $\mathcal{J}_-$ will be described best by $\psi(v)$ the closer it propagates to R_0 the more it is adequately described in terms of (V): $\psi(V)$. At the origin this will, according to (3.112), turn into a $\psi(U)$, which is finally best described as a function of (u): $\psi(u)$. Unfortunately the connection functionals that are needed for this procedure are not known and therefore a closer look at the matching between the two coordinate systems $(u,\ v)$ and $(U,\ V)$ on the star′s surface is necessary: On the star′s surface $(r = R(\tau))$ there is

$$\begin{aligned}
\mathrm{dr} &= \partial_\tau R \mathrm{d}\tau \quad , \\
\mathrm{dr}^* &= \tfrac{1}{1-2M/r}\mathrm{dr} \quad , \\
\mathrm{dU} &= (1 - \partial_\tau R)\mathrm{d}\tau \quad , \\
\mathrm{dV} &= (1 + \partial_\tau R)\mathrm{d}\tau \quad , \\
\mathrm{du} &= \mathrm{d}\tau - \tfrac{\partial_\tau \mathrm{R}}{1-2\mathrm{M/r}}\mathrm{d}\tau \text{ and} \\
\mathrm{dv} &= \mathrm{d}\tau - \tfrac{\partial_\tau \mathrm{R}}{1-2\mathrm{M/r}}\mathrm{d}\tau \quad .
\end{aligned} \tag{3.113}$$

Plugging this into the definitions of the two metrics one finds on the curve $r = R(\tau)$

$$\mathrm{dt} = \mathrm{d}\tau \left(\frac{\mathrm{A}}{1-2\mathrm{M/r}} (1 - (\partial_\tau \mathrm{R})^2) \left(\frac{\partial_\tau \mathrm{R}}{1-2\mathrm{M/r}} \right)^2 \right)^{\frac{1}{2}} \quad . \tag{3.114}$$

From this the derivatives of the coordinate transformations (3.103) are found:

$$\begin{aligned}
\tfrac{\mathrm{dU}}{\mathrm{du}} &= \tfrac{1-\partial_\tau R}{(1-2M/r)(A(1-2M/r)(1-(\partial_\tau R)^2)+(\partial_\tau R)^2)^{\frac{1}{2}}-\partial_\tau R} \quad , \\
\tfrac{\partial U}{\partial v} &= 0 \quad , \\
\tfrac{\mathrm{dV}}{\mathrm{dv}} &= \tfrac{1+\partial_\tau R}{(1-2M/r)(A(1-2M/r)(1-(\partial_\tau R)^2)+(\partial_\tau R)^2)^{\frac{1}{2}}+\partial_\tau R} \quad , \\
\tfrac{\partial V}{\partial u} &= 0 \quad .
\end{aligned} \tag{3.115}$$

A first order taylor series around the point $(1-2M/r=0)$ simplifies eq. (3.115) to

$$\begin{array}{ll} \frac{\mathrm{dU}}{\mathrm{du}} & = \frac{\partial_\tau R-1}{2\partial_\tau R}(1-2M/r) \\ \frac{\mathrm{dv}}{\mathrm{dV}} & = \frac{A(1-\partial_\tau R)}{2\partial_\tau R} \end{array} \quad . \tag{3.116}$$

At the time τ_h the star′s radius will drop below it′s Schwarzschild radius $(R(\tau_h)=R_h)$. The surface velocity at this point shall be $\partial_\tau R(\tau)|_{\tau_h} = -\nu$ and so

$$R(\tau) = R_h\nu(\tau_h-\tau) + \mathcal{O}(\tau_h-\tau)^2 + \ldots \quad . \tag{3.117}$$

With the approximate expressions

$$\begin{array}{rl} \left(1-\frac{2M}{R}\right) & = 2\kappa(R(\tau)-R_h) + \mathcal{O}(\tau_h-\tau)^2 \ , \ \ 2\kappa = \partial_R\left(1-\frac{2M}{R}\right)\big|_{r=R_h} \\ U & = \tau_h - R_h - (\nu+1)(\tau_h-\tau) + R_0 \end{array} \tag{3.118}$$

the approximate differential equation (3.116) simplifies to

$$-\kappa\frac{\mathrm{du}}{\mathrm{dU}} = \frac{1}{U+R_h-\tau_h-R_0} \quad . \tag{3.119}$$

The solution to this is

$$-\kappa u = -\ln|U+R_h-R_0-\tau_0| + \text{ constant} \quad , \tag{3.120}$$

or the inverted relation

$$U \propto e^{-\kappa u} + \text{constant} \quad . \tag{3.121}$$

At the formation of the horizon the solution (3.120) shows that

$$\lim_{U\to\tau_h+R_0-R_h} u = +\infty \quad . \tag{3.122}$$

The distance Δ_u for two different outgoing rays $(u_1 = u+\frac{\Delta_u}{2},\ u_2 = u-\frac{\Delta_u}{2})$ will be much smaller than, the distance Δ_U between the corresponding $(U_1 = U+\frac{\Delta_U}{2},\ U_1 = U-\frac{\Delta_U}{2})$, especially for large u, as $\lim\limits_{u\to\infty}\frac{\Delta_U}{\Delta_u} = 0$. Also the corresponding $(V_1,\ V_2)$ obey $\lim\limits_{u\to\infty}\frac{\Delta_V}{\Delta_u} = 0$. As for $\gamma \approx 0$ and $\frac{\mathrm{dA}}{\mathrm{dV}} \approx 0$

$$v \approx -A\frac{1+\nu}{2\nu}V + \text{const.} \quad , \tag{3.123}$$

one finds the same behavior for the incoming rays $v\ \lim\limits_{u\to\infty}\frac{\Delta_v}{\Delta_u} = 0$. There is a last ray, v_l, that can escape (exponentially red shifted) from the event horizon and all possible observable rays in the future will have to come (mostly quite close) from before this ray. This causes a different density of rays in the

future than in the past.
Now all transformations are available to trace an initial ray

$$\phi(v) \sim e^{-\omega v} \tag{3.124}$$

that starts from $\mathcal{J}_-$. With the help of the equations (3.123, 3.112) and (3.122) it can be followed via V, U to u at $\mathcal{J}_+$. At $\mathcal{J}_+$ one finds for this ray

$$\phi(u) \sim e^{i\omega(ce^{-\kappa u}+d)} \quad , \tag{3.125}$$

where c and d are constants which depend on A, ν, κ, R_0, ω and R_h. This is true for $v < v_l$, but for $v > v_l$ the rays are lost behind the horizon and can not be detected at $\mathcal{J}_+$.
For finding the Bogolubov coefficients for this setup, one has to calculate the vacuum expectation value of $e^{i\omega' u}$ modes and the modes from (3.125), which are both defined at the hypersurface $\mathcal{J}_+$. Fortunately the integrals that appear in this calculation have mostly been done in the previous subsection. Since the solutions in Rindler coordinates (3.82) have the same exponential form compared to free Minkowski solutions as the $e^{i\omega' u}$ solutions have compared to (3.125).
Proceeding the analogous steps as for the Unruh case one finds that an observer sitting at $\mathcal{J}_+$ beside a black hole and that measures the vacuum $\left|{}^I 0_-\right\rangle$ of the time before the black hole was formed $\mathcal{J}_-$, will be surprised by

$$N_\omega = \langle 0_-| \, a_\omega^\dagger a_\omega \, |0_-\rangle = \mathrm{A}_\infty \, \frac{1}{\exp(\frac{2\pi\omega}{\kappa}) - 1}. \tag{3.126}$$

Like in the Unruh case, the overall constant A_∞ is divergent, which is natural, as already the underlying plane wave solutions are not normalizable. Leaving this aside the observer of the late collapse stadium of a black hole at $\mathcal{J}_+$ sees a Planck distributed black body radiation with the temperature

$$T = \frac{\kappa}{2\pi k_B} \quad , \tag{3.127}$$

where k_B is the Boltzmann constant. For very massive black holes of mass M this temperature is quite small

$$T = \frac{\hbar c^3 M_P^2}{8\pi M k_B} \approx 10^{-6} \frac{M_\odot}{M} \mathrm{K} \quad , \tag{3.128}$$

where $M_\odot$ stands for the solar mass. The Hawking temperature is important for our later studies and therefore one should note at this point that the approximations made here, do not hold any more as soon the temperature becomes comparable to the mass of the black hole.

3.5 Limitations of the theory of general relativity

The physics of fundamental particles, excited particle states, or microscopical bound states, such as the hydrogen atom, can only be described in the language of a quantum theory. General relativity, as a classical theory, can not address this regime of physical phenomena in general and already semi classical approaches as described in the previous section become difficult.
On the other side GR is the theory of space and time and, therefore, has to be an ingredient of any fundamental theory. Unfortunately it turns out to be challenging to rephrase GR consistently and predictive in the language of quantum theories. As it has been shown in the previous section, already the formulation of a quantum theory on a purely classical and exactly solvable gravitational background is rather difficult. The problem becomes even worse, as soon as quantum fluctuations of gravitational fields are taken into account.
We conclude that the consistent and predictive rephrasing of GR in the language of quantum theories can be considered a crucial step in the search for a fundamental theory of all forces.

Chapter 4

Basics of physics with extra dimensions

It is an unwritten law of theoretical physics that the more a theory is believed to be "fundamental" the higher is the level of abstraction at which this theory is formulated. High level of abstraction again leads to low level of comprehensibility or intuitiveness (at least according to "common" sense). To the authors opinion the high interest in physics with extra dimensions partially originates from the fact that this kind of physics promises new understanding without the introduction of a new extremely abstract formalism. Of course one has to admit that physics with extra dimensions introduces extra dimensions, but this is purely geometry and therefore formulated in a language which is already well known and intuitive.

4.1 Kaluza-Klein theory

One of the most remarkable attempts was suggested in 1921 by Theodor Kaluza [23]. In its original ansatz Kaluza extended the four-dimensional metric $g_{\mu\nu}$ to a five-dimensional one $\hat{g}_{NJ}$ by introducing one aditional component and choosing

$$\hat{g}_{NJ} = e^{\phi/\sqrt{3}} \begin{pmatrix} g_{\mu\nu} + e^{-\sqrt{3}\phi} A_\mu A_\nu & e^{-\sqrt{3}\phi} A_\nu \\ e^{-\sqrt{3}\phi} A_\mu & e^{-\sqrt{3}\phi} \end{pmatrix} \tag{4.1}$$

as the ansatz for the higher-dimensional metric, where the capital indices $N,\ J$ run from one to four and the $\hat{}$ marks the higher-dimensional objects. The spin 0 dilaton field ϕ is defined differently throughout literature [24, 25, 26, 27] and was originally (and inconsistently) set to zero by Kaluza and Klein. The classical equations of motion for this metric are the analog of

Einstein's equations (3.1) generalized for one extra coordinate eq. (4.9). One obtains three separate systems of equations

$$R_{\mu\nu} - \frac{1}{2} g_{\mu\nu} R = -8\pi G T_{\mu\nu} \quad , \tag{4.2}$$

where the energy momentum tensor is defined as $T_{\mu\nu} = \frac{1}{4} e^{-\sqrt{3}\phi} F_{\mu\rho} F^{\rho}_{\nu} + \frac{\partial_\mu \phi \partial_\nu \phi}{2}$,

$$\partial_\mu (\partial^\nu A^\mu - \partial^\mu A^\nu) = 0 \tag{4.3}$$

and

$$\partial_\mu \partial^\mu \phi = \frac{-\sqrt{3}}{4} e^{-\sqrt{3}\phi} F_{\mu\nu} F^{\mu\nu} \quad . \tag{4.4}$$

The first system of equations is the four-dimensional form of Einstein's equations (3.1), the second is Maxwell's equations and the third is the relativistic equation for a scalar field, which lacks compelling interpretation. The second system of equations shows that Maxwell's electromagnetism is an inevitable consequence of this ansatz. Despite this astonishing results, Kaluzas idea suffered from obvious drawbacks. It could not give a good reasoning why the fields A_μ and ϕ should only depend on the $3+1$ dimensions and closely related to this, why the fifth dimension was not visible at all. In 1926, Oskar Klein solved those problems [28, 29]. He assumed the fifth dimension to have circular (S^1) topology by imposing the periodic boundary conditions $0 \leq \frac{y}{R} \leq 2\pi$ on the fifth coordinate y. Thus the spacial coordinates have a $R^3 + S^1$ topology. He could resolve the problem of the invisibility of the fifth dimension. In his setup, as soon as the compactification Radius R is small enough, the S^1 topology which is attached to every single point of our three-dimensional space, can not be resolved by our measurements and therefore the y coordinate is invisible to us. The questions why the fields A_μ are only depending on the $3+1$-dimensional x coordinate can be resolved in this setup as well. To see this it is useful to consider Kleins proposal from the "modern" perspective of Lagrangians.

The action of pure gravity in five dimensions is

$$\mathcal{S} \sim \int d^5\hat{x} \sqrt{-\hat{g}} \hat{R} \quad . \tag{4.5}$$

The ansatz for the five-dimensional metric $\hat{g}$ is exactly the same as in (4.1), just that the fields A_μ, ϕ and $g_{\mu\nu}$ are allowed to have y dependence as well. Due to the periodicity in y one may expand $A_\mu(x,y)$, $\phi(x,y)$ and $g_{\mu\nu}(x,y)$

in a Fourier series

$$\begin{aligned} g_{\mu\nu}(x,y) &= \sum_{n=-\infty}^{n=\infty} g_{\mu\nu\,n}(x) e^{in\frac{y}{R}} \quad , \\ A_{\mu}(x,y) &= \sum_{n=-\infty}^{n=\infty} A_{\mu\,n}(x) e^{in\frac{y}{R}} \quad , \\ \phi(x,y) &= \sum_{n=-\infty}^{n=\infty} \phi_n(x) e^{in\frac{y}{R}} \end{aligned} \tag{4.6}$$

with

$$g^*_{\mu\nu\,n}(x) = g_{\mu\nu\,-n}(x) \tag{4.7}$$

etc. Thus the Kaluza-Klein theory describes an infinite number of four-dimensional fields. The $n = 0$ modes $A_{\mu\,0}(x)$, $\phi_{\,0}(x)$ and $g_{\mu\nu\,0}(x)$ are just Kaluzas graviton, photon and dilaton. Substituting eq. (4.1) and eq. (4.6) into the action (4.5) integrating over y and retaining just the $n = 0$ one obtains

$$S \sim \int d^4x \sqrt{-g_0} \left[R_0 - \frac{1}{2}\partial_\mu\phi_0\partial^\mu\phi_0 - \frac{1}{4}e^{\sqrt{3}\phi_0} F_{\mu\nu}F^{\mu\nu} \right] \quad , \tag{4.8}$$

where $F_{\mu\nu} = \partial_\mu A_{\nu\,0} - \partial_\nu A_{\mu\,0}$. Considering the $n \neq 0$ modes, any derivative with respect to y results in an extra factor $\frac{n}{R}$. In a quantized version of this field theory such terms have to be interpreted as apparent mass terms in the effective four-dimensional Lagrangian (4.8). For small R those fields are therefore suppressed by factors of $\frac{n}{R}$, which explains, why in a low energy approximation only the $n = 0$ modes dominate. The amazing thing here is that the topological S^1 symmetry in the fifth coordinate could be integrated out of the five-dimensional Lagrangian to give electromagnetism which is the classical theory of local $U(1)$ gauge symmetry. It can be shown that this is not just coincidence, but also works for arbitrary gauge groups [27], although it is difficult to include fermions into this model [30]. This theory leaves the question of a consistent quantization of gravity unanswered, but still branches of this old idea live on in very popular attempts to reduce D-dimensional supergravity (the point limit of some string theory) down to effective four-dimensional field theories [31, 32].

4.2 Compactiefied extra dimensions and the ADD model

The concept of introducing additional spatial dimensions and thereby solving problems of theories with 3 spatial dimensions is an old approach in theoretical physics. As shown in section 4.1 in the year 1921 Theodor Kaluza

[23] used a 4+1-dimensional metric to unifiy the theoretical description of gravity with classical electromagnetism. Apart from the exciting possibility of obtaining classical gauge symmetries, extra dimensions in carefully chosen scenarios might as well help to explain (or at least weaken) the strong hierarchy between gravity and the electroweak theory as suggested by Antoniadis [33]. This can be seen explicitly in the so called ADD model, which was introduced by Arkani-Hamed, Dimopoulos and Dvali in 1998 [34]. In this section a short introduction of the ADD model will be given which is based on the work by [35, 36].

4.2.1 Einstein's equations in higher-dimensional spaces

Einstein's field equations with $3+d$ spatial dimensions are a straight forward generalisation of the three dimensional case [37]. However all the indices N,M run from $0 \ldots 3+d$ instead of $0 \ldots 3$, i.e.

$$R_{MN} - \frac{1}{2} g_{MN} R = -8\pi G T_{MN} \quad . \tag{4.9}$$

The trace of this gives the Ricci scalar R

$$R(1 - \frac{4+d}{2}) = -8\pi G T^N_N. \tag{4.10}$$

From this one finds the $(3+d)$-dimensional Ricci-tensor R_{MN} as

$$R_{MN} = -8\pi G(T_{MN} - \frac{1}{2+d} g_{MN} T^L_L), \tag{4.11}$$

and therefore the $3+d$-dimensional gravitational source term $\mathcal{S}_{MN}$ can be defined as

$$\mathcal{S}_{NM} := (T_{NM} - \frac{1}{2+d} g_{MN} T^L_L) \quad , \tag{4.12}$$

a definition which will be usefull later, when deriving the calssical graviton production cross section.

4.2.2 The reduced fundamental mass scale

In theories with gravity only large extra dimenions it is possible to relate the measured gravitational coupling constant $G^{-1} = 8\pi M_P^2$ (where M_P is the ordinary Planck mass) to the Planck mass M_D of the $D = 4+d$ dimensional theory [38]

$$G^{-1} = 8\pi R^d M_D^{2+d} \quad . \tag{4.13}$$

This equation is found by assuming that in addition to the four $(3+1)$ observable dimensions (**brane**) there are d additional spatial dimensions (**bulk**) which are compactified on tori with radius R. This $U(1)$ compactification on tori is the most simple scenario, as most other approaches like S^2 would lead to surface tension on the brane and therefore to further non trivial source terms on the effective source terms. However, one can hope that the brane surface tension does not exceed the fundamental scale M_D and that at distances from the brane much bigger than $1/M_D$, the metric looks essentailly flat and surface tension does not play an important role any more. To check the relation (4.13) in terms of a perturbative approach to gravity in large extra dimensions we introduce the reduced Planck mass $\bar{M}_D$ by writing eq. (4.9) as

$$R_{MN} - \frac{1}{2} g_{MN} R = -\frac{T_{MN}}{\bar{M}_D^{2+d}} \quad . \tag{4.14}$$

and then finding the connection between $\bar{M}_D^{2+d}$ and M_D^{2+d}. In order to make this comparison and to varify eq. (4.13) we have to find the effective four-dimensional description of eq. (4.14) and compare it to the known Einstein equations (3.1). In a perturbative approach one studies the emission of "soft" gravitons, with a momentum transverse to the brane $q_t \ll M_D$. This allows the perturbative expansion of the metric g_{AB} around the flat Minkowski metric

$$g_{AB} = \eta_{AB} + 2\frac{h_{AB}}{\bar{M}^{1+d/2}} \quad . \tag{4.15}$$

Expanding eq. (4.14) to first oder in h_{AB} gives

$$\begin{aligned} -\bar{M}_D^{-1-d/2} T_{AB} = \; & \partial^C \partial_C h_{AB} - \partial^C \partial_B h_{CA} - \partial^C \partial_A h_{CB} \partial_A \partial_B h_C^C \\ & -\eta_{AB} \partial^C \partial_C h_D^D + \eta_{AB} \partial^C \partial^D h_{CD} \quad , \end{aligned} \tag{4.16}$$

where in this limit the raising and lowering of indices is achieved by the flat spacetime metric η. The same equations of motion can be obtained from the effective Lagrangian density for small perturbations in $D = 4+d$ dimensions

$$\begin{aligned} \mathcal{L}_D = \; & h^{AB} \left(\partial^C \partial_C h_{AB} - 2\partial^C \partial_B h_{CA} + \partial_A \partial_B h_C^C \right) \\ & -h_A^A \left(\partial^C \partial_C h_D^D + \partial^C \partial^D h_{CD} \right) + \bar{M}_D^{-1-d/2} h^{AB} T_{AB}(z) \quad . \end{aligned} \tag{4.17}$$

Now the periodicity comes into play by demanding the boundary conditions for the d extra-dimensional coordinates

$$y_j = y_j + 2\pi R \;\; \text{with } j = 1, \ldots, d \quad , \tag{4.18}$$

where R is the compactification radius [1]. This implies that all fields that are functions of this D-dimensional spacetime ($z = (x_i, y_j)$ with $i = 0, 1, 2, 3$ and

[1] Note that the notation $j,\ k\ l$ will be used for the extra-dimensional indices in the following.

$j = 1,\ ...,\ d$) can be Fourier expanded in the y coordinates

$$h_{AB} = \sum_{n_1=-\infty}^{+\infty} ... \sum_{n_d=-\infty}^{+\infty} \frac{h^n_{AB}(x)}{\sqrt{V_d}} e^{i\frac{n^l y_l}{R}} \quad , \tag{4.19}$$

where $n = (n_1,\ ...,\ n_d)$ and

$$V_d = (2\pi R)^d \tag{4.20}$$

is the volume element of the compactified space. The $h^n_{AB}(x)$ are called Kaluza-Klein modes and they only live on the four-dimensional brane. The crucial assumption that ordinary matter is confined to the brane is implemented by the definition of the energy momentum tensor in eq. (4.17)

$$T_{AB}(z) = \eta^\mu_A \eta^\nu_B T_{\mu\nu}(x)\delta^d(y) \text{ with } \mu,\ \nu = 0,\ 1,\ 2,\ 3 \quad . \tag{4.21}$$

An observer who has very low energy available for testing his theory, will also have a very bad spatial resolution, and therefore he will miss effects that come due to the extra dimensions. He just can measure the effective four-dimensional version $\mathcal{L}_4$ of the Lagrangian $\mathcal{L}_D$. This Lagrangian is found by integration out the d extra dimensions.

$$\mathcal{L}_4 = \int \mathrm{d}y^d \mathcal{L}_D \quad . \tag{4.22}$$

Due to the periodic expansion (4.19) the integration over the kinetic terms of $\mathcal{L}_D$ is only non zero for $n = (0,\ ...,\ 0)$ (therefore the superscripts 0 will not be written down explicitly and h stands now for $h^{(0)}$) and the integration over the source term is trivial due to the delta function $\delta^d(y)$ giving

$$\begin{aligned}
\mathcal{L}_4 = \quad & h^{\mu\nu}\left(\partial^\alpha\partial_\alpha h_{\mu\nu} - 2\partial^\alpha\partial_\nu h_{\alpha\mu} + \partial_\mu\partial_\nu h^\alpha_\alpha\right) \\
& -h^\mu_\mu\left(\partial^\alpha\partial_\alpha h^\beta_\beta + \partial^\alpha\partial^\beta h_{\alpha\beta}\right) + \frac{h^{\mu\nu}}{\sqrt{V^d}\bar{M}_D^{+1+d/2}} T_{\mu\nu}(z) \\
& +h^{\mu\nu}\partial_\mu\partial_\nu h^i_i + h^i_i\partial_\mu\partial_\nu h^{\mu\nu} - h^i_i\partial^\alpha\partial_\alpha h^\mu_\mu - h^\mu_\mu\partial^\alpha\partial_\alpha h^i_i \\
& +2h^{\mu i}\partial^\alpha\partial_\alpha h_{\mu i} - 2h^{\mu i}\partial_\mu\partial^\nu h_{\nu i} \\
& +h^{ij}\partial^\alpha\partial_\alpha h_{ij} - h^i_i\partial^\alpha\partial_\alpha h^j_j \quad .
\end{aligned} \tag{4.23}$$

The first two lines in this Lagrangian look like the Lagrangian of a purely four-dimensional theory would look like, the third line couples the four-dimensional components $h_{\mu\nu}$ to the trace of the extra-dimensional components h^i_i and the last two lines contain only kinetic terms for h^i_i or $h^{\mu i}$ and are independent of $h_{\mu\nu}$. Because of the couplings in the third line the effective Lagrangian $\mathcal{L}_4$ does not yet fall apart into a purely four-dimensional part

and a part that comes due to the extra dimensions. This can be achieved by redefining the block- diagonal gravitational fields according to

$$\begin{aligned} G^{\mu\nu} &= h^{\mu\nu} - \eta^{\mu\nu} H^0 \quad , \\ h^i_i &= -2H^0 \quad . \end{aligned} \tag{4.24}$$

The Lagrangian (4.23) in terms of those variables is

$$\begin{aligned} \mathcal{L}_4 = \; & G^{\mu\nu}\partial^\alpha\partial_\alpha G_{\mu\nu} - 2G^{\mu\nu}\partial^\alpha\partial_\nu G_{\mu\alpha} + G^{\mu\nu}\partial^\mu\partial_\nu G^\beta_\beta + G^\beta_\beta\partial^\mu\partial_\nu G^{\mu\nu} \\ & - G^\beta_\beta\partial^\alpha\partial_\alpha G^\gamma_\gamma + \tfrac{G^{\mu\nu}+\eta^{\mu\nu}H^0}{\sqrt{V^d}\bar{M}_D^{1+1+d/2}} T_{\mu\nu}(z) \\ & + 2h^{\mu i}\partial^\alpha\partial_\alpha h_{\mu i} - 2h^{\mu i}\partial_\mu\partial^\nu h_{\nu i} \\ & + h^{ij}\partial^\alpha\partial_\alpha h_{ij} \quad , \end{aligned} \tag{4.25}$$

where the four-dimensional field $G^{\mu\nu}$ is not mixing dynamically to the extra-dimensional components $h^{\mu i}$, h^{ij} any more. The first two lines of eq. (4.25) match to the ordinary weak field expansion of Einstein's field equations (with the Planck mass $\bar{M}_P = M_p/\sqrt{8\pi}$) if and only if

$$\bar{M}_P^2 = V_d \bar{M}_D^{2+d} = (2\pi R)^d \bar{M}_D^{2+d} = R^d M_D^{2+d} \quad . \tag{4.26}$$

Therefore, we have derived the connection between the original Plank mass M_P and the reduced Planck mass M_D and come to an agreement with eq. (8.2), where just a different convention is used.

4.2.3 Feynman rules for the ADD model

For high energy processes the extra dimensions might be resolvable by the experiment. Therefore, instead of integrating out all the $n \neq (0, ..., 0)$ modes one has to take them all into account and rewrite the resulting Lagrangian in terms of those modes. The resulting equations of motion will again be coupled so one has to find a transformation analogous to eq. (4.24) that decouples the equations of motion [35]. For $d > 1$ this transformation is [2]

$$\begin{aligned} G^{(n)}_{\mu\nu} &= h^{(n)}_{\mu\nu} + \tfrac{\kappa}{3}\left(\eta_{\mu\nu} + \tfrac{\partial_\mu\partial_\nu}{n^2}\right) H^{(n)} - \partial_\mu\partial_\nu P^{(n)} + \partial_\mu Q^{(n)}_\nu + \partial_\nu Q^{(n)}_\mu \quad , \\ V^{(n)}_{\mu j} &= \tfrac{1}{\sqrt{2}}\left[ih^{(n)}_{\mu j} - \partial_\mu P^{(n)}_j - n_j Q^{(n)}_\mu\right] \quad , \\ S^{(n)}_{jk} &= g^{(n)}_{jk} - \tfrac{\kappa}{d-1}\left(\eta_{jk} + \tfrac{n_j n_k}{n^2} H^{(n)} + n_j P^{(n)}_k + n_k P^{(n)}_j - n_j n_k P^{(n)}\right) \quad , \\ H^{(n)} &= \tfrac{1}{\kappa} h^{(n)j}_j + n^2 P^{(n)} \quad , \\ Q^{(n)}_\mu &= -i\tfrac{n^j}{n^2} h^{(n)}_{j\mu} \quad , \\ P^{(n)}_j &= \tfrac{n^l}{n^2} h^{(n)}_{lj} + n_j P^{(n)} \quad , \\ P^{(n)} &= \tfrac{n^j n^k}{n^4} h^{(n)}_{jk} \quad , \end{aligned} \tag{4.27}$$

[2] Please note that n^j is the j-th component of the d-tupel n and that $n^2 = n^j n_j$.

where κ is chosen to be

$$\kappa = \sqrt{\frac{3(d-1)}{d+2}} \quad . \tag{4.28}$$

The number of superficial degrees of freedom of the variables in (4.27) is larger than the degrees of freedom in h_{AB}, which can be canceled by the $5+2d$ identities $n^j V_{\mu j}^{(n)} = n^j S_{jk}^{(n)} = S_j^{(n)j} = P_j^{(n)} = 0$. The fields $G_{\mu\nu}^{(n)}$, $V_{\mu j}^{(n)}$, $S_{jk}^{(n)}$ and $H^{(n)}$ are invariant under general coordinate tranformations

$$z_A \to z_A{}' = z_A + \epsilon_A(z) \quad . \tag{4.29}$$

This infinitesimal coordinate transformation induces a variation of the metric such that

$$\delta_\epsilon h_A B = -\partial_A \epsilon_B - \partial_B \epsilon_A \quad . \tag{4.30}$$

Under this coordinate transformation (gauge) $5+d$ degrees of freedom that are incorporated in the fields $Q_\mu^{(n)}$, $P_j^{(n)}$, and $P^{(n)}$ are gauge dependent. Therefore, it is possible to choose a gauge where $Q_\mu^{(n)} = P_j^{(n)} = P^{(n)} = 0$, which we will refer to as the unitary gauge. In this gauge the Lagrangian (4.17) becomes the sum over Kaluza-Klein modes

$$\begin{aligned}
\mathcal{L}_D = \sum_n & -\tfrac{1}{2} G^{(-n)\mu\nu}(\partial^\alpha \partial_\beta + m^2) G_{\mu\nu}^{(n)} + \tfrac{1}{2} G_\mu^{(-n)\mu}(\partial^\alpha \partial_\beta + m^2) G_\nu^{(n)\nu} \\
& - G^{(-n)\mu\nu} \partial_\mu \partial_\nu G_\lambda^{(n)\lambda} + G^{(-n)\mu\nu} \partial_\mu \partial_\lambda G_\nu^{(n)\lambda} - \tfrac{1}{4} \left| \partial_\mu V_{\nu j}^{(n)} - \partial_\nu V_{\mu j}^{(n)} \right|^2 \\
& + \tfrac{m^2}{2} V^{(-n)\mu j} V_{\mu j}^{(n)} - \tfrac{1}{2} S^{(-n)jk}(\partial^\alpha \partial_\beta + m^2) S_{jk}^{(n)} \\
& - \tfrac{1}{2} H^{(-n)}(\partial^\alpha \partial_\beta + m^2) H^{(n)} - \tfrac{1}{R^{d/2} M_D^{1+d/2}} \left[G^{(n)\mu\nu} - \tfrac{\kappa}{3} \eta^{\mu\nu} H^{(n)} \right] T_{\mu\nu} \quad .
\end{aligned} \tag{4.31}$$

From this Lagrangian the graviton ($G_{\mu\nu}^{(n)}$) propagator can be found in momentum space

$$< 0 | G_{\mu\nu}^{(n)} G_{\alpha\beta}^{(n)}(k) | 0 > = \frac{i P_{\mu\nu\alpha\beta}}{k^2 - m^2} \quad , \tag{4.32}$$

with

$$\begin{aligned}
P_{\mu\nu\alpha\beta} = & \tfrac{1}{2}(\eta_{\mu\alpha}\eta_{\nu\beta} + \eta_{\nu\alpha}\eta_{\mu\beta} - \eta_{\mu\nu}\eta_{\alpha\beta}) \\
& - \tfrac{1}{2m^2}(\eta_{\mu\alpha} k_\nu k_\beta + \eta_{\nu\alpha} k_\mu k_\beta + \eta_{\mu\beta} k_\nu k_\alpha + \eta_{\nu\beta} k_\mu k_\alpha) \\
& \tfrac{1}{6}\left(\eta_{\mu\nu} + \tfrac{2}{m^2} k_\mu k_\nu\right)\left(\eta_{\alpha\beta} + \tfrac{2}{m^2} k_\beta k_\alpha\right) \quad .
\end{aligned} \tag{4.33}$$

The spin-sum of the polarization tonsor is

$$\sum_s e_{\nu\mu}(k,s) e_{\alpha\beta}(ks) = P_{\mu\nu\alpha\beta} \tag{4.34}$$

and it satisfies the conditions

$$\eta^{\alpha\beta} P_{\mu\nu\alpha\beta} = 0 = k^\alpha P_{\mu\nu\alpha\beta} \quad . \tag{4.35}$$

All couplings of ordinary matter to the Kaluza-Klein gravitons comes due to the energy momentum tensor of this matter. From the Lagrangian of a Yang Mills theory coupled to fermions in the background in curved spacetime

$$\begin{aligned}\mathcal{L} = \quad & \sqrt{-g}\left(\bar{\psi}(i\gamma^l e_l^\mu(\partial_\mu + \tfrac{i}{2}e_\nu^m e_\lambda^n \Gamma^\nu{}_\mu{}^\lambda \Sigma_{mn} - ig_s A_\mu^a t^a) - m)\psi \right. \\ & \left. -\tfrac{1}{4}F_{\mu\nu}^a F_a^{\mu\nu}\right) \quad ,\end{aligned} \tag{4.36}$$

just as in equation (B.21) with the additional t^a terms that are the gauge group generators in the fundamental representation. The kinetic part of the gauge fields A_μ^a is written in terms of $F_{\mu\nu}^a = \partial_\mu A_\nu^a - \partial_\nu A_\mu^a - g_s f^{abc} A_\mu^b A_\nu^c$ where $a,\ b,\ c$ are group indices and f^{abc} are the structure constants. The energy momentum tensor for this Lagrangian is [3]

$$\begin{aligned}T_{\mu\nu} = \quad & \tfrac{i}{4}\bar{\psi}(\gamma_\mu\partial_\nu + \gamma_\nu\partial_\mu)\psi - \tfrac{i}{4}(\partial_\mu\bar{\psi}\gamma_\nu + \partial_\nu\bar{\psi}\gamma_\mu)\psi \\ & +\tfrac{1}{2}g_s t^a\bar{\psi}(\gamma_\mu A_\nu^a + \gamma_\nu A_\mu^a)\psi + F_{\mu\lambda}^a F_\nu^{a\lambda} + \tfrac{1}{4}\eta_{\mu\nu}F^{a\lambda\rho}F_{\lambda\rho}^a \quad .\end{aligned} \tag{4.37}$$

Plugging the energy momentum tensor (4.37) into the ADD Lagrangian (4.31) gives the couplings of gravitons to the Yang Mills theory:

- Fermion, fermion, graviton:

$$u(k_1)\ ,\ \bar{u}(k_2)\ ,\ G_{\mu\nu}^{(n)}\ :\quad -\frac{i}{4\bar{M}_P}(W_{\mu\nu} + W_{\nu\mu}) \tag{4.38}$$

  with

$$W_{\mu\nu} = (k_1 + k_2)_\mu\gamma_\nu \quad . \tag{4.39}$$

- Gauge boson, gauge boson, graviton:

$$A_\alpha^a\ ,\ A_\beta^b\ ,\ G_{\mu\nu}^{(n)}\ :\quad -\frac{i}{\bar{M}_P}\delta^{ab}(W_{\mu\nu\alpha\beta} + W_{\nu\mu\alpha\beta}) \tag{4.40}$$

  with

$$\begin{aligned}W_{\mu\nu\alpha\beta} = \quad & \tfrac{1}{2}\eta_{\mu\nu}(k_{1\beta}k_{2\alpha} - k_1k_2\eta_{\alpha\beta}) + \eta_{\alpha\beta}k_{1\mu}k_{2\nu} \\ & +\eta_{\mu\alpha}(k_1k_2\eta_{\nu\beta} - k_{1\beta}k_{2\alpha}) - \eta_{\mu\beta}k_{1\nu}k_{2\alpha} \quad .\end{aligned} \tag{4.41}$$

- Fermion, fermion, gauge boson, graviton:

$$u\ ,\ \bar{u}\ ,\ A_\alpha^a\ ,\ G_{\mu\nu}^{(n)}\ :\quad -\frac{i}{\bar{M}_P}g_s t^a(X_{\mu\nu\alpha} + X_{\nu\mu\alpha}) \tag{4.42}$$

  with

$$X_{\mu\nu\alpha} = \gamma_\mu\eta_{\nu\alpha} \quad . \tag{4.43}$$

[3] Note that for the gauge group $SU(2)$ of the standard model the gauge bosons Z, W^+ and W^- acquire a mass due to the Higgs mechanism, which leads to additional terms in the energy momentum tensor (4.37).

- Gauge boson, gauge boson, gauge boson, graviton:

$$A^a_\alpha(k_1),\ A^b_\beta(k_2),\ A^c_\gamma(k_3),\ G^{(n)}_{\mu\nu}\ :\quad \begin{aligned}&\tfrac{g_s}{M_P} f^{abc}(Y_{\mu\nu\alpha\beta\gamma}(k_1)+Y_{\mu\nu\beta\gamma\alpha}(k_2)\\ &+Y_{\mu\nu\gamma\alpha\beta}(k_3)+Y_{\nu\mu\alpha\beta\gamma}(k_1)\\ &+Y_{\nu\mu\beta\gamma\alpha}(k_2)+Y_{\nu\mu\gamma\alpha\beta}(k_1))\end{aligned} \tag{4.44}$$

where

$$\begin{aligned} Y_{\mu\nu\alpha\beta\gamma}(k) = \quad & k_\mu(\eta_{\nu\beta}\eta_{\alpha\gamma}-\eta_{\nu\gamma}\eta_{\alpha\beta})\\ + \quad & k_\beta(\eta_{\mu\alpha}\eta_{\nu\gamma}-1/2\eta_{\mu\nu}\eta_{\alpha\gamma})\\ - \quad & k_\gamma(\eta_{\mu\alpha}\eta_{\nu\beta}-1/2\eta_{\mu\nu}\eta_{\alpha\beta}) \quad . \end{aligned} \tag{4.45}$$

Those Feynman rules allow for the study of experimental signatures of the ADD model in particle collisions like energy loss due to graviton emission or enhancement of cross sections due to virtual graviton exchange. Such studies can be performed in lowest order perturbation theory. Unfortunately going to higher orders will not bring better or new insight, as the couplings with negative mass dimension show that the theory is non renormalizable.

4.2.4 Black holes in the ADD model

Apart from the modification of standard model cross sections theories with large extra dimensions offer another touchstone for their positive testing or falsification. By assuming a static $\Re^2 \times S^{2+d}$ symmetry (where d is the number of the extra spatial dimensions), Einstein's field equations in the vacuum region (outside of the mass distribution) can be solved exactly [37]. The solutions are generalizations of the 4-dimensional Schwarzschild solution (3.58)

$$ds^2 = \left(1-\frac{16\pi M G_{4+d}}{(2+d)A_{2+d}r^{1+d}}\right)dt^2 - \left(1-\frac{16\pi M G_{4+d}}{(2+d)A_{2+d}r^{1+d}}\right)^{-1} dr^2 - r^2 d\Omega^2_{2+d} \quad , \tag{4.46}$$

where A_{2+d} is the surface area of the dimensional unit sphere in $3+d$ dimensions

$$A_{2+d} = \frac{2\pi^{(3+d)/2}}{\Gamma((3+d)/2)} \tag{4.47}$$

and M is the mass of the spherical object. For this solution in the ADD model (with 4.13) the assumption of infinitely extended extra dimensions is approximately true as long as the Schwarzschild radius in the extra-dimensional scenario

$$R_S = \frac{1}{M_f}\left(\frac{16\pi}{A_{2+d}(2+d)}\frac{M}{M_f}\right)^{\frac{1}{1+d}} \tag{4.48}$$

is much smaller than the compactification radius R:

$$R_S \ll R \quad . \tag{4.49}$$

For a TeV range reduced Planck mass $M_f \sim 1$ TeV this condition means that the solution (4.46) is valid for black hole masses

$$M \ll \frac{A_{2+d}(2+d)}{16\pi} 10^{35} \times 10^{32\,d}\ \text{GeV} \quad , \tag{4.50}$$

which is certainly valid for all collider accessible energies.

4.2.5 Black hole production and evaporation in the ADD model

The most intuitive argument for the formation of black holes in high energy collisions is based on Thorne's hoop conjecture [39]. It predicts that high energy collisions where the center of mass energy substantially exceeds the Planck mass or the reduced Planck mass respectively would produce black holes [40]. The naive estimate that a black hole is formed as soon as the impact parameter of two colliding particles is smaller than the black hole horizon radius $R_S(\sqrt{s})$ for the invariant scattering energy $\sqrt{s}$, leads to a rough estimate of the black hole production cross-section of

$$\sigma \sim \pi R_S^2(\sqrt{s}) \quad . \tag{4.51}$$

When the Planck scale is due to some mechanism lowered down to the ∼TeV scale this raises the exciting prospect that black holes can be produced in the energy range of the large hadron collider (LHC) [40, 41, 42].

A more quantitative argument for the production of mini black holes in high energy collisions was given by Eardley and Giddings [42] who took the gravitational solution of incoming particles as the Schwarzschild solution and boosted it into the Lab-frame to obtain two shock waves described by the Aichelburg-Sexl solution [43]. Due to the large Lorentz boost the solutions of both particles could not interact causally before collision and therefore the total solution of the system is described by the sum of both solutions. In the moment of collision this changes instantly and it could be shown that for zero impact parameter a marginally trapped surfaces $\mathcal{S}$ [4] at the union of the shock waves are formed in the flat $D-2$ region with the radius

$$\rho_c = \left(\frac{4\pi G\sqrt{s}}{\Omega_{D-3}}\right)^{1/(D-3)} \sim r_H(\sqrt{s}) \quad . \tag{4.52}$$

[4] If a light ray crosses a surface $\mathcal{S}$ not reaching the infinite distance on the other end, this surface is called marginally trapped. This leads to the obvious conjecture that the existence of such surfaces indicates the formation of a black hole.

The intersection area of this surface with the 4-dimensional brane is then supposed to give the production cross section for the black hole production, which agrees with eq. (4.51). This argument has been improved for a non zero impact parameter and angular momentum modifications leading to corrections of order one [42]. Still the cross section is probably not correct for the production of very massive mini black holes $M_{BH}(\sqrt{s}) \gg M_f$, as it is exponentially suppressed [44] relatively to the lighter black holes $M_{BH}(\sqrt{s}) \sim M_f$ by the Gibbons-Hawking action [45, 37]. This leads to the unsatisfactory situation that for light black holes ($M_{BH}(\sqrt{s}) \sim M_f$) the semiclassical derivation of the cross section (4.51) is not good and for heavier black holes ($M_{BH}(\sqrt{s}) \gg M_f$) the cross section (4.51) might be exponentially suppressed. Fortunately it has been shown recently that large curvature and quantum fluctuations near the apparent horizon are an artifact of the point particle assumption for the incoming particles [46]. So curvature and quantum fluctuations near the apparent horizon of the closed trapped surfaces are small and the semiclassical approach and its resulting cross section (4.51) should still be reliable even for lighter black holes [46].

4.3 Randall Sundrum models

In the previous section it has been shown how the volume of at least two compact extra dimensions can lead to a reduced Planck scale ($M_f \sim 1$ TeV see eq. (4.13)) without contradicting actual measurements of Newtons law down to the millimeter range. Such an approach relies on a factorizable extra-dimensional metric.
In 1999, Lisa Randall and Raman Sundrum showed that dropping this assumption of a factorizable metric, a solution with only a single extra dimension can be found which allows a ∼TeV Planck mass [47]. Models with such a non factorizable metric are called Randall Sundrum (RS) type models.

4.3.1 The first Randall Sundrum model

The first model announced in this setup is in a five-dimensional space with the standard 3+1 coordinates x^μ and ϕ for the one extra-dimensional coordinate. ϕ is taken in the range from $-\pi$ to π and so on the periodic space S^1/Z_2. The connection to a $3+1$-dimensional theory is obtained by considering the purely four-dimensional components of the five-dimensional bulk metric (G) on the boundaries $\phi = 0,\ \pi$,

$$g^I_{\mu\nu}(x) = G_{\mu\nu}(x^\mu, \phi = \pi), \quad g^{II}_{\mu\nu}(x) = G_{\mu\nu}(x^\mu, \phi = 0) \quad . \tag{4.53}$$

The total action of this setup is assumed to consist of two parts living on the $3+1$ branes and on purely gravitational part living in the bulk as well

$$\begin{aligned} S &= S_I + S_{II} + S_{grav} \quad , \\ S_{grav} &= \int d^4x \int_{-\pi}^{\pi} d\phi \sqrt{-G}\{-\Lambda + 2M^3 R\} \quad , \\ S_I &= \int d^4x \sqrt{g_I}\{\mathcal{L}_I - V_I\} \\ S_{II} &= \int d^4x \sqrt{g_{II}}\{\mathcal{L}_{II} - V_{II}\} \quad , \end{aligned} \tag{4.54}$$

where V_I, V_{II} can be interpreted as cosmological terms on the brane and Λ is the cosmological term in the bulk. The five-dimensional Einstein's equations for the above action are

$$\begin{aligned} \sqrt{-G}\left(R_{MN} - \tfrac{1}{2}G_{MN}R\right) &= -\tfrac{1}{4M^3}\left[\Lambda\sqrt{-G}G_{MN} + (V_I\sqrt{-g_I}g^I_{\mu\nu}\delta(\phi-\pi)\right. \\ &\quad \left. + V_{II}\sqrt{-g_{II}}g^{II}_{\mu\nu}\delta(\phi))\delta^\mu_M\delta^\nu_N\right] \quad . \end{aligned} \tag{4.55}$$

If one assumes that the solution to (4.55) obeys four-dimensional Poincare invariance, the four-dimensional components of G have to be proportional to the proportional to the flat $3+1$-dimensional Minkowski metric $\eta_{\mu\nu}$. This justifies the metric ansatz

$$ds^2 = e^{-2\sigma(\phi)}\eta_{\mu\nu}dx^\mu dx^\nu + r_c^2 d\phi^2 \quad , \tag{4.56}$$

where r_c is a ϕ independent constant that is taking the place of the compactification radius R in the separable orbifold ansatz. With the ansatz (4.56) the $_{55}$ component of eq (4.55) reduces to

$$\frac{6\sigma'^2}{r_c^2} = \frac{-\Lambda}{4M^3} \tag{4.57}$$

and the $_{\mu\nu}$ component reduces to

$$\frac{3\sigma''}{r_c^2} = \frac{V_{II}}{4M^3 r_c}\delta(\phi) + \frac{V_I}{4M^3 r_c}\delta(\phi-\pi) \quad , \tag{4.58}$$

where σ' stands for $\partial_\phi\sigma$. Integrating eq. (4.57) gives

$$\sigma(\phi) = r_c\,|\phi|\,\sqrt{\frac{-\Lambda}{24M^3}} = r_c\phi\sqrt{\frac{-\Lambda}{24M^3}}\,(2\theta(\phi) - \theta(\phi+\pi) - \theta(\phi-\pi)) \quad , \tag{4.59}$$

where the absolute vale (expressed in terms of θ functions) assures a $\phi \to -\phi$ symmetry. This solution is unique up to an over all additive constant, which

corresponds to a scaling of all x^μ coordinates. A second derivative of the solution (4.59) and the 2π boundary condition give

$$\sigma'' = 2r_c\sqrt{\frac{-\Lambda}{24M^3}}\left[\delta(\phi) - \delta(\phi - \pi)\right] \quad . \tag{4.60}$$

Comparing this to the second differential equation (4.58) we find that the cosmological terms V_I, V_{II} and Λ are related in terms of a single scale k

$$V_{II} = -V_I = 24M^3k, \;\; \Lambda = -24M^3k^2 \quad . \tag{4.61}$$

Assuming a relatively small bulk cosmological constant $|\Lambda| < M^5$ (or $k < M$) so that the classical nature of the solution can be trusted we find the metric

$$ds^2 = e^{-2k|\phi|}\eta_{\mu\nu}dx^\mu dx^\nu + r_c^2 d\phi^2 \quad . \tag{4.62}$$

At this point, it is necessary to specify the physical interpetation of the branes V_I and V_{II}: The standard model particles are assumed to live on the brane $V_I = V_{vis}$ where as the brane V_{II} is assumed to be hidden $V_{II} = V_{hid}$. Fluctuations of this classical metric will provide the gravitational field of the effective four-dimensional theory. The zero modes of the classical solution only depend on x and can be written as

$$ds^2 = d^{-2kT(x)|\phi|}\left[\eta_{\mu\nu} + h_{\mu\nu}\right]dx^\mu dx^\nu + T^2(x)d\phi^2 \quad . \tag{4.63}$$

Here the $h_{\mu\nu}$ is the graviton of the four-dimensional theory

$$g_{\mu\nu}(x) = \eta_{\mu\nu} + h_{\mu\nu}(x) \tag{4.64}$$

and $T(x)$ is a real function and the so called modulus field. The structure of the modulus field is unknown but as its vacuum expectation value has to be the compactification radius r_c this problem is postponed (for an introduction to the problem see e.g. [48]). Next we replace T by r_c. Note that for the present approach no isometries are known that would allow the emerging of an electro-magnetic field $A_\mu dx^\mu d\phi$ from the off diagonal part of the bulk metric, like in the Kaluza Klein approach (see section 4.1). By plugging the metric (4.63) into the bulk action of (4.54) the curvature part of the Lagrangian is

$$L_{eff} \supset 2M^3 r_c e^{-2k_c|\phi|}\sqrt{-\det(g_{\mu\nu})}R_4 \quad , \tag{4.65}$$

where R_4 is the four-dimensional curvature scalar of $g_{\mu\nu}$. The ϕ integral can be explicitly performed, and gives the purely four-dimensional gravitational

part S_{4eff} of the action (4.65)

$$S_{4eff} = \int d^4x \left\{ \int_{-\pi}^{\pi} d\phi 2M^3 r_c e^{-2kr_c|\phi|} \right\} \sqrt{-\det(g_{\mu\nu})} R_4 \quad , \tag{4.66}$$

where R_4 denotes the four-dimensional Ricci scalar. In order to match this action to the four-dimensional GR action the part in the curly brackets has to be equal to two times the square effective four-dimensional Planck mass [5]

$$2M_{pl}^2 = 2M^3 r_c \int_{-\pi}^{\pi} d\phi e^{-2kr_c|\phi|} = \frac{M^3}{k} \left[1 - e^{-2kr_c\pi}\right] \quad . \tag{4.67}$$

Thus for large kr_c the effective Planck mass only depends very weakly on r_c and is indirect proportional to k. The coupling of standard matter to gravity on the visible brane is determined by eq. (4.55) and by the visible 4-d metric $g_{\mu\nu}^{vis} = e^{-2kr_c\pi} g_{\mu\nu}$, $\sqrt{-g^{vis}} = e^{-4kr_c\pi}\sqrt{-det(g_{\mu\nu})} = e^{-4kr_c\pi}\sqrt{-g}$. The metric on the hidden brane is in contrast $g_{\mu\nu}^{hid} = g_{\mu\nu}$. For simplicity we will consider the Lagrangian of a massive (m_0) scalar field Φ in the visible brane:

$$S_{vis} \supset \int d^4x \sqrt{-g^{vis}} \left\{ \partial_\mu \Phi g_{vis}^{\mu\nu} \partial_\nu \Phi - m_0^2 \Phi^2 \right\} \tag{4.68}$$

In terms of the metric $g_{\mu\nu}$ this is

$$S_{vis} \supset \int d^4x \sqrt{-g} e^{-4kr_c\pi} \left\{ \partial_\mu \Phi g^{\mu\nu} e^{+2kr_c\pi} \partial_\nu \Phi - m_0^2 \Phi^2 \right\} \tag{4.69}$$

Rewriting the wave function, $\Phi \to e^{kr_c\pi}\Phi$ gives

$$S_{vis} \supset \int d^4x \sqrt{-g} \left\{ \partial_\mu \Phi g_{vis}^{\mu\nu} \partial_\nu \Phi - m_0^2 e^{-2kr_c\pi} \Phi^2 \right\} \quad . \tag{4.70}$$

This shows that a mass parameter m_0 on the visible brane corresponds to a physical mass

$$m = e^{-kr_c\pi} m_0 \quad . \tag{4.71}$$

This mechanism works exactly the same way for realistic standard model fields and the Higgs vacuum expectation value v_0.
This shows that the gravitational mass m is exponentially suppressed in

[5] Note that in the ADD approach the perturbations of the metric were defined to have a mass dimension $1 + d/2$, which is not the case here and therefore the factor M_{pl}^2 is needed for the effective action to be dimensionless.

comparison to the mass on the visible brane m_0. For example a TeV scale m_0 with a $kr_c \approx 12$ would lead to a $m \approx 10^{19}$ GeV$\approx M_{Pl}$.
Like in the ADD model (or UXD models), there exist higher excitations of the gravitational (all physical) fields which can be found by solving the equations of motion with a product ansatz for the wave function. But in contrast to those models the spacing in the mass tower in the RS model [49] is given by

$$m_n = x_n k e^{-kr_c\pi} \quad , \tag{4.72}$$

where x_n are zeros of the Bessel function $J_1(x_n) = 0$ and therefore of order one. The energy scale from which one could expect new physical effects is determined here by the mass of the first Kaluza-Klein excitation. For an appropriate kr_c this scale could be in the TeV range without contradicting any known experiment.

4.3.2 Randall Sundrum model with infinite extra dimension

In the previous subsection we saw that for solving the hierarchy problem in the RS approach one needs $kr_c \approx 12$. For a $k \approx M_{Pl}$ this gives a size of the extra dimension of $r_c = \frac{12}{M_{Pl}}$. This very small distance finally determines the mass gap in the spectrum (4.72) and therefore the validity regime of standard physics. But this mass gap is not necessary in a slightly modified version of the scenario described before [47]. In this approach the interpretation of the branes is reversed so that the brane V_{II} is " visible" and the brane V_I is not visible. Therefore, the vacuum energy densities of the two branes change signs so that the standard model particles are assumed to be bound to the brane with a positive cosmological term $V^{vis} = 24M^3k$. Nevertheless this does not change the effective lower-dimensional Lagrangian and therefore does not alter the relation between the higher and lower-dimensional Planck mass (4.67). Taking the brane distance to infinity $r_c \to \infty$ the hidden brane is effectively removed from the setup and it follows that

$$M_{Pl}^2 = \frac{M^3}{k} \quad . \tag{4.73}$$

Still one has to check whether this also reproduces 4-d gravity. To see this we have to study small perturbations ($h_{\mu\nu}$) on top of the classical vacuum state solution to eq. (4.63):

$$G_{\mu\nu} = e^{-2k|y|}\eta_{\mu\nu} + h_{\mu\nu}(x, y) \quad . \tag{4.74}$$

Plugging this expansion into eq. (4.55) gives a differential equation for $h_{\mu\nu}$. In lowest order in h and in the gauge harmonic $\partial^\mu h_{\mu\nu} = 0 = h^\mu_\mu$ this equation reads

$$\left[\frac{1}{2}e^{2k|y|}\partial_\alpha\partial^\alpha - \frac{1}{2}\partial_y^2 - 2k\delta(y) + 2k^2\right] h_{\mu\nu}(x,y) = 0 \quad . \tag{4.75}$$

A further separation of variables $h_{\mu\nu}(x,y) = \psi_{\mu\nu}(x)e^{ipx}$ under the assumption of orbifold boundary conditions gives

$$\left[\frac{-m^2}{2}e^{2k|y|}\partial_\alpha\partial^\alpha - \frac{1}{2}\partial_y^2 - 2k\delta(y) + 2k^2\right] \psi_{\mu\nu}(x) = 0 \quad , \tag{4.76}$$

with $p^2 = m^2$. By replacing $s = \mathrm{sgn}(y)\left(e^{k|y|} - 1\right)/k$ and defining $\hat{\psi}(z) = \psi(y)e^{k|y|/2}$ this turns into the well known form of a one-dimensional Schrödinger equation,

$$\left[-\frac{1}{2}\partial_z^2 + V(z)\right] \hat{\psi}z = m^2\hat{\psi} \quad , \tag{4.77}$$

with the potential

$$V(z) = \frac{15k^2}{8(k\,|z| + 1)^2} - \frac{3k}{2}\delta(z) \quad . \tag{4.78}$$

The delta function in this potential is responsible for the existence of a single normalizable gravitational bound state mode on the visible brane. The rest of the potential supports continuum modes that are scattered from the repulsive part of the potential. Those modes have no gap but they are suppressed near the origin, due to the potential barrier near $z = 0$ and they fill all states $m^2 > 0$. Due to this suppression the only mode that really contributes at the origin is the zero mode from the δ function.
This gives rise to a standard graviton propagator $\sim \frac{P_{\mu\nu\alpha\beta}}{k^2}$ which corresponds to a radial potential for the zero mode

$$V_0(r) \sim G_N \frac{m_1 m_2}{r} \quad . \tag{4.79}$$

The continuum modes can be determined and normalized explicitly in terms of Bessel functions. The potential corresponding to one of those solutions is

$$V_C(r) \sim \int_0^\infty dm \frac{G_N}{k} \frac{m_1 m_2 m e^{-mr}}{kr} \quad , \tag{4.80}$$

where the Yukawa part of the potential originates from the massive Kaluza-Klein(KK) states, the additional m/k part originates from the wave function

suppression at the origin and the integral is the continuum version of the sum over the KK mass tower. $G_N = k/M^3$ denotes the coupling strength of gravity. Putting the last two equations together and performing the integral, one finds

$$V(r) = V_0(r) + V_C(r) = G_N \frac{m_1 m_2}{r} \left(1 + \frac{1}{r^2 k^2}\right) \quad . \tag{4.81}$$

This is exactly the Newtonian potential plus a $\frac{1}{r^2k^2}$ correction. The deviations from the Newton law will therefore be visible on distance scales $r < \frac{1}{k}$ which is way below experimental reach for a $k \sim \mathcal{O}(M)$. Apart from this Newtonian limit (close to the brane) this model has been studied in terms of gravitational radiation, graviton self coupling and gravity effects in larger distance from the brane. For a more detailed discussion on those topic the reader is referred to [47, 50, 51] and references therein.

Chapter 5

Black hole remnants

The final fate of black holes is an unresolved subject of ongoing research. The last stages of the evaporation process are closely connected to the information loss puzzle. The black hole emits thermal radiation, whose sole property is the temperature, regardless of the initial state of the collapsing matter. So, if a black hole completely decays into statistically distributed particles, unitarity can be violated. This happens when the initial state is a pure quantum state and then evolves into a mixed state [52, 53].

When one tries to avoid the information loss problem, two possibilities are left. Either the information is regained by some unknown mechanism or a stable black hole remnant is formed which keeps the information. Besides the fact that it is unclear in which way the information should escape the horizon [54, 55, 56, 57, 58, 59] there are several other arguments for black hole remnants (BHR) such as [60, 61, 62, 63, 64, 65, 66, 67, 68, 69]:

- The uncertainty relation: The Schwarzschild radius of a black hole with Planck mass is of the order of the Planck length. Since the Planck length is the wavelength corresponding to a particle of Planck mass, a problem arises when the mass of the black hole drops below Planck mass. Then one has trapped a mass inside a volume which is smaller than allowed by the uncertainty principle [70]. To avoid this problem, Zel'dovich [71] has proposed that black holes with masses below Planck mass should be associated with stable elementary particles. Also, the occurrence of black hole remnants within the framework of a generalized uncertainty principle has been investigated in [72].

- Corrections to the Lagrangian: The introduction of additional terms, which are quadratic in the curvature, yields a decrease of the evaporation temperature towards zero [73, 74]. This holds also for extra-dimensional scenarios [75] and is supported by calculations in the low

energy limit of string theory [76, 77, 78]. The production of TeV-scale black holes in the presence of Lovelock higher-curvature terms has been examined in [79] and it was found that these black holes can become thermodynamically stable since their evaporation takes an infinite amount of time.

- Further reasons for the existence of remnants have been suggested to be black holes with axionic charge [80], the modification of the Hawking temperature due to quantum hair [81] or magnetic monopoles [82, 83]. Coupling of a dilaton field to gravity also yields remnants, with detailed features depending on the dimension of spacetime [84, 85].

- The calculation of lowest order quantum gravity effects leads to stable remnants as well, as shown by [86].

- One might also see the arising necessity for remnant formation by applying the geometrical analogy to black holes and quantizing the radiation into wavelengths that fit on the surface, i.e. the horizon [87]. The smaller the size of the black hole, the smaller the largest possible wavelength and the larger the smallest possible energy quantum that can be emitted. Should the energy of the lowest energy level already exceed the total mass of the black hole, then no further emission is possible. Not surprisingly, this equality happens close to the Planck scale and results in the formation of a stable remnant.

Of course these remnants, which in various context have also been named Maximons, Friedmons, Cornucopions, Planckons or Informons, are not a miraculous remedy but bring some new problems along. Such as the necessity for an infinite number of states which allows the unbounded information content inherited from the initial state.

5.1 Charged black holes

The black hole produced in a deep inelastic proton-proton collision can carry an electric charge which it inherits from the initial quarks. The evaporation spectrum contains all particles of the SM and so, a certain fraction of the final black hole remnants will also carry net electric charge. In the following, these charged black hole remnants will be denoted BH^+ and BH^-, and the neutral ones BH^0, respectively. Since the $BH^\pm$'s undergo an electromagnetic interaction, their cross section is enhanced and they can be examined closely. This makes them extremely interesting candidates for the investigation of Planck scale physics.

The metric of a charged black hole in higher dimensions has been derived in [37]. This solution assumes the electric field to be spherical symmetric in all dimensions whereas in the scenario with LXDs the SM fields are confined to our brane. This has also been pointed out in ref. [88].

The exact solution for this system in a spacetime with compacitfied extra dimensions is known only implicitely [89, 37, 90, 91, 92, 93, 94]. However, for our purposes, it will be sufficient to estimate the charge effects by taking into account that we expect the brane to have a width of about $1/M_{\rm f}$. Up to this width, also the gauge fields can penetrate the bulk which is essentially a scenario of embedding universal extra dimensions as a fat brane into the large extra dimensions. Note, that this does not modify the electromagnetic coupling constants as there is no hierarchy between the inverse width and the radius of the fat brane. Following the same arguments leading to the Newtonian potential, we see that the Coulomb potential receives a modification to

$$\phi_{\rm C} = \frac{\alpha}{M_{\rm f}^{d+1}} \frac{Q}{r^{d+1}} \quad , \tag{5.1}$$

where α is the fine structure constant and Q is the dimensionless charge in units of the unit charge e. But this higher-dimensional potential will already turn into the usual $1/r$ potential at a distance $r = 1/M_{\rm f}$ which means that the pre-factors cancel and α does not collect any volume factors.

One can estimate the exact solution for the system by assuming it to be spherical symmetric up to the horizon radius. This yields

$$g_{tt} = \gamma(r) = 1 - 2\phi(r) \quad , \tag{5.2}$$

where ϕ is the potential containing the gravitational energy and the Coulomb energy of the source whose electric field is now also higher-dimensional. The weak field limit of Einstein's field equations yields the Poisson equation

$$-\Delta\phi(r) = \Omega_{(d+3)}\delta(r)\frac{M}{M_{\rm f}^{d+2}} + \frac{\alpha}{M_{\rm f}^{2(d+1)}}\frac{Q^2}{r^{2(d+2)}} \quad , \tag{5.3}$$

where $\Omega_{(d+3)}$ is the surface of the $d+3$-dimensional unit sphere

$$\Omega_{(d+3)} = \frac{2\pi^{\frac{d+3}{2}}}{\Gamma(\frac{d+3}{2})} \quad , \tag{5.4}$$

and the delta-function is already converted into spherical coordinates. Using the spherical symmetry and applying Gauss' Law yields then

$$\partial_r\phi(r) = -\frac{M}{M_{\rm f}^{d+2}}\frac{1}{r^{d+2}} + \frac{\alpha}{M_{\rm f}^{2(d+1)}}\frac{Q^2}{d+1}\frac{1}{r^{2d+3}} \quad . \tag{5.5}$$

Thus we find

$$\phi(r) = \frac{1}{d+1}\frac{1}{M_{\rm f}^{d+2}}\frac{1}{r^{d+1}}\left[M - \frac{\alpha Q^2}{2(d+1)}\frac{M_{\rm f}^{-d}}{r^{d+1}}\right] \quad . \tag{5.6}$$

The horizon R_H is located at the zero of $\gamma(r)$. In case there exists no (real) solution for R_H, the metric is dominated by the contribution of the electromagnetic field and the singularity will be a naked one. The requirement of γ having a zero, yields the constraint [1]

$$\alpha Q^2 \leq \left(\frac{M}{M_{\rm f}}\right)^2 \quad . \tag{5.7}$$

With $M =$ few $\times M_{\rm f}$, and Q being close by e, the left hand side is at least by a factor 100 smaller than the right hand side. So, the charge contribution to the gravitational field, which is described by the second term of eq. (5.6), will be negligible at the horizon location $R_H \sim 1/M_{\rm f}$. For the typical collider produced black holes, the singularity will not be naked. For the same reason, modifications of the Hawking evaporation spectrum can be neglected in the charge range under investigation.

Let us briefly comment on the assumption that the electromagnetic field is spherical symmetric up to a brane width of $\sim 1/M_{\rm f}$. If the field is confined to a thinner brane, the charge contribution to the gravitational potential will obey a different functional behaviour. It will drop slower at large distances but therefore be less divergent at small distances. This means, if the above inequality is fulfilled it will still hold because the singularity is even better shielded.

Usually, the Hawking-radiation for very small charged black holes necessarily leads to naked singularities which are hoped to be excluded by the (unproven) cosmic censorship hypothesis. The reason is that once the mass of a charged black hole becomes smaller than the mass of the lightest charged particle - i.e. the electron or positron, respectively - it could never get rid of its charge by radiating it off. Then, it would either end as a naked singularity or as a tiny remnant of mass about the electron mass. This case, however, can not occur in the here discussed setting, as we assume the remnant mass to be close by $M_{\rm f}$ and therefore much above the electron mass.

[1] Note, that these relations do only agree with the relations in [37] up to geometrical pre-factors. This is due to the fact that our additional dimensions are compactified and the higher-dimensional coupling constants are fixed by eq. (8.2) and (5.1).

5.2 Black hole remnants from cosmic rays

Cosmic ray data provides a valuable tool to test the assumption of stable remnant formation, because detailed examinations on the production probabilities of high mass low charge particles have been put forward [95, 96]. The hypothesis of stable black hole remnant formation therefore has to be confronted with these constraints. The production rate of black holes from highest energetic cosmic ray events has been studied [97, 98] and it was found that, for the most optimistic scenario, the black hole production rate, n, in an ice cube of volume ~ 1 km^3 ($m_{\rm cube} \approx 0.9 \times 10^{12}$kg) near the surface of the earth is roughly 10 black holes per year.

To give an upper limit, we assume that this production rate does not decrease when going deeper into the earth. The total number of black holes, N, that have been produced over the earth's existence time, $t_{\rm earth}$, can then be estimated by

$$N = n\ t_{\rm earth} \frac{m_{\rm earth}}{m_{\rm cube}} \quad , \tag{5.8}$$

with $t_{\rm earth} = 4.5$ Gy, $m_{\rm earth} = 5.97 \times 10^{24}$ kg. By this, one finds that about 300×10^{21} events have occurred in earth's history. If all these remnants would have been trapped in the earth, which is only likely for the charged fraction, the 45×10^{21} charged remnants with a mass of the order of 1 TeV form in total ~ 510 g black hole matter distributed all over the planet.

A stable black hole (charged or not) would have a very low charge to mass ratio. Such particles have been searched for in different types of matter [99, 100]. Ordinary mass spectrometry and accelerator mass spectrometry give upper limits on the relative abundance (X/nucleon) of such particles between 10^{-8} and 10^{-24} [100] depending on the mass of the remnant. The most optimistic concentration of black hole remnants as derived above is $n\frac{m_{\rm nucleon}}{m_{cube}} t_{\rm earth} = 8.6 \times 10^{-30}$/nucleon. This is still way below the observational limits. For enriched D_2O the sensitivity goes even down to concentrations as low as 10^{-29}. However, note that this experimental constraint relies on some assumptions of the chemical behaviour of the heavy charged particles and is only valid for masses up to 1 TeV.

Therefore, we conclude that charged remnants can not be excluded by present experimental data. However, it will be interesting to await new experimental results which might be able to reach a precision that allows to directly observe black hole remnants in ordinary matter.

5.3 Modified Hawking evaporation

We now attempt to construct a numerically applicable model for modifications of the black hole's temperature in order to simulate the formation of a black hole remnant. Though the proposals of remnant formation in the literature are built on various different theoretical approaches, they have in common that the temperature of the black hole drops to zero already at a finite black hole mass. We will denote the mass associated with this finite remnant size with $M_{\rm R}$ and make the reasonable identification $M_{\rm R} = M_{\rm min}$. Instead of deriving such a minimal mass within the frame of a specific model, we aim in this work to parametrize its consequences for high energy collisions.

For our purposes, we will assume that we are dealing with a theory of modified gravity which results in a remnant mass and parametrize the deviations of the entropy $S(M)$. This entropy now might differ from the Hawking-entropy by correction terms in $M_{\rm R}/M$. For black hole masses M much larger than $M_{\rm R}$ we require to reproduce the standard result. The expansion then reads

$$S(M) = \mathcal{A}_{(d+3)} M_f^{d+2} \left[a_0 + a_1 \left(\frac{M_{\rm R}}{M} \right) + a_2 \left(\frac{M_{\rm R}}{M} \right)^2 + \dots \right] \tag{5.9}$$

with dimensionless coefficients a_i depending on the specific model (see e.g. [72, 73, 77, 85]). $\mathcal{A}$ is the surface of the black hole

$$\mathcal{A}_{(d+3)} \;=\; \Omega_{(d+3)} R_H^{d+2} \tag{5.10}$$

where $\Omega_{(d+3)}$ is the surface of the $d+3$-dimensional unit sphere

$$\Omega_{(d+3)} = \frac{2\pi^{\frac{d+3}{2}}}{\Gamma(\frac{d+3}{2})} \quad . \tag{5.11}$$

As T_H is a function of M, A is a function of M as well. For the standard scenario one has

$$a_0 = \frac{d+1}{d+2} \frac{2\pi}{\Omega_{(d+3)}} \quad , \quad a_{i>1} = 0 \quad . \tag{5.12}$$

Note that in general

$$S_0 = S(M = M_{\rm R}) \tag{5.13}$$

will differ from the unmodified black hole entropy since the Schwarzschild-radius can be modified.

It should be understood that an underlying theory of modified gravity will allow to compute $M_{\rm R} = M_{\rm R}(a_i)$ explicitly from the initially present

parameters. This specific form of these relations however, depends on the ansatz. $M_{\rm R}$ will be treated as the most important input parameter. Though the coefficients a_i in principle modify the properties of the black hole's evaporation, the dominating influence will come from the existence of a remnant mass itself, making the a_i hard to extract from the observables.

To make this point clear, let us have a closer look at the evaporation rate of the black hole by assuming a remnant mass. Note, that the Hawking-evaporation law can not be applied towards masses that are comparable to the energy of the black hole because the emission of the particle will have a non-negligible back reaction. In this case, the black hole can no longer be treated in the micro canonical ensemble but instead, the emitted particles have to be added to the system, allowing for a loss of energy into the surrounding of the black hole. Otherwise, an application of the Hawking-evaporation down to small masses comparable to the temperature of the black hole, would yield the unphysical result that the evaporation rate diverges because one has neglected that the emitted quanta lower the mass of the black hole.

This problem can be appropriately addressed by including the back reaction of the emitted quanta as has been derived in [101, 102, 103, 104, 105, 106, 107, 108, 109, 110]. It is found that in the regime of interest here, when M is of order $M_{\rm f}$, the emission rate for a single particle micro state is modified and given by the change of the black hole's entropy

$$n(\omega) = \frac{\exp[S(M-\omega)]}{\exp[S(M)]} \quad . \tag{5.14}$$

If the average energy of the emitted particles is much smaller than M, as will be the case for $M \gg M_{\rm f}$, one can make the approximation

$$S(M) - S(M-\omega) \approx \frac{\partial S}{\partial M}\omega = \frac{\omega}{T} \tag{5.15}$$

which, inserted in eq. (5.14) reproduces the familiar relation. The single particle distribution can be understood by interpreting the occupation of states as arising from a tunnelling probability [110, 111, 112]. From the single particle number density (Eq. 5.14) we obtain the average particle density by counting the multi particle states according to their statistics

$$n(\omega) = \left(\exp[S(M) - S(M-\omega)] + s\right)^{-1} \quad , \tag{5.16}$$

where

$$\begin{aligned} s &= 1 \quad \text{for Fermi-Dirac statistic} \quad , \\ s &= 0 \quad \text{for Boltzmann statistic} \quad , \\ s &= -1 \quad \text{for Bose-Einstein statistic} \quad , \end{aligned} \tag{5.17}$$

and $\omega \leq M - M_{\mathrm{R}}$, such that nothing can be emitted that lowers the energy below the remnant mass. Note, that this number density will assure that the remnant is formed even if the time variation of the black hole's temperature (or its mass respectively) is not taken into account.

For the spectral energy density we then use this particle spectrum and integrate over the momentum space. Since we are concerned with particles of the standard model which are bound to the 3-brane, their momentum space is the usual 3-dimensional one. This yields

$$\varepsilon = \frac{\Omega_{(3)}}{(2\pi)^3} \int_0^{M-M_{\mathrm{R}}} \frac{\omega^3 \, \mathrm{d}\omega}{\exp[S(M) - S(M-\omega)] + s} \quad . \tag{5.18}$$

We are dealing with emitted particles bound to the brane and the surface through which the flux disperses is the 2-dimensional intersection of the black hole's horizon with the brane. Therefore, the black hole mass evolution is given by the surface integral of eq. (5.18)

$$\frac{\mathrm{d}M}{\mathrm{d}t} = \frac{\Omega_{(3)}^2}{(2\pi)^3} R_H^2 \int_0^{M-M_{\mathrm{R}}} \frac{\omega^3 \, \mathrm{d}\omega}{\exp[S(M) - S(M-\omega)] + s} \quad . \tag{5.19}$$

From this, we obtain the evaporation rate in the form a Stefan-Boltzmann law.

Inserting the modified entropy eq. (5.9) into the derived expression eq. (5.19), one sees that the evaporation rate depends not only on M_{R} but in addition on the free parameters a_i. However, for large M the standard scenario is reproduced and we can apply the canonical ensemble. E.g. for the Fermi-Dirac statistic one obtains

$$\frac{\mathrm{d}M}{\mathrm{d}t} = \frac{\Omega_{(3)}^2}{(2\pi)^3} R_H^2 \zeta(4)\Gamma(4) T^4 \quad \text{for} \quad M \gg M_{\mathrm{R}} \quad . \tag{5.20}$$

Whereas for $M/M_{\mathrm{R}} \to 1$, the dominant contribution from the integrand in eq. (5.19) comes from the factor ω^3 and the evaporation rate will increase with a power law. The slope of this increase will depend on S_0. From this qualitative analysis, we can already conclude that the coefficients a_i will influence the black hole's evaporation only in the intermediate mass range noticeably. If we assume the coefficients to be in a reasonable range – i.e. each a_i is of order 1 or less and the coefficient a_{i+1} is smaller[2] than the coefficient a_i and the series breaks off at a finite i – then the deviations from the standard evaporation are negligible as is demonstrated in figures 5.3, 5.2 and 5.3.

[2]From naturalness, one would expect the coefficients to become smaller with increasing i by at least one order of magnitude see e.g. [79].

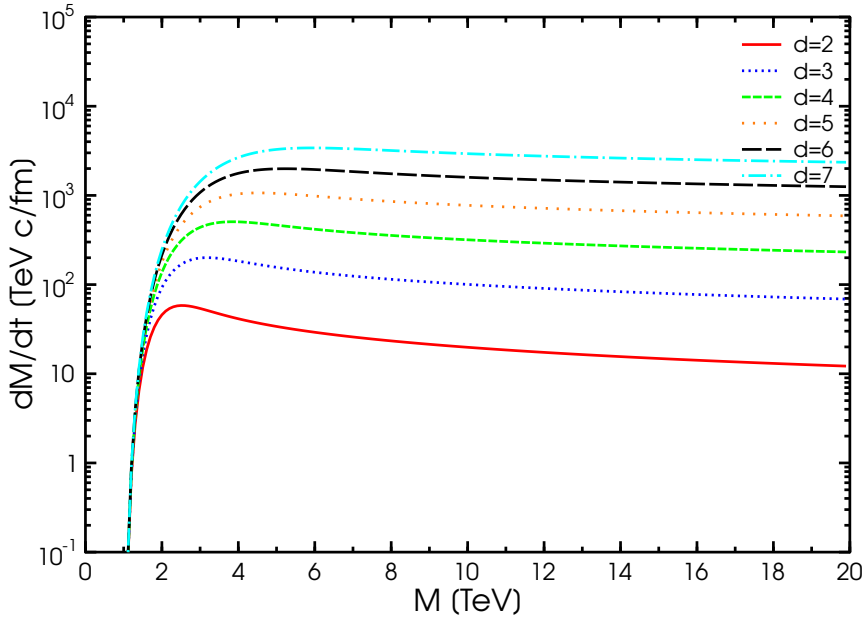

Figure 5.1: The evaporation rate eq. (5.19) for various d for $M_{\mathrm{R}} = M_{\mathrm{f}} = 1$ TeV and the standard entropy, i.e. the parameter set eq. (5.12). Here, Boltzmann- statistic was used.

Figure 5.3 shows the evaporation rate eq. (5.19) for various d with the standard parameters (5.12). Figure 5.2 and 5.3 show various choices of parameters for $d = 3$ and $d = 5$ as examples. Note, that setting a_3 to 1 is already in a very extreme range since a natural value is several orders of magnitude smaller: $a_3 \leq 10^{-3}$ (in this case the deviations would not be visible in the plot). For our further numerical treatment, we have included the possibility to vary the a_i but one might already at this point expect them not to have any influence on the characteristics of the black hole's evaporation except for a slight change in the temperature-mass relation.

From the evaporation rate eq. (5.19) one obtains by integration the mass evolution $M(t)$ of the black hole. This is shown for the continuous mass case in Figure 5.4. For a realistic scenario one has to take into account that the mass loss will proceed by steps by radiation into the various particles of the standard model.

5.4 A consistently modified black hole entropy

In this section another effective modification to the black hole entropy under the assumption of a BHR is derived.

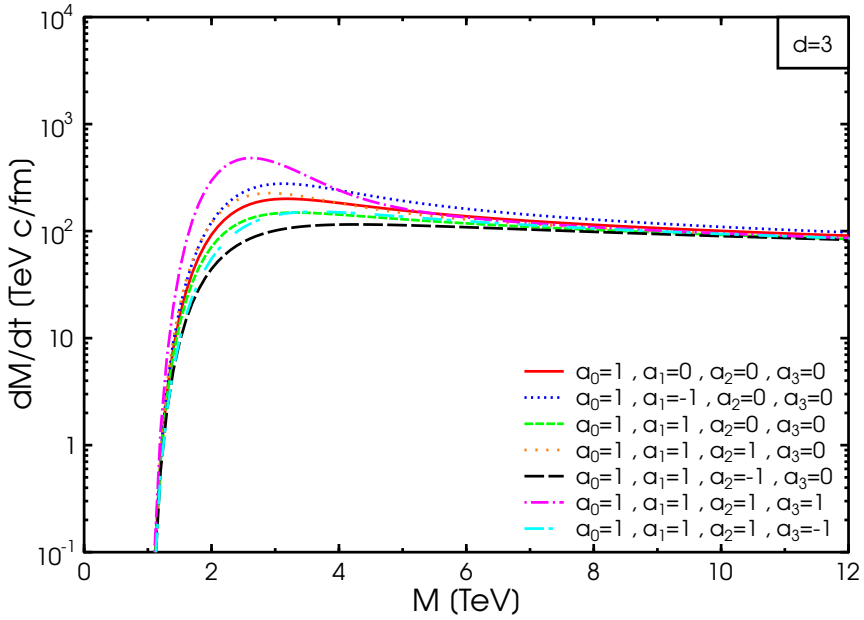

Figure 5.2: The evaporation rate for the black hole with $M_{\rm R} = M_{\rm f} = 1$ TeV and $d = 3$ for various parameters a_i. Here, Boltzmann-statistic was used.

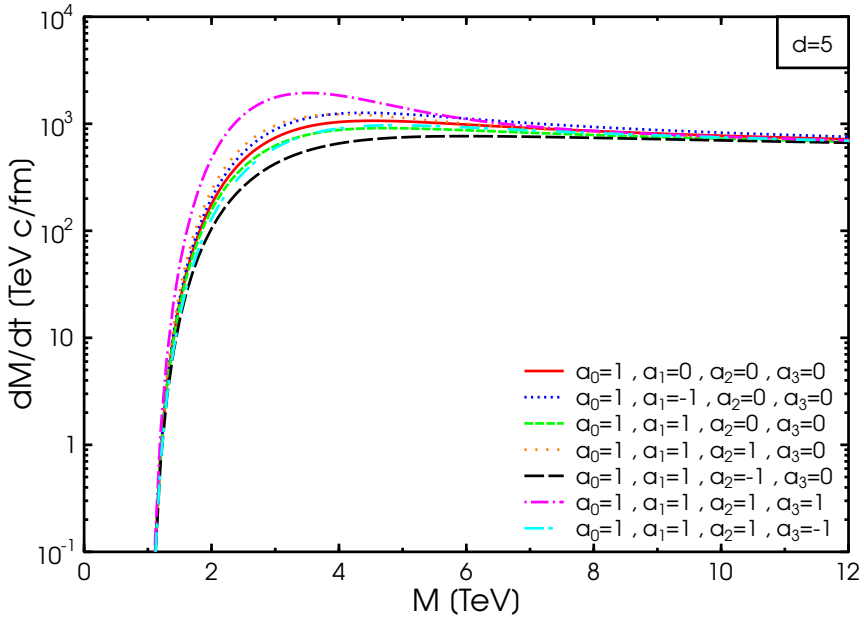

Figure 5.3: The evaporation rate for the black hole with $M_{\rm R} = M_{\rm f} = 1$ TeV and $d = 5$ for various parameters a_i. Here, Boltzmann-statistic was used.

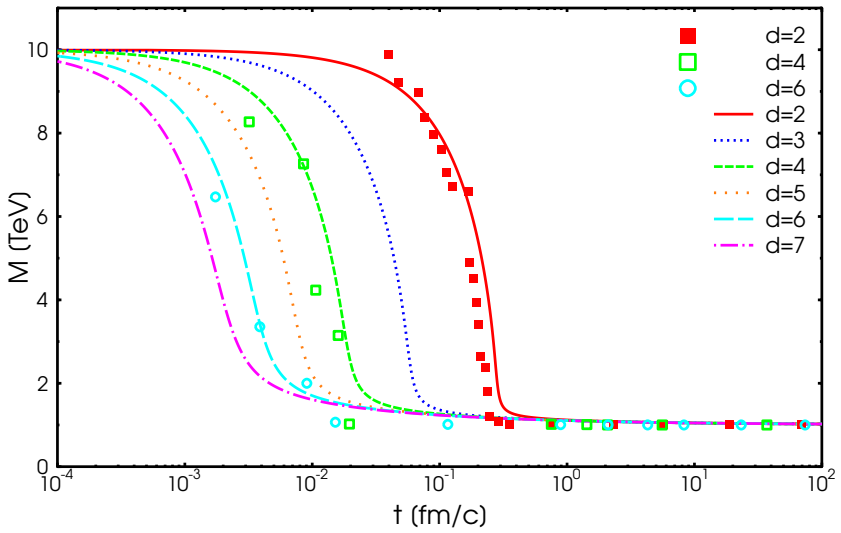

Figure 5.4: The mass evolution for a black hole of initial mass $M = 10$ TeV and various d. Here, we set $M_{\rm R} = M_{\rm f} = 1$ TeV. The full lines show the analytical calculation. The numerical results are shown as symbols. Note that each numerical example shows a single event only.

- Assumption I:
  Black hole remnants with certain mass M_R are the final state of any microscopic black hole

- Assumption II:
  The BHs can be described by a standard spectral function $n(\omega, M)$ (the hope is that it can be found from a entropy S) which leads in a smooth way to the formation of the BHR. With smooth we mean:

$$\lim_{\omega \to M - M_R} n(\omega, M) = 0 \tag{5.21}$$

  and

$$\lim_{\omega \to M - M_R} \partial_\omega (n(\omega, M)\omega^3) = \text{finite} \quad . \tag{5.22}$$

The straight forward ansatz for the spectral function is

$$n = \frac{1}{\exp(S(M) - S(M-\omega)) + s} \quad , \tag{5.23}$$

where we set for simplicity $s = 0$ although it could be ± 1 as well. From condition (5.21) we learn that $\lim_{\omega \to M - M_R} S(M) - S(M-\omega) = \infty$. As we want the entropy for $M > M_R$ to be always greater than zero we have no choice but defining

$$S(M) = k + S_1(M) \tag{5.24}$$

where k is an infinite constant and $S_1(M)$ is the finite part of S as long as $M > M_R$ and has to cancel the infinity at $M = M_R$ so that

$$S(M_R) = 0 \quad . \tag{5.25}$$

For $M \gg M_R$ and infinitesimal ω the Hawking temperature must be re-obtained

$$\partial_M S(M)|_{M \gg M_R} = 1/T_H = \frac{1}{M_f}\left(\frac{M}{M_f}\right)^{1/(d+1)} \tag{5.26}$$

and therefore S_1 must contain a part that obeys this condition but does not disturb condition (5.21):

$$S(M) = k + S_1(M) = k + \frac{d+1}{d+2}\left(\frac{M - M_R}{M_f}\right)^{\frac{2+d}{1+d}} + S_2(M) \quad . \tag{5.27}$$

The infinite constant k is now canceled by S_2: $k + S_2(M_R) = 0$. Instead of dealing with infinities directly it is useful to regularize them by
$k = -a_0 \ln(\epsilon)$ and $S_2(M) = a_0 \ln(M - M_R + \epsilon)$ so that

$$S(M) = -a_0 \ln(\epsilon) + \frac{d+1}{d+2}\left(\frac{M - M_R}{M_f}\right)^{\frac{2+d}{1+d}} + a_0 \ln(M - M_R + \epsilon) \quad , \tag{5.28}$$

where a is a positive constant. From condition (5.22) we find that the spectral density $n(\omega, M)\omega^3$ only behaves well at $\omega = M - M_R$ if $a_0 \geq 1$. One further finds that for $a > 1$ the spectral density softly approaches zero in this limit $\lim_{\omega \to M - M_R} \partial_\omega (n(\omega, M)\omega^3) = 0$. This is found by inserting the solution (5.28) into the ansatz (5.23) and computing the spectral density $n(\omega, M)\omega^3$ and its derivatives and finally taking the limit $\epsilon \to 0$.
Analogue corrections to the given entropy which also fulfill the boundary conditions can be implemented in the choice of a_0 and by terms like

$$\frac{a_n}{n+1}\left(\left(\frac{M_f}{\epsilon}\right)^n - \left(\frac{M_f}{M - M_R + \epsilon}\right)^n\right) \tag{5.29}$$

for $n > 0$. Expressing those corrections and the logarithmic terms by an integral, we find the general solution for the BHR entropy under the conditions (5.21) and (5.22):

$$S(M) = \frac{d+1}{d+2}\left(\frac{M - M_R}{M_f}\right)^{\frac{2+d}{1+d}} + \frac{1}{M_f}\int_{\epsilon}^{M - M_R + \epsilon} \sum_{n=0}^{\infty} a_n \left(\frac{M_f}{x}\right)^{n+1} dx \quad , \tag{5.30}$$

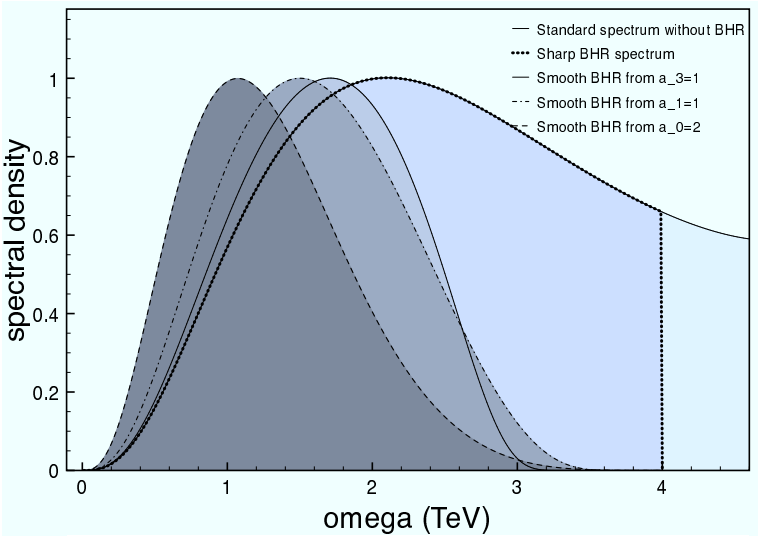

Figure 5.5: Normalized spectra of the first emission of a BH with $M = 5$ TeV, $d = 2$, $M_f = 1$ TeV and M_R=1TeV for the standard, the sharp BHR and the soft BHR spectral density with the parameters: $a_0 = 2$; $a_1 = 1$; $a_3 = 1$ (where all other coefficients $a_n = 0$).

where all coefficients $a_n \geq 0$.

So we have found the general analytic form for the spectral function (5.23) and the entropy (5.30) that fulfills the conditions (5.21) and (5.22). As an example the normalized spectral density $n(\omega, M)\omega^3$ is plotted in fig. (5.5) and compared to the spectral density from standard black body radiation (as implemented in the current event generators for black holes) and the spectral density for BHRs as suggested in the previous section.

One clearly sees in fig. (5.5) that the soft BHR spectrum leads to softer Hawking-radiation at any stage of the evaporation process. This statement is practically independent of the choice of the coefficients a_i.
Corrections of the type $\frac{M_R}{M}$ as suggested in the previous section could therefore be replaced by the equation that matches the physical boundary conditions (5.30) in order to obtain a smooth thermal radiation. Never the less the key experimental signal is expected to come from the pure existence of the BHR and not from the detailed study of it thermal spectrum. Because of this most of the signatures which will be discussed in the upcoming chapter under the assumption of the hard BHR spectrum will probably also be valid for a soft spectrum discussed in this section. Further spectrum modifications have been discussed in [113].

Chapter 6

Detection of black hole remnants

6.1 Direct detection of black hole remnants

Following the assumption of the previous chapter that the evaporation process slows down in the final stages of a black hole one wants to derive physical observables for this model. The simplest way to confirming the formation of a black hole remnant would be its direct detection. As only charged particles can produce direct measurable tracks in a detector one has to discuss the question of charged black holes first.
Black holes are typically formed from valence quarks as those carry the largest available momenta of the partonic system. So, the black holes formed in a proton-proton collision will have an average charge of $\sim 4/3$. The black holes decay with an average multiplicity of $\approx 10 - 25$ into particles of the SM, most of which will be charged. The details of the multiplicity depend on the number of extra dimensions [114]. After the black holes have evaporated off enough energy to be stable at the remnant mass, some have accumulated a net electric charge. According to purely statistical considerations, the probability for being left with highly charged black hole remnants drops fast with deviation from the average. The largest fraction of the black holes should have charges ± 1 or zero.

For a detailed analysis, we have estimated the fraction of charged black hole remnants with the PYTHIA event generator and the CHARYBDIS program [115, 116]. For our purposes, we turned off the final decay of the black hole and the charge minimization. Figure 6.1 shows the results for a simulation of proton-proton collisions at the LHC with an estimated center of mass energy of $\sqrt{s} = 14$ TeV.

We further assumed as an applicable model, worked out in [114], that the effective temperature of the black hole drops towards zero for a finite remnant mass M_{R}. This mass of the remnant is a few $\times M_{\mathrm{f}}$ and a parameter of the model. Even though the temperature-mass relation is not clear from the present status of theoretical examinations, such a drop of the temperature can be implemented into the simulation. However, the details of the modified temperature as well as the value of M_{R} do not noticeably affect the investigated charge distribution as it results from the very general statistical distribution of the charge of the emitted particles.

Therefore, independent of the underlying quantum gravitational assumption leading to the remnant formation, we find that about 27.5% of the remnants carry zero electric charge, whereas we have $\approx 17.7\%$ of BH^- and $\approx 23.5\%$ of BH^+.

The total number of produced black hole remnants depends on the total cross section for black holes [117, 118, 119, 120, 121, 122, 123, 124, 125, 126, 127, 128]. Ongoing investigations on the subject reveal a strong dependence on M_{f} and a slight dependence on d and suggest the production of $\approx 10^8$ black holes per year. Thus, following the above given results we predict the production of about 10^7 single charged $BH^{\pm}$ remnants per year. If the

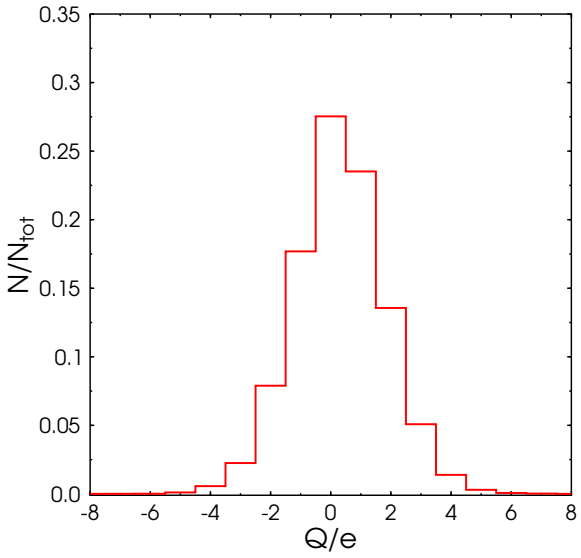

Figure 6.1: Distribution black hole remnant charges in PP-interactions at $\sqrt{s} = 14$ TeV calculated with the PYTHIA event generator.

time-of-flight (TOF) resolution of the detector can determine the velocity (see figure 6.2) of one of these charged remnants, the bended path in the magnetic field would allow direct determination of the remnants mass [129]. For the standard acceptance of the ALICE TPC (time projection chamber)

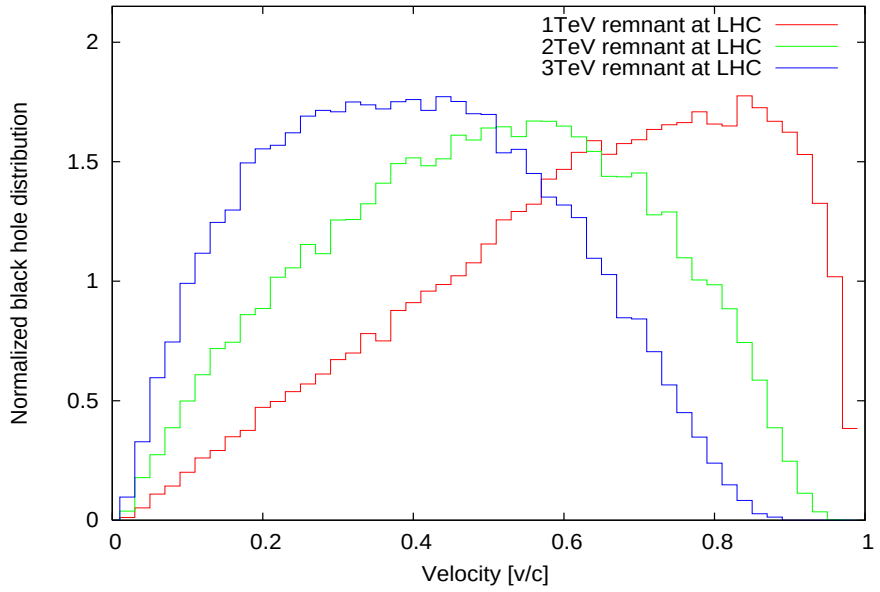

Figure 6.2: Normalized remnant velocities for the masses $M_R = 1, 2, 3$ TeV.

and the velocity distribution given from 6.2 the accuracy of the possible mass reconstruction for black hole remnants ($M_R = 1,\ 2\ , 3$ TeV) is shown in figure (6.3) [130]. But one can think even further and not only measure the tracks of those charged remnants but also try to single them out in an experiment before they are neutralized in a detector. As their electromagnetic interaction further allows to trap and keep them in an electromagnetic field.

For the specific scenario discussed here, the average momenta of the black hole remnants are of the order of $p \sim 1$ TeV. We suggest to use a similar approach as used for the trapping of anti-protons at LEAR/TRAP [131]. This means, first the remnants are decelerated in a decelerator ring from some GeV/c down to 100 MeV/c. Then they have to be further slowed down by electric fields to a couple of keV. This is slow enough to allow for a capture of the remnants in a Penning trap with low temperature. Then positrons (or electrons) are loaded into the trap. The positrons/electrons cool down to the temperature of the Penning trap by the emission of cyclotron radiation. Unfortunately, the lower cyclotron frequency of the heavy (thus slow) remnants makes this cooling mechanism less efficient for black hole remnants. However,

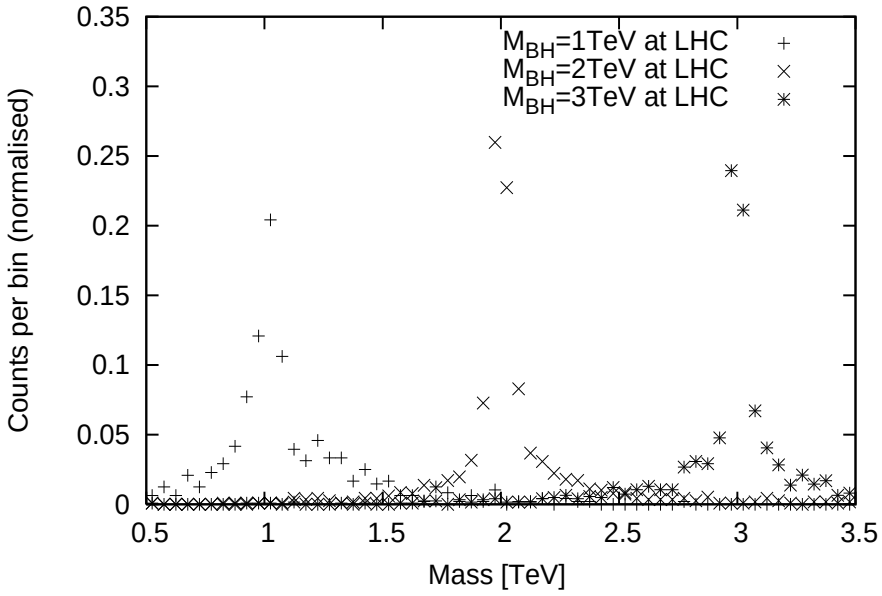

Figure 6.3: Black hole mass reconstruction in the ALICE TPC for the masses $M_R = 1, 2, 3$ TeV.

they can be cooled indirectly by Coulomb interaction with the positrons or electrons. In the case of anti-protons, the above discussed method allowed the TRAP collaboration to store the anti-protons for many month. This time would be sufficient to collect a huge amount of black hole remnants for study, even if only a small percentage will have low enough energies for deceleration. Another approach to collect black hole remnants might be to slow down the charged remnants by energy loss in matter - a similar approach was suggested by [132] to stop gluinos. The energy loss experienced by a charged particle when travelling through matter can be calculated using the Bethe-Bloch equation. From the average momentum of the remnants, we conclude that 50% of the remnants will have velocities $\beta \leq 0.3$. These remnants can be decelerated in matter e.g. in an iron block of 8 cm ($\beta = 0.1$), 1.3 m ($\beta = 0.2$) or 6.4 m ($\beta = 0.3$) length. This method would allow to include even high momentum remnants into the trapping process. Thus, these approaches allow to accumulate separated BH^+ and BH^- over a long period of time. In a second stage, the BH^+s can be merged with the BH^-s which increases the horizon in the process $BH^+ + BH^- \rightarrow BH^0$. During this process, the charge of the forming black hole is neutralized and the mass is increased to $2M_{\mathrm{R}}$. This will make a new evaporation possible which can then be analyzed in an environment clean of background from the proton-proton collision. In particular, the characteristics of the late stages of the decay can be observed

closely. After the merged black holes have shrunk again to remnant mass, most of them will be neutral and escape the experimentally accessible region due to their small cross section. Figure 5.2 shows results from a simulation of such reactions for a sample of 10^6 events of $BH^+ + BH^- \rightarrow BH^0$ with CHARYBDIS modified to incorporate the remnant production according to [114]. Here, it has been assumed that the black holes have been slowed down enough to make the initial momentum negligible. The total energy of the collision is then $2 \times M_{\mathrm{R}}$. Even though the parameter of the model might be difficult to extract (the dependence on d and M_{f} would require initial states of varying masses) a measurement of such spectrum would be a very important input to examine the signatures from the PP collision at the LHC. In such a way, the remnants would allow to extract the properties of the black hole's decay and remove theoretical uncertainties by allowing to quantify them directly from experimental measurements. This would substantially increase the precision by which the parameters of the underlying extra-dimensional model can be determined.

6.2 Indirect signatures for black holes and black hole remnants

We have included the evaporation rate, parametrized according to the previous section, into the black hole event generator CHARYBDIS and examined the occurring observables within the PYTHIA environment. Since these black hole remnants are stable, they are of special interest as they are available for close investigations. Especially those remnants carrying an electric charge offer exciting possibilities as investigated in [133].

It has also been shown in [133] that no naked singularities have to be expected for reasonably charged black holes and that the modification of the Hawking-radiation due to the electric charge can be neglected for the parameter ranges one expects at the LHC. This means in particular that the interaction of emitted charged particles with the black hole does not noticeably modify the emission probability. Although there might be uncertainties in the low energy limit where QED or QCD interactions might have unknown consequences for the processes at the horizon.

The formation of a remnant indeed solves a (technical) problem occuring within the treatment of a final decay: it might in principle have happened that during its evaporation process, the black hole has emitted mostly electrically charged particles and ended up with an electric charge of order ten. In such a state, it would then be impossible for the black hole to decay into less

than ten particles of the SM, whereas the standard implementation allows only a decay into a maximum of 5 particles.

Therefore, in the original numerical treatment, the process of Hawking-radiation has before been assumed to minimize the charge of the evaporating hole in each emission step. In such a way, it is assured that the object always has a small enough charge to enable the final decay in ≤ 5 particles without any violation of conservation laws. This situation changes if the remnant is allowed to keep the electric charge. In the here presented analysis, the assumption of charge minimization has therefore been dropped as it is no longer necessary. However, the in- or exclusion of charge minimization does not modify the observables investigated [1].

When attempting to investigate slowly decaying objects, one might be concerned whether these decay in the collision region or might be able to leave the detector, thereby still emitting radiation. As shown for the continuous case in fig. 5.4, the average energy of the emitted particles drops below an observable range within a 10 fm radius. Even if one takes into account the large γ-factor, the black hole will have shrunken to remnant-mass safely in the detector region. This is shown for a sample of simulated events in fig. 5.4 (symbols) which displays the mass evolution of these collider produced black holes. Here, the time, t, for the stochastic emission of a quanta of energy E was estimated to be $1/E$. This numerical result agrees very well with the expectations from the continuous case.

To understand the fast convergence of the black hole mass, recall the spectral energy density which enters in eq. (5.19) and which dictates the distribution of the emitted particles. Even though the spectrum is no longer an exactly Planckian, it still retains a maximum at energies $\sim 1/T$. If the black hole's mass decreases, the emission of the high energetic end of the spectrum is no longer possible. For masses close to the Planck scale, the spectrum has a maximum at the largest possible energies that can be emitted. Thus, the black hole has a high probability to emit its remaining energy in the next emission process. However, theoretically, the equilibrium time goes to infinity (because the evaporation rate falls to zero, see fig. 5.3) and the black hole will emit an arbitrary amount of very soft photons. For practical purposes, the evaporation was cut off as soon as the black hole reached the mass $M_{\mathrm{R}} + 0.1$ GeV. This is done by disabeling emission of objects carrying color after the maximally possible energy drops below the mass of the lightest meson, i.e. the pion.

Figure 6.4 shows the rapidity of the produced black hole remnants in

[1] The differences in the finally observable charged particle distributions from the black hole decay are changed by less than 5% compared to the charge minimization setting.

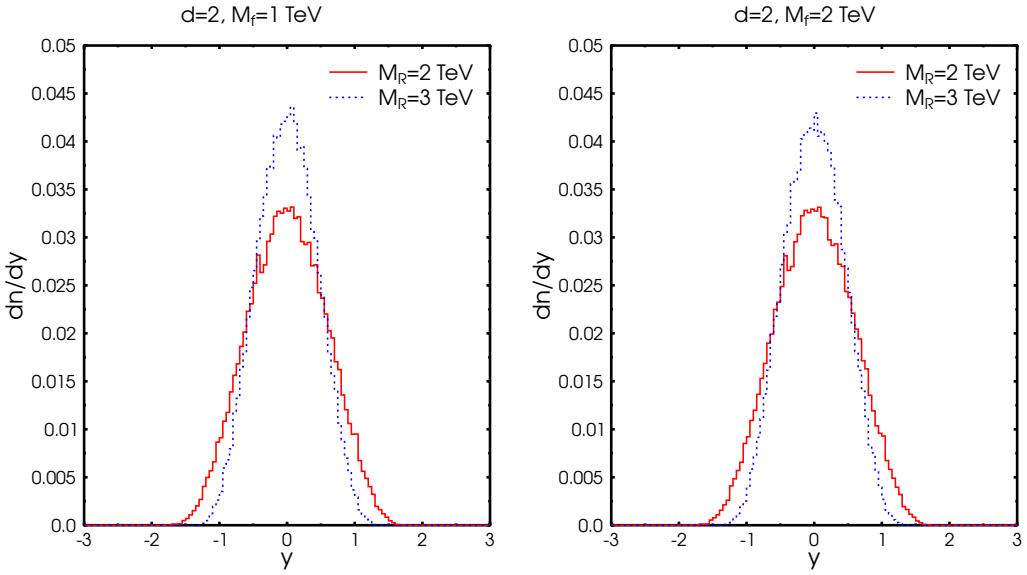

Figure 6.4: Rapidity distribution of the black hole remnants in pp interactions at $\sqrt{s} = 14$ TeV for $d = 2$. The curves for different number of extra dimensions d differ from the depicted ones by less than 5% and are not shown.

a proton-proton collision at $\sqrt{s} = 14$ TeV. All plots are for $d = 2$ since a higher number of extra dimensions leads to variations of less than 5%. The reader should be aware that the present numerical studies assume the production of one black hole in every event. To obtain the absolute cross sections the calculated yields have to be multiplied by the black hole production cross section $\sigma(\mathrm{pp} \to BH)$. Due to the uncertainties in the absolute production cross section of black holes this factor is taken explicitely out. For the present examination a sample of 50,000 events has been initialized. The black hole remnants are strongly peaked around central rapidities, making them potentially accessible to the CMS and ATLAS experiments. In Figure 6.5 the distribution of the produced black hole remnants as a function of the transverse momentum is shown.

Figure 6.6 shows the transverse momentum, p_T, of the decay products as it results from the modified multi particle number density eq. (5.16) before fragmentation. Figure 6.7 shows the p_T-spectrum after fragmentation. In both cases, one clearly sees the additional contribution from the final decay which causes a bump in the spectrum which is absent in the case of a remnant formation. After fragmentation, this bump is slightly washed out but still present. However, from the rapidity distribution and the fact that the black hole event is spherical, a part of the high p_T-particles will be at large y

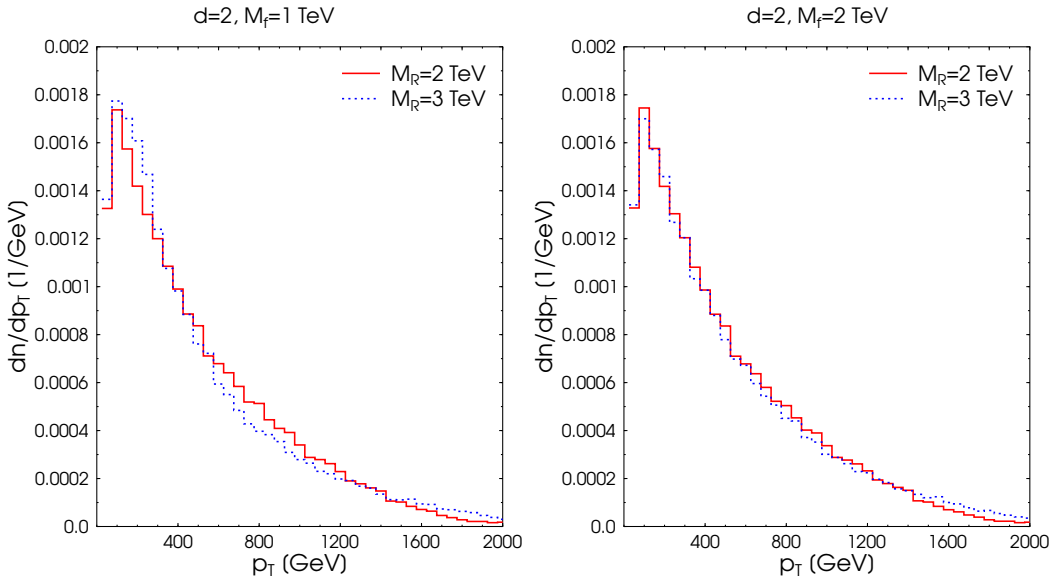

Figure 6.5: Transverse momentum distribution of the black hole remnants in pp interactions at $\sqrt{s} = 14$ TeV.

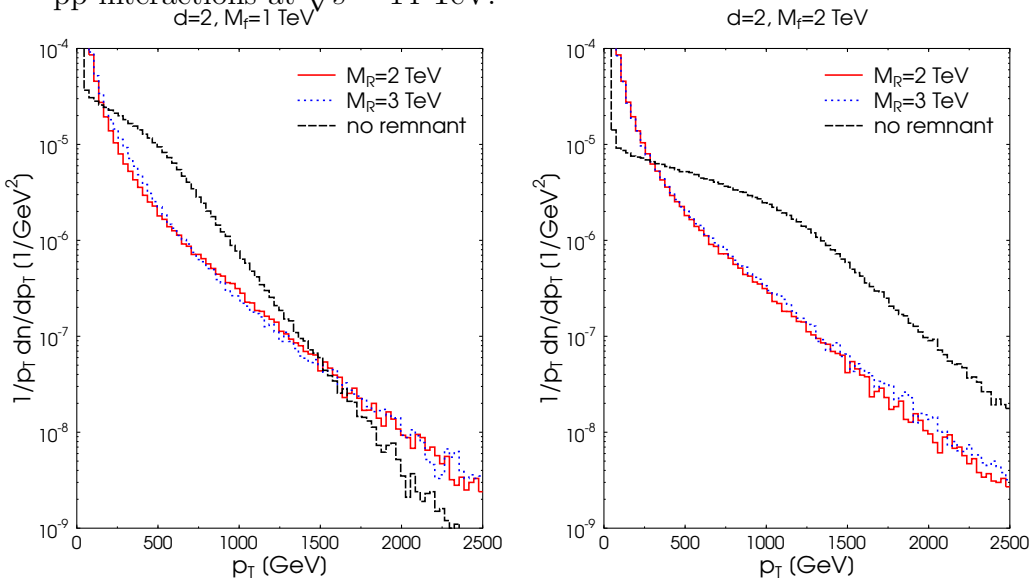

Figure 6.6: Transverse momentum distribution of initially emitted particles (i.e. before the fragmentation of the emitted partons) with final (two-body) decay in contrast to the formation of a black hole remnant.

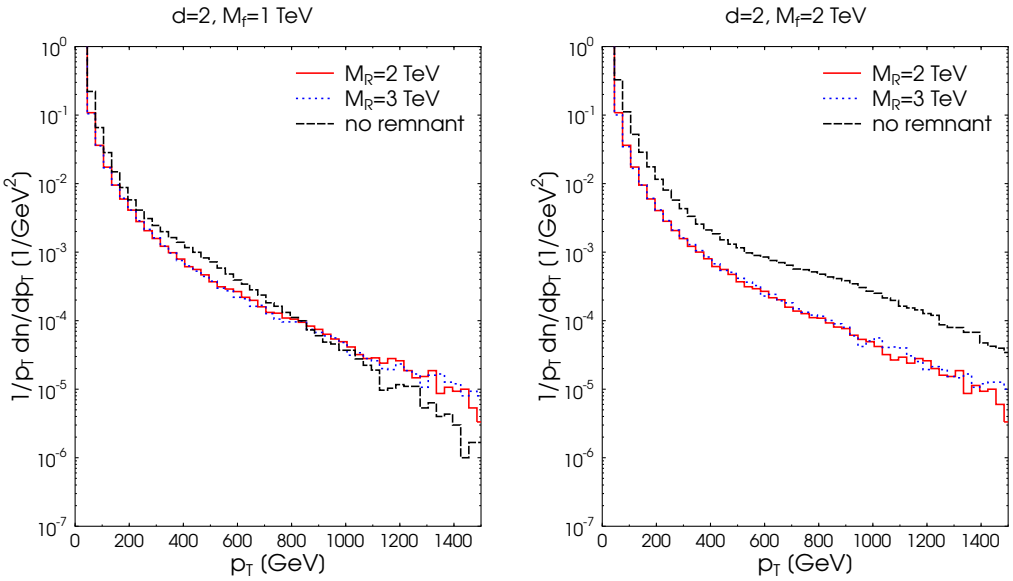

Figure 6.7: Transverse momentum distribution after fragmentation with final (two-body) decay in contrast to the formation of a black hole remnant.

and thus be not available in the detector. Therefore one has to include the experimental acceptance in detail if one wants to compare to experimental observables.

Figure 6.8 shows the total multiplicities of the event. When a black hole remnant is formed, the multiplicity is increased due to the additional low energetic particles that are emitted in the late stages instead of a final decay with $2-5$ particles. Note that this multiplicity increase is not an effect of the remnant formation itself, but stems from the treatment of the decay in the micro-canonical ensemble used in the present calculation. I.e. the black hole evaporates a larger amount of particles with lower average energy.

Figure 6.9 shows the sum over the transverse momenta of the black holes' decay products. To interpret this observable one might think of the black hole event as a multi-jet with total Σp_T. As it is evident, the formation of a remnant lowers the total Σp_T by about M_{R}. This also means, that the signatures of the black hole as previously analyzed are dominated by the doubtful final decay and not by the Hawking phase. It is interesting to note that the dependence on M_{f} is dominated by the dependence on M_{R}, making the remnant mass the primary observable, leading to an increase

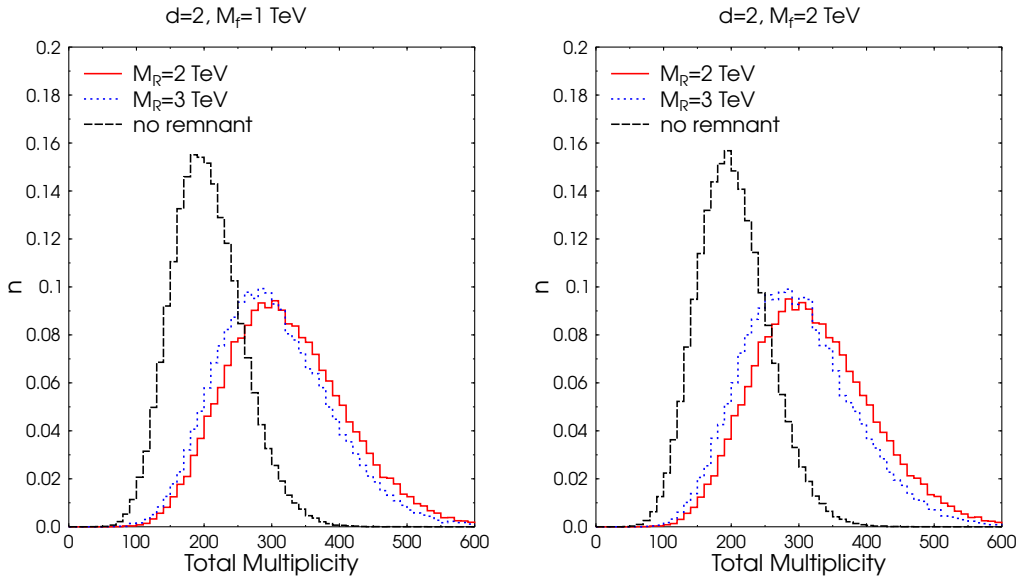

Figure 6.8: Total multiplicity with final (two-body) decay in contrast to the formation of a black hole remnant for $d = 2$.

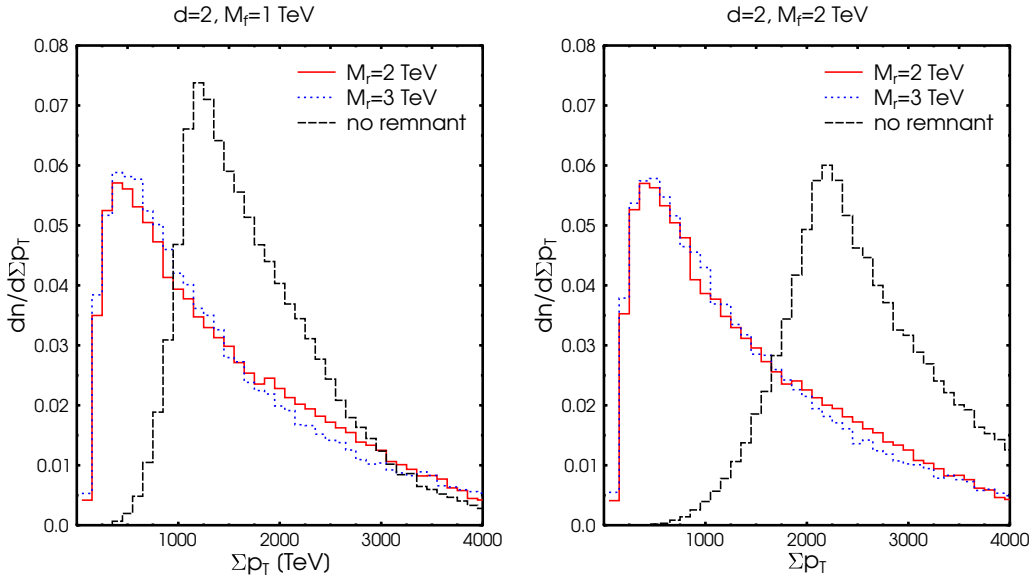

Figure 6.9: The total sum of the transverse momenta of the decay products.

in the missing energy. All those inderect signatures for black holes and black hole remnants are model dependent as they rely on the momentum and multiplicty distributions of secondary particles. But their qualitative difference should be present in any model that simulates some kind of final black hole decay or the formation of a stable remnant.

Up to now, one of the most prominent signatures for black hole production which is the suppression of high energetic dijets [134, 88, 135] has not been discussed. The most violent parton parton collisions in the standard model would result in two high energetic dijet. In a model with large extra dimension exactly those collisions would form a microscopic black hole, which then isotropically radiates its energy away and therefore does not produce very high energetic dijets. Motivated by this prominent signal, dijet correlations in the Charybidis model and with standard phythia as shown in figure 6.10 have been studied [130]. It turns out that in the Charybdis model the angular correlation of black hole decay products still shows a weak two bump structure. This is due to the assumption of a strict n-body decay of the black hole as soon as its mass reaches the critical scale M_f. If this implementation would be physical it could blur the signal of strong dijet suppression. As dijet pattern is expected to be much weaker for the decay procedure with a stable black hole remnant, it might be easier to detect stable or quasistable black hole remnants than black holes with a rapid final decay.
Even if, due to some unknown mechanism, the argumentation in favor of charged black hole remnants does not hold and neutral black hole remnants form the final state of a microscopic black hole, one still can hope to detect these with indirect measurements. As neutral particles do not leave tracks in detectors one can look for missing transverse momentum in the hadronic signature of a scattering event. As shown in figure 6.11 most black holes will be produced close to the production thresh hold. For those relatively light black holes it is very likely to relax to the remnant mass by evaporating just a few high energetic particles. The evaporated particles (as they are just a few of them) can recoil the black hole considerably into a transversal direction. If this black hole forms a neutral remnant, it would carry momentum not visible in the detector. Therefore such a black hole can produce a hadronic missing energy and missing momentum signature, which is distinct from the missing energy and missing momentum signature of neutrinos. The simulated output of a single event with an initial black hole mass of 1263 GeV and a final remnant mass of 1000 GeV is shown in figure 6.12.

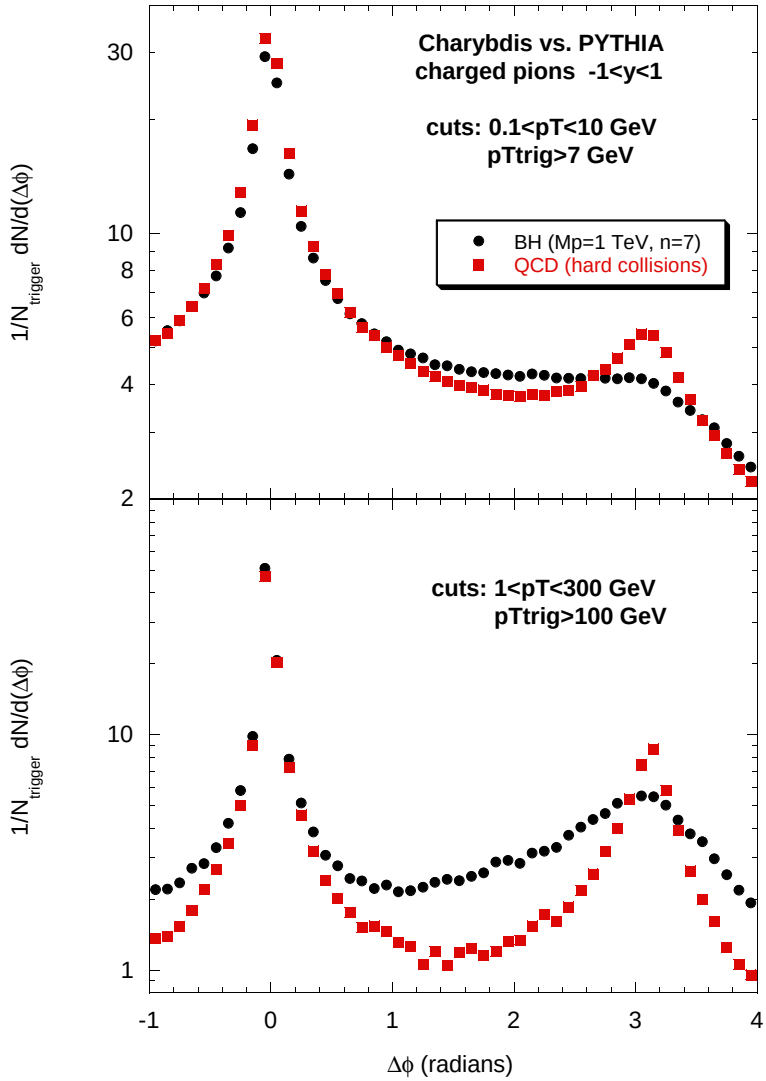

Figure 6.10: $\Delta\phi$ correlation for the ALICE tracking acceptance for simulated BH and QCD events in two different kinematic regions.

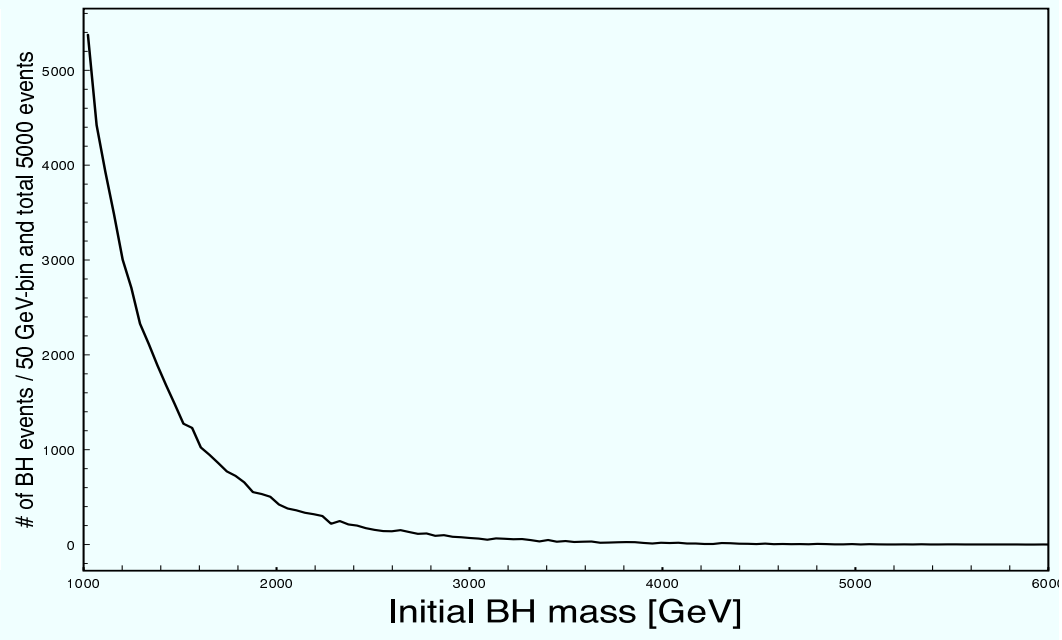

Figure 6.11: Distribution of initial black hole masses for a 14 TeV collider, for $M_f = 1$ TeV and $d = 6$.

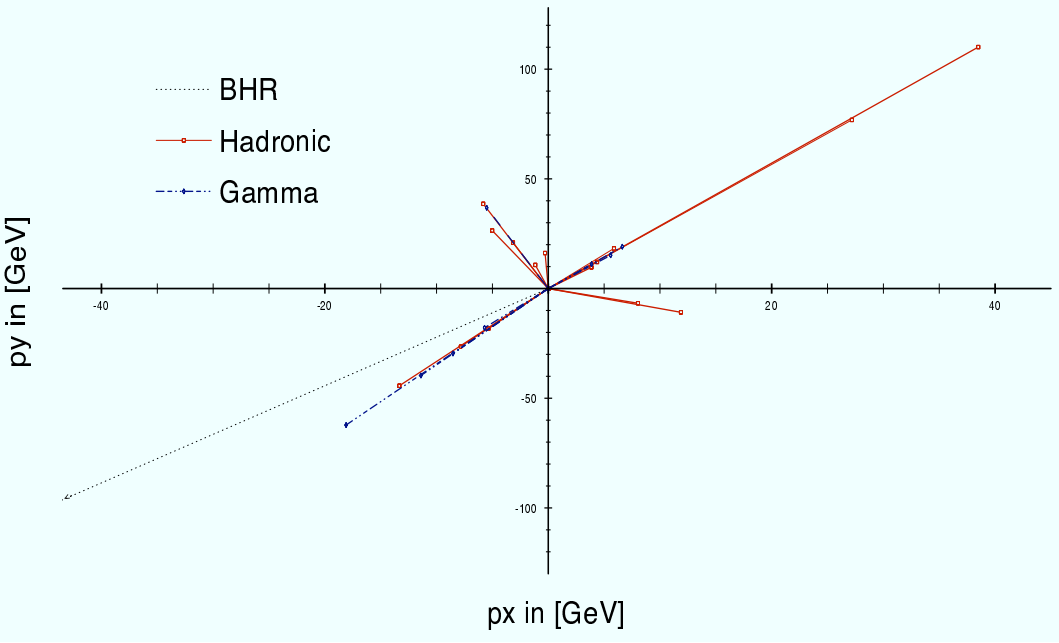

Figure 6.12: Transversal event shape of a single black hole with a p_T cut of 10 GeV for an initial black hole mass of 1263 GeV, $M_f = M_R = 1$ TeV, and $d = 6$.

Chapter 7

Gravitational radiation from elastic scattering

In this chapter the gravitational radiation from elastic scattering is derived and discussed.

7.1 Gravitational radiation in the ADD model

7.1.1 Gravitational waves in $3+d$ spatial dimensions

Assuming small perturbations h_{MN} from the $3+d$-dimensional Minkowski metric η_{NM} with the signature $(+,-,-,-,-,\dots)$ the following ansatz for the metric tensor is chosen

$$g_{NM} = \eta_{MN} + h_{MN}. \tag{7.1}$$

Inserting this ansatz into eq. (4.11), yields Einstein's field equations to first order in the perturbation h

$$\partial_L \partial^L h_{MN} - \partial_L \partial_N h^L_M - \partial_L \partial_M h^L_N + \partial_M \partial_N h^L_L = -8\pi G \mathcal{S}_{MN}. \tag{7.2}$$

Here the definition of the $3+d$-dimensional Riemann tensor used:

$$\begin{aligned} R_{MNOP} &= \tfrac{1}{2}\left[\partial_N\partial_P g_{MO} - \partial_M\partial_P g_{NO} - \partial_N\partial_O g_{MP} + \partial_M\partial_O g_{NP}\right] \\ &\quad + g_{AB}\left[\Gamma^A_{OM}\Gamma^B_{NP} - \Gamma^A_{PM}\Gamma^B_{N0}\right] \\ &:= \tfrac{1}{2}\left[\partial_N\partial_P g_{MO} - \partial_M\partial_P g_{NO} - \partial_N\partial_O g_{MP} + \partial_M\partial_O g_{NP}\right] + \Delta \quad . \end{aligned} \tag{7.3}$$

is used. Notice that Δ contributes only with quadratic and higher order terms in h. Next, we exploit the gauge invariance of Einstein's field equations. The harmonic gauge is chosen, with

$$g^{KL}\Gamma^N_{KL} = 0 \quad . \tag{7.4}$$

Using the definition of the Christoffel symbol

$$\Gamma^A_{BC} = \frac{1}{2} g^{AD} \left[\partial_C g_{BD} + \partial_B g_{CD} - \partial_D g_{BC} \right] \tag{7.5}$$

and expanding eq. (7.4) to first order in h gives

$$\partial_L h^L_N = \frac{1}{2} \partial_L h^N_N \quad . \tag{7.6}$$

Inserting eq. (7.6) in eq. (7.2) one find

$$\partial^L \partial_L h_{MN} = -16\pi G \mathcal{S}_{MN} \quad . \tag{7.7}$$

The retarded ($\tau = t - t_0 - |x - y| > 0$) solution of eq. (7.7) can be obtained with the help of the $3 + d$-dimensional Greens function $G^{(3+d)}(|x - y|)$. This gives

$$h_{MN}(t, x) = N \int dt_0 \int d^{3+d}\underline{y} G^{(3+d)}_{ret}(t - t_0, |\underline{x} - \underline{y}|) \mathcal{S}_{MN}(t_0, \underline{y}) \quad , \tag{7.8}$$

with a normalisation constant $N = -16\pi G$. Let us examine the $3 + d$-dimensional retarded Greens function [136, 137, 138] closer:

$$G^{3+d}_{ret}(t, x) = -\frac{1}{(2\pi)^{4+d}} \int d^{3+d}\underline{k} e^{i\underline{kx}} \int dk_0 \frac{e^{-ik_0(t-T_0)}}{k_0^2 - \underline{k}^2}. \tag{7.9}$$

For an even number of flat extra dimensions the integrands can be analytically evaluated and give according to [137]

$$G^{3+d}_{ret}(t, x) = \frac{1}{4\pi} \left[\frac{-1}{2\pi r} \frac{\partial}{\partial r} \right]^{d/2} \left[\frac{\delta\left((t - t_0) - r\right)}{r} \right] \ , d \text{ even} \quad . \tag{7.10}$$

In the present study, we restrain ourselves to the discussion of scenarios with even numbers of extra dimension. It is convenient to shift all derivatives in eq. (7.10) to the right hand side. Therefore, we define the commutator brackets

$$\begin{array}{lcl} \left[\partial_r, \frac{1}{r}\right]_{-1} & := & 1, \\ \left[\partial_r, \frac{1}{r}\right]_{0} & := & \frac{1}{r}, \\ \left[\partial_r, \frac{1}{r}\right]_{1} & := & \frac{-1}{r^2}, \\ & \ldots & \\ \left[\partial_r, \frac{1}{r}\right]_{n} & := & (-1)^n n! \frac{1}{r^{n+1}}. \end{array} \tag{7.11}$$

Now $(\partial_r \frac{1}{r})^n \delta$ is decomposed into a number ($\mathrm{A}(k, n)$) times the k^{th} derivative of the δ-function with respect to its argument

$$(\partial_r \frac{1}{r})^n \delta := \sum_{k=0}^{n} A(k, n) \delta^{(k)} \quad . \tag{7.12}$$

Using the defining equations (7.11) and (7.12) a recursion equation for eq. (7.10) can be obtained. Thus, knowing the Greens function for $d-2$ extra dimensions the Greens function for d extra dimensions can be calculated from

$$\begin{aligned} G_{ret}^{3+d}(t,x) &= \tfrac{1}{4\pi r}\left(\tfrac{1}{2\pi}\right)^{d/2}\sum_{i=0}^{d/2}\left\{\sum_{l=0}^{d/2-i}\left|\left[\partial_r,\tfrac{1}{r}\right]_l\right|\mathrm{A}(l+i-1,d/2-1)\tfrac{(l+i)!}{l!i!}\right\} \\ &\quad\times\delta^{(i)}\left[(t-t_0)-r\right] \\ &:= \tfrac{1}{4\pi r}\left(\tfrac{1}{2\pi}\right)^{d/2}\sum_{i=0}^{d/2}K(r,i)\delta^{(i)}\left[(t-t_0)-r\right]. \end{aligned} \tag{7.13}$$

For the cases of $d=0,2,4,6$ the explicit calculation gives the retarded Greens $G_{ret}^{3+d}(t,x)$ functions as:

$$\begin{aligned} G_{\mathrm{ret}}^{3}(t,x) &= \tfrac{\delta[(t-t_0)-r]}{4\pi r}, \\ G_{\mathrm{ret}}^{3+2}(t,x) &= \tfrac{\delta[(t-t_0)-r]+r\delta^{(1)}[(t-t_0)-r]}{8\pi^2 r^3}, \\ G_{\mathrm{ret}}^{3+4}(t,x) &= \tfrac{\delta^{(2)}[(t-t_0)-r]r^2+3\delta^{(1)}[(t-t_0)-r]r+3\delta[(t-t_0)-r]}{16\pi^3 r^5}, \\ G_{\mathrm{ret}}^{3+6}(t,x) &= \tfrac{\delta^{(3)}r^3+6\delta^{(2)}[(t-t_0)-r]r^2+15\delta^{(1)}[(t-t_0)-r]r+15\delta[(t-t_0)-r]}{32\pi^4 r^7}. \end{aligned} \tag{7.14}$$

Next it is assumed that the observer ($|\underline{x}|$) is at large distance in comparison to the extension of the source ($|\underline{y}|$). This means for $|\underline{x}| \gg |\underline{y}|$ that

$$\tau = t - t_0 - |\underline{x}-\underline{y}| \approx t - t_0 - |\underline{x}| + \underline{y}\frac{\underline{x}}{|\underline{x}|}. \tag{7.15}$$

Keeping this in mind, eq. (7.8) gives

$$\begin{aligned} h_{MN}(x) &= N\int dt_0\int d^3y_\parallel d^dy_\perp G_{ret}^{(3+d)}(t-t_0,|\underline{x}-\underline{y}|)\mathcal{S}_{MN}(t_0,\underline{y}) \\ &= \int dt_0\int d^3y_\parallel d^dy_\perp \tfrac{N}{4\pi|\underline{x}-\underline{y}|}(\tfrac{1}{2\pi})^{d/2}\sum_{i=0}^{d/2}K(|\underline{x}-\underline{y}|,i) \\ &\quad\times\delta^{(i)}(t-t_0-|\underline{x}-\underline{y}|)\mathcal{S}_{MN}(t_0,\underline{y}). \end{aligned} \tag{7.16}$$

Partial integration with respect to t_0 allows to shuffle the derivatives from the δ-function to the source $\mathcal{S}_{MN}$ and one obtains

$$\begin{aligned} h_{MN}(x) = &\int dt_0\int d^3y_\parallel d^dy_\perp \tfrac{N}{4\pi|\underline{x}-\underline{y}|}(\tfrac{1}{2\pi})^{d/2}\sum_{i=0}^{d/2}K(|\underline{x}-\underline{y}|,i) \\ &\delta(t-t_0-|\underline{x}-\underline{y}|)(\tfrac{\partial}{\partial t_0})^i\mathcal{S}_{MN}(t_0,\underline{y}). \end{aligned} \tag{7.17}$$

The delta function fixes the time at which to evaluate $\mathcal{S}_{MN}(t_0,\underline{y})$. The source term $\mathcal{S}$ is positive definite and can be expressed by its Fourier integral

$$\mathcal{S}_{MN}(\tau,\underline{y}) = \frac{1}{\sqrt{2\pi}}\int_0^\infty d\omega\mathcal{S}_{MN}(\omega,\underline{y})e^{-i\omega\tau} + c.c. \quad . \tag{7.18}$$

Every derivative with respect to the time generates a factor $-i\omega$ from eq. (7.18). After using eq. (7.15) and integrating out the δ-functions this leads to

$$\begin{aligned} h_{MN}(x) &= N\tfrac{1}{\sqrt{2\pi}4\pi}\tfrac{1}{(2\pi)^{d/2}}\int d\omega \exp\left(-i\omega(t-|\underline{x}|)\right) \\ &\quad \sum_{j=0}^{d/2} K(|\underline{x}-\underline{y}|,j)\int d^3y_\parallel d^dy_\perp \tfrac{1}{|\underline{x}|}(i\omega)^j \mathcal{S}_{MN}(\omega,\underline{y})\exp\left(-i\omega\underline{y}\tfrac{\underline{x}}{|\underline{x}|}\right). \end{aligned} \tag{7.19}$$

The monopole part of this gravitational wave is found by taking $|\underline{y}|/|\underline{x}| \ll 1$ and therefore to lowest order $1/|\underline{x}-\underline{y}|^j \approx 1/|\underline{x}|^j$ and $K(|\underline{x}-\underline{y}|,j) \approx K(|\underline{x}|,j)$,

$$\begin{aligned} h^{(0)}_{MN}(x) &= N\tfrac{1}{\sqrt{2\pi}4\pi}\tfrac{1}{(2\pi)^{d/2}}\int d\omega \exp\left(-i\omega(t-|\underline{x}|)\right) \\ &\quad \sum_{j=0}^{d/2} K(|\underline{x}|,j)\int d^3y_\parallel d^dy_\perp \tfrac{1}{|\underline{x}|}(i\omega)^j \mathcal{S}_{MN}(\omega,\underline{y})\exp\left(-i\omega\underline{y}\tfrac{\underline{x}}{|\underline{x}|}\right) \\ &= \int d\omega \exp\left(-i\omega(t-|\underline{x}|)\right) e_{MN}(\underline{x},\omega) \quad , \end{aligned} \tag{7.20}$$

which has the form of a plane wave solution. As the final result of this subsubsection it is shown that the polarisation tensor e_{MN} of the induced gravitational wave is given by

$$\begin{aligned} e_{MN}(\underline{x},\omega) &= N\tfrac{1}{4\pi}\tfrac{1}{(2\pi)^{d/2}\sqrt{2\pi}}\sum_{j=0}^{d/2} K(|\underline{x}|,j)\tfrac{1}{|\underline{x}|}(i\omega)^j\int d^3y_\parallel d^dy_\perp \\ &\quad \mathcal{S}_{MN}(\omega,\underline{y})\exp\left(-i\omega\underline{y}\tfrac{\underline{x}}{|\underline{x}|}\right) + c.c. \\ &= N\tfrac{1}{4\pi}\tfrac{1}{(2\pi)^{d/2}\sqrt{2\pi}}\sum_{j=0}^{d/2} K(|\underline{x}|,j)\tfrac{1}{|\underline{x}|}(i\omega)^j\hat{\mathcal{S}}_{MN}(\omega) + c.c. \quad . \end{aligned} \tag{7.21}$$

The charge conjugated part (abbr. as c.c.) is not shown explicitly, but is taken into account in the further calculations.

In section 7.1.4 the source term $\mathcal{S}_{MN}(\omega,\underline{y})$ will be explicitly calculated. When doing so, it is useful to remember that the " time" coordinate corresponding to ω is τ from Eq. (7.15) and not t.

7.1.2 The Greens function in compactified space

In the ADD model the Greens functions for gravitational radiation have to fulfill the boundary conditions

$$G^{3+d}_{\rm ret}(t,\boldsymbol{x},y_i) = G^{3+d}_{\rm ret}(t,\boldsymbol{x},y_i+2\pi R) \quad . \tag{7.22}$$

Therefore, $G^{3+d}_{\rm ret}(t,\boldsymbol{x},y_i)$ can be expressed in form of its discrete Fourier modes

$$G^{3+d}_{\rm ret}(t,\boldsymbol{x},y) = \sum_{(n)} \frac{G^{3+d\,(n)}_{\rm ret}(t,\boldsymbol{x})}{\sqrt{V_d}}\exp(\mathrm{i}\frac{\mathrm{n^j y_j}}{\mathrm{R}}) \quad , \tag{7.23}$$

where $(n) = (n_1, .., n_d)$ and V_d is the volume of the compactified space

$$V_d = (2\pi R)^d. \tag{7.24}$$

From the ansatz (7.23) the retarded Greens function for eq. (7.7) is found by the reverse transformation of the solution in Fourier space

$$\begin{aligned} G^{3+d}_{\rm ret}(t, \boldsymbol{x}, y) = & \frac{-1}{(2\pi)^4\sqrt{V_d}} \sum_{(n)} \int d^3\boldsymbol{k} \int dk_0 \, e^{i\boldsymbol{k}\boldsymbol{x}} e^{-ik_0(t)} e^{i\sum_i \frac{n^i y_i}{R}} \\ & \times \frac{1}{(k_0 - i\epsilon)^2 - \boldsymbol{k}^2 - \sum_i \frac{n^i y_i}{R}} \quad . \end{aligned} \tag{7.25}$$

After performing a contour integral for $\int dk_0$ and the angular integrals from $d^3\boldsymbol{k} = |\boldsymbol{k}|^2 \cos(\beta) d|\boldsymbol{k}| \, d\alpha \, d\beta$ one is left with

$$\begin{aligned} G^{3+d}_{\rm ret}(t, \boldsymbol{x}, y) = & \frac{1}{(2\pi)^2\sqrt{V_d}} \sum_{(n)} \int d|\boldsymbol{k}| \exp(i \sum_i \frac{n^i y_i}{R}) \\ & \times \frac{\theta(t)|\boldsymbol{k}| \sin\left(t\sqrt{|\boldsymbol{k}|^2 + \sum_i \frac{n^i}{R}}\right) \sin(|\boldsymbol{k}||\boldsymbol{x}|)}{|\boldsymbol{x}|\sqrt{|\boldsymbol{k}|^2 + \sum_i \frac{n^i}{R}}} \quad . \end{aligned} \tag{7.26}$$

Due to the non-trivial factors $\sqrt{|\boldsymbol{k}|^2 + \sum_i \frac{n^i y_i}{R}}$, the integral $\int d|\boldsymbol{k}|$ can not be performed in general. Still from eq. (7.26) the long wave length limit $\omega \to 0$ can be obtained by taking the $(n) = (0, ...0)$ part of $\sum_{(n)}$. This corresponds to the case of mass-less gravitons in field theory where the integral $\int d|\boldsymbol{k}|$ can be performed and gives

$$G^{3+d}_{\rm ret}(t, \boldsymbol{x}, y)|_{n=0} = \frac{1}{4\pi\sqrt{V_d}} \frac{\delta(t - |\boldsymbol{x}|)}{|\boldsymbol{x}|}. \tag{7.27}$$

So it has been shown that in the long wave length limit $\omega \to 0$ the polarization tensor (7.21) has to approach

$$e_{MN}(x, \omega)_{\omega \to 0} \to N \frac{1}{4\pi\sqrt{2\pi}\sqrt{V_d}} \frac{1}{|\underline{x}|} \hat{\mathcal{S}}_{MN}(\omega) + c.c. \tag{7.28}$$

and therefore

$$\frac{1}{(2\pi)^{d/2}} \sum_{j=0}^{d/2} K_d(|\underline{x}|, j) \Big|_{\omega \to 0} \to \frac{1}{(2\pi)^{d/2}} K_d(|\underline{x}|, 0) = \frac{1}{\sqrt{V_d}} \quad . \tag{7.29}$$

7.1.3 The energy and momentum of a gravitational wave

In this subsubsection the energy momentum tensor t_{MN} of the gravitational wave given in Eq. (7.20) will be derived. When we derived eq. (7.2) only the first order contributions of h in R_{MN} were included. Considering the approximate solution eq. (7.8) in the complete field equations Eq. (4.9) one finds the energy momentum tensor t_{MN} of the gravitational wave eq. (7.8). Expanding and rearranging eq. (4.9) with $R^{(1)}_{MN} - 1/2\eta_{MN}R^{(1)}$ gives

$$\begin{aligned} R^{(1)}_{MN} - \tfrac{1}{2}\eta_{MN}R^{(1)} = \; & -8\pi G \left[T_{MN} + \tfrac{1}{8\pi G}(R_{MN} - \tfrac{1}{2}\eta_{MN}R \right. \\ & \left. -R^{(1)}_{MN} + \tfrac{1}{2}\eta_{MN}R^{(1)})\right] \quad . \end{aligned} \tag{7.30}$$

Now the energy momentum tensor of eq. (7.16) can be defined.

$$t_{MN} := \frac{1}{8\pi G}(R_{MN} - \frac{1}{2}\eta_{MN}R - R^{(1)}_{MN}\frac{1}{2}\eta_{MN}R^{(1)}) \quad , \tag{7.31}$$

and the total energy momentum tensor of the gravitational wave becomes

$$\tau_{MN} = T_{MN} + t_{MN} \quad . \tag{7.32}$$

The total energy momentum tensor in eq. (7.32) consists of two parts: the energy momentum tensor of the source T_{MN} and the energy momentum tensor t_{MN} of the propagating wave itself. In order to evaluate eq. (7.31), the $3+d$-dimensional Riemann tensor Eq. (7.3) has to be expanded to second order in h. Noting that

$$\begin{aligned} R_{AB} &= R^{(1)}_{AB} + R^{(2)}_{AB} + \mathcal{O}(h^3), \\ R &= g^{AB}R_{AB} = \eta^{AB}R^{(1)}_{AB} + \eta^{AB}R^{(2)}_{AB} + h^{AB}R^{(1)}_{AB} + \mathcal{O}(h^3), \\ R^{A(1)}_{A} &= \eta^{AB}R^{(1)}_{AB} \quad , \end{aligned} \tag{7.33}$$

eq. (7.31) takes the form

$$t_{MN} = \frac{1}{8\pi G}\left[R^{(2)}_{MN} - \frac{1}{2}h_{MN}R^{(1)} - \frac{1}{2}\eta_{MN}(\eta^{AB}R^{(2)}_{AB} + h^{CD}R^{(1)}_{CD})\right] + \mathcal{O}(h^3). \tag{7.34}$$

For the freely propagating gravitational wave, the metric $g_{MN} = \eta_{MN} + h_{MN}$ satisfies the first-order Einstein equation $R^{(1)}_{MN} = 0$. The first order terms in Eq. (7.34) drop out and Eq. (7.34) simplifies to

$$t_{MN} = \frac{1}{8\pi G}\left[R^{(2)}_{MN} - \frac{1}{2}\eta_{MN}\eta^{AB}R^{(2)}_{AB}\right] + \mathcal{O}(h^3). \tag{7.35}$$

The next task is to derive the h dependence of $R^{(2)}_{MN}$. First we calculate the h^2 dependence of Δ_{MN} in eq. (7.3). As the Christoffel symbols (Γ) in Δ_{MN} (see Eq. (7.3)) contain derivatives of the metric G_{MN} and Δ_{MN} is proportional to Γ^2, the second order part of Δ_{MN} contains only terms of the form $(\partial h)(\partial h)$ in particular

$$\begin{aligned}\Delta^{(2)}_{MN} = \tfrac{1}{4} \quad & \Big[(2\partial_L h^L_S - \partial_S h^{\grave{L}}_{\grave{L}})(\partial_M h^S_P + \partial_M h^S_P - \partial^S h_{MN}) \\ & -(\partial_N h^L_S + \partial^L h_{NP} - \partial_S h^L_N)(\partial_M h^S_L + \partial_L h^S_M - \partial^S h_{ML})\Big] \ .\end{aligned} \tag{7.36}$$

The first part of eq. (7.3) contributes with terms proportional to h times second derivatives of h, in particular

$$\begin{aligned}R^{(2)}_{MN}\Big|^{\text{first}}_{\text{part}} &= h^{LS} R^{(1)}_{MLSN} \\ &= \tfrac{1}{2} h^{LS}(\partial_M \partial_N h_{LS} - \partial_L \partial_M h_{NS} - \partial_S \partial_N h_{ML} + \partial_L \partial_S h_{MN}) \quad .\end{aligned} \tag{7.37}$$

Combining eq. (7.36) and (7.37) one obtains the second order of R in h

$$\begin{aligned}R^{(2)}_{MN} &= R^{(2)}_{MN}\Big|^{\text{first}}_{\text{part}} + \Delta^{(2)}_{MN} \\ &= \tfrac{1}{2} h^{LS}(\partial_M \partial_N h_{LS} - \partial_L \partial_M h_{NS} - \partial_S \partial_N h_{ML} + \partial_L \partial_S h_{MN}) + \\ &\quad \Big[(2\partial_L h^L_S - \partial_S h^{\grave{L}}_{\grave{L}})(\partial_M h^S_P + \partial_M h^S_P - \partial^S h_{MN}) \\ &\quad -(\partial_N h^L_S + \partial^L h_{NP} - \partial_S h^L_N)(\partial_M h^S_L + \partial_L h^S_M - \partial^S h_{ML})\Big] \ .\end{aligned} \tag{7.38}$$

Now one uses the plane wave solution eq. (7.19) and inserts it into eq. (7.38) and (7.35). This yields a quite lengthy result which depends on the phase factors from eq. (7.19). However, averaging over a spatial region that is large compared to $1/|k|$ one can integrates out these phase factors. The average is indicated by the $\langle \dots \rangle$ brackets. By using $k_L k^L = 0$ and the harmonic coordinate system condition eq. (7.6), the averaged energy momentum tensor of a plane gravitational wave is obtained:

$$\begin{aligned}\langle t_{MN} \rangle &= \langle R^{(2)}_{MN} \rangle \\ &= \tfrac{k_M k_N}{16\pi G}(\langle e^{SL*}(\underline{x},\tau) e_{SL}(\underline{x},\tau)\rangle - \tfrac{1}{2}|\langle e^L_L \rangle|^2) \quad .\end{aligned} \tag{7.39}$$

Note that eq. (7.39) still depends on the polarisation tensor e_{MN}. The polarisation tensor itself depends on the energy momentum tensor of the given source.

7.1.4 Energy momentum tensor of a quasi-elastic collision

In this subsubsection the focus will be on the energy momentum tensor of collisions of standard model particles. As discussed in the previous subsubsection, this tensor is needed, because it defines the source term for the gravitational wave production eq. (7.18). In the ADD model [38] all standard model particles are confined to a 3-brane. Thus, the total energy momentum tensor for one of the standard model particles is defined using a δ-function on the extra-dimensional part of the $3+d$ dimensional brane coordinates [1](see e.g. [35, 36]),

$$T_{MN}(x) = \eta^{\mu}_{M}\eta^{\nu}_{N}T_{\mu\nu}(x)\delta^{d}(x_{\perp}) \quad . \tag{7.40}$$

The energy momentum tensor can be decomposed into an incoming and outgoing part

$$T_{MN} = T^{(in)}_{MN} + T^{(out)}_{MN} \quad . \tag{7.41}$$

The incoming and outgoing energy momentum tensors are given in terms of the 4-momenta of C colliding particles

$$\begin{aligned} T^{(in)}_{MN} &= \delta^{(d)}(x_{\perp})\eta_{M\mu}\eta_{N\nu}\sum_{j=1}^{C}\frac{P^{\mu}_{(j)}P^{\nu}_{(j)}}{P^{0}_{(j)}}\delta^{(3)}(x_{\parallel}-v_{(j)\parallel}t)\theta(-t) \\ &=: \delta^{(d)}(x_{\perp})\eta_{M\mu}\eta_{N\nu}T^{\mu\nu}_{(in)} \\ T^{(out)}_{MN} &= \delta^{(d)}(x_{\perp})\eta_{M\mu}\eta_{N\nu}\sum_{j=1}^{C}\frac{P^{\mu}_{(j)}P^{\nu}_{(j)}}{P^{0}_{(j)}}\delta^{(3)}(x_{\parallel}-v_{(j)\parallel}t)\theta(t) \\ &=: \delta^{(d)}(x_{\perp})\eta_{M\mu}\eta_{N\nu}T^{\mu\nu}_{(out)}. \end{aligned} \tag{7.42}$$

The source term eq. (4.12) for incoming states is therefore

$$\begin{aligned} \mathcal{S}^{(in)}_{MN}(t,x) &= T^{(in)}_{MN} - \tfrac{1}{2+d}\eta_{MN}T^{(in)L}_{L} \\ &= \delta^{(d)}(x_{\perp})(\eta_{M\mu}\eta_{N\nu} - \tfrac{1}{2+d}\eta_{MN}\eta_{\mu\nu})T^{\mu\nu}_{(in)}(t,x_{\parallel}). \end{aligned} \tag{7.43}$$

The incoming and the outgoing $\mathcal{S}_{MN}$ will now be used as source terms for the induced gravitational wave eq. (7.20). In order to calculate the polarisation tensor of the wave Eq. (7.20) one has to perform the $3+d$ dimensional y integral

$$\begin{aligned} \hat{\mathcal{S}}_{MN}(\omega) &= \int d^{3}y_{\parallel}d^{d}y_{\perp}\mathcal{S}_{MN}(\omega,y)\exp\left(-i\omega\underline{y}\tfrac{\underline{x}}{|\underline{x}|}\right) \\ &= \tfrac{1}{\sqrt{2\pi}}\int d\tilde{t}\int d^{3}y_{\parallel}d^{d}y_{\perp}\mathcal{S}_{MN}(\tilde{t},y)\exp\left(-i\omega(\tilde{t}+\underline{y}\tfrac{\underline{x}}{|\underline{x}|})\right) \quad . \end{aligned} \tag{7.44}$$

[1]One should note, that in models different from the ADD or RS setting (e.g. those with universal extra dimensions (UXD) [33, 139]) this delta function restriction is not needed. The discussion presented in this subsubsection can easily be translated to models of this type as well.

For the incoming particles, as well as for the outgoing particles the δ-function in eq. (7.43) simplifies the integral. The last part of eq. (7.44) reads

$$\begin{aligned}\int d^3y_\parallel d^dy_\perp \quad & \mathcal{S}_{MN}(\tilde{t},y)\exp\left(-i\omega\underline{y}\tfrac{\underline{x}}{|\underline{x}|}\right) = \int d^3y_\parallel d^dy_\perp \mathcal{S}^{(in)}_{MN}(\tau,\underline{y})\exp\left(-i\omega\underline{y}\tfrac{\underline{x}}{|\underline{x}|}\right)\\ = \quad & (\eta_{M\mu}\eta_{N\nu}-\tfrac{1}{2+d}\eta_{MN}\eta_{\mu\nu})\sum_{j=1}^{C}\frac{P^\mu_{(j)}P^\nu_{(j)}}{P^0_{(j)}}\int d^3y_\parallel\delta^{(3)}(y_\parallel-v_{(j)\parallel}\tau)\\ & \times\theta(-\tau)\exp\left(-i\omega\underline{y}\tfrac{\underline{x}}{|\underline{x}|}\right)\\ =: \quad & (\eta_{M\mu}\eta_{N\nu}-\tfrac{1}{2+d}\eta_{MN}\eta_{\mu\nu})\sum_{j=1}^{C}\frac{P^\mu_{(j)}P^\nu_{(j)}}{P^0_{(j)}}J^{(in)} \quad .\end{aligned} \tag{7.45}$$

After some transformations, $J^{(in)}$ can be cast in a form compatible with the Fourier decomposition of h_{MN}:

$$\begin{aligned}J^{(in)} &= \int d^3y_\parallel\delta^{(3)}((y_\parallel-v_{(j)\parallel}\tau)\theta(-\tau))\exp\left(-i\omega\underline{y}\tfrac{\underline{x}}{|\underline{x}|}\right)\\ &= \int d^3y_\parallel\int\tfrac{d^3k_\parallel}{(2\pi)3}\exp\left(ik_\parallel(y_\parallel-v_{(j)}\tau)\right)\int\tfrac{d\omega_0}{-2\pi i}\frac{e^{-i\omega_0\tau}e^{-i\omega\underline{y}\frac{\underline{x}}{|\underline{x}|}}}{\omega_0-i\epsilon}\\ &= \int d^3y_\parallel\int\tfrac{d^3k_\parallel}{(2\pi)3}\exp\left(ik_\parallel(y_\parallel)\right)\int\tfrac{d\omega_0}{-2\pi i}\frac{e^{-i(\omega_0+v_{(j)}k_\parallel)\tau}e^{-i\omega\underline{y}\frac{\underline{x}}{|\underline{x}|}}}{\omega_0-i\epsilon}\\ &= \int d^3y_\parallel\int\tfrac{d^3k_\parallel}{(2\pi)3}\exp\left(ik_\parallel(y_\parallel)\right)\int\tfrac{d\tilde{\omega}}{-2\pi i}\frac{e^{-i(\tilde{\omega})\tau}e^{-i\omega\underline{y}\frac{\underline{x}}{|\underline{x}|}}}{\tilde{\omega}-k_\parallel v_{(j)}-i\epsilon}\\ &= \int d\tilde{\omega}e^{-i\tilde{\omega}\tau}\int\tfrac{d^3k_\parallel}{-i(2\pi)4}\int d^3y_\parallel\frac{e^{ik_\parallel y_\parallel}e^{-i\omega\underline{y}\frac{\underline{x}}{|\underline{x}|}}}{\tilde{\omega}-k_\parallel v_{(j)}-i\epsilon} \quad .\end{aligned} \tag{7.46}$$

Here, first the Fourier transforms of the δ-function and the θ-function are used, then the terms under the integrals are rearranged and the substitution $\tilde{\omega}:=\omega_0+k_\parallel v_{(j)}$ is introduced. Now the definition of the Fourier transform of the δ-function is used in order to evaluate the two three-dimensional integrals

$$\begin{aligned}J^{(in)} &= \int d\tilde{\omega}e^{-i\tilde{\omega}\tau}\int\tfrac{d^3k_\parallel}{-i(2\pi)4}\frac{1}{\tilde{\omega}-k_\parallel v_{(j)}-i\epsilon}\int d^3y_\parallel\exp\left(-i(\omega\tfrac{x_\parallel}{|x_\parallel|}-k_\parallel)y_\parallel\right)\\ &= \int d\tilde{\omega}e^{-i\tilde{\omega}\tau}\frac{1}{-i2\pi}\frac{1}{\tilde{\omega}-\underline{k}v_{(j)}-i\epsilon} \quad .\end{aligned} \tag{7.47}$$

From $\underline{k}v_{(j)}=k_\parallel v_{(j)}$, $k_\parallel$ can be replaced by $\underline{k}$. For outgoing particles the procedure is similar, however here one has to use the Fourier transform of $\theta(-t)$

$$J^{(out)} = -\int d\tilde{\omega}e^{-i\tilde{\omega}\tau}\frac{1}{-i2\pi}\frac{1}{\tilde{\omega}-\underline{k}v_{(j)}+i\epsilon} \quad . \tag{7.48}$$

We see that the difference between the incoming and outgoing J can be expressed by a change of the sign of J and ϵ. These results can be inserted back into Eq. (7.45). For high energetic particles the denominator is $P^0_{(j)}(\omega-\underline{k}v_{(j)})=k\cdot P_{(j)}$. As this is positive one can drop the ϵ. Using equations (7.44, 7.45, 7.47, 7.48) one finally obtains the source term eq. (7.49) for the incoming

particles

$$\hat{\mathcal{S}}^{(in)}_{MN}(\omega) =: \hat{T}^{(in)}_{MN} - \eta_{MN}\hat{T}^{(in)L}_{L} = (\eta_{M\mu}\eta_{N\nu} - \frac{1}{2+d}\eta_{MN}\eta_{\mu\nu})\sum_{j=1}^{C}\frac{P^{\mu}_{(j)}P^{\nu}_{(j)}}{P_{(j)}k} \tag{7.49}$$

and for the outgoing particles

$$\hat{\mathcal{S}}^{(out)}_{MN}(\omega) =: \hat{T}^{(out)}_{MN} - \eta_{MN}\hat{T}^{(out)L}_{L} = -(\eta_{M\mu}\eta_{N\nu} - \frac{1}{2+d}\eta_{MN}\eta_{\mu\nu})\sum_{j=1}^{C}\frac{P^{\mu}_{(j)}P^{\nu}_{(j)}}{P_{(j)}k} \quad . \tag{7.50}$$

7.1.5 Gravitational radiation from quasi-elastic scattering

Based on the discussion in the previous subsections let us now calculate the classically radiated energy into gravitational waves from a quasi-elastic scattering.

7.1.6 Radiated energy and the energy momentum tensor

The momentum P^i of an extended object is defined as the volume integral over the density of the t^{0i} component of the energy momentum tensor. In $3+d$ dimensions this is

$$P^i = \int_V d^{3+d}x t^{0i} \quad . \tag{7.51}$$

The energy change in time $dE/d\tau$ of a system can be rewritten by using the conservation of the energy momentum tensor

$$\frac{dE}{d\tau} = \int_V d^{3+d}x\, \partial_0 t^{00} = \int_V d^{3+d}x\, \partial_i t^{0i} = \partial_i P^i \quad . \tag{7.52}$$

Applying Gauss law to $\partial_i P^i$ and using eq. (7.51) gives

$$\partial_i P^i = \int_V d^{3+d}x\, \partial_i P^i = \int_{\mathcal{O}(V)} dS\, n_i t^{0i} = \int_{\mathcal{O}(V_E)} d\Omega\, |x|^{2+d} n_i t^{0i} \quad . \tag{7.53}$$

By differentiating eq. (7.52) by $d\Omega$, averaging over the space, integrating over $d\tau$ and using eq. (7.53) one obtains the average energy radiated into the spatial element $d\Omega$

$$\frac{d\langle E\rangle}{d\Omega} = \int d\tau \frac{\langle \partial_i P^i\rangle}{d\Omega} = \int d\tau |x|^{2+d} n_i \langle t^{0i}\rangle \quad . \tag{7.54}$$

7.1.7 Radiated gravitational energy

Using the general relation between radiated energy and the energy momentum tensor t^{MN} (see previous subsubsection) we can now quantify how much energy is radiated away by the gravitational wave. Therefore, one has to insert the energy momentum tensor of this wave Eq. (7.39) into Eq. (7.54). In the Fourier formulation of eq. (7.54) one uses eq. (7.39) and $k_0^2 = k_i^2 = \omega$. This gives

$$\begin{aligned} \frac{dE}{d\Omega} &= \frac{1}{2\pi}\int\int\int d\tau d\tilde{\omega} d\omega |\underline{x}|^{2+d} \frac{\tilde{\omega}\omega}{16\pi G}(\langle e^{SL*}(\underline{x},\omega) e_{SL}(\underline{x},\tilde{\omega})\rangle \\ &\quad -\frac{1}{2}\langle e_L^{L*}(\underline{x},\omega)\rangle\langle e_L^L(\underline{x},\tilde{\omega})\rangle) e^{i\tau(\tilde{\omega}-\omega)} \\ &= \int d\omega |\underline{x}|^{2+d}\frac{\omega^2}{16\pi G}(\langle e^{SL*}(\underline{x},\omega) e_{SL}(\underline{x},\omega)\rangle - \frac{1}{2}|\langle e_L^L(\underline{x},\omega)\rangle|^2) \quad . \end{aligned} \tag{7.55}$$

Moving $d\omega$ to the l.h.s gives

$$\begin{aligned} \frac{dE}{d\Omega d\omega} &= |x|^{2+d} n_i \langle t^{0i}\rangle \\ &= |x|^{2+d}\frac{\omega^2}{16\pi}(\langle e^{SL*}(\underline{x},\omega) e_{SL}(\underline{x},\omega)\rangle - \frac{1}{2}|\langle e_L^L\rangle|^2) \quad . \end{aligned} \tag{7.56}$$

Next, the relation $\omega = |k^0| = |n_i k^i|$ and from Eq. (7.21) can be used to get the polarisation tensors e_{MN} of the radiated gravitational wave,

$$\langle e_{MN}(\underline{x},\omega)\rangle = N\frac{1}{4\pi}\frac{1}{(2\pi)^{d/2}\sqrt{2\pi}}\hat{\mathcal{S}}_{MN}(\omega)\langle\sum_{j=0}^{d/2} K(|\underline{x}|,j)\frac{1}{|\underline{x}|}(i\omega)^j\rangle, \tag{7.57}$$

by defining $\hat{\mathcal{S}}_{MN}(\omega) := (\hat{T}_{MN}(\omega) - 1/(2+d)\eta_{MN}\hat{T}_L^L(\omega))$, which is the Fourier transform of $(\hat{\mathcal{S}}_{MN}(\tau)^{(in)} + \hat{\mathcal{S}}_{MN}(\tau)^{(out)})$ (c.f. Eq. (7.45)). The $\langle e^{MN} e^*_{MN}\rangle$ part of Eq. (7.56) gives by using Eq. (7.57)

$$\begin{aligned} \langle e^{SL*}(\underline{x},\omega) e_{SL}(\underline{x},\omega)\rangle = \; & \frac{N^2}{32\pi(2\pi)^d}\sum_{j,k=0}^{d/2}\langle K(|\underline{x}|,j)K(|\underline{x}|,k)\frac{1}{|\underline{x}|^2}(i\omega)^{j+k}\rangle \\ & \hat{\mathcal{S}}^{SL}(\omega)\hat{\mathcal{S}}^*_{SL}(\omega) \\ & = \frac{8G^2}{\pi(2\pi)^d}\sum_{j,k=0}^{d/2}\langle K(|\underline{x}|,j)K(|\underline{x}|,k)\frac{1}{|\underline{x}|^2}(i\omega)^{j+k}\rangle \\ & (\hat{T}^{SL}(\omega)\hat{T}^*_{SL}(\omega) - \frac{d}{(2+d)^2}|T_K^K|^2) \quad . \end{aligned} \tag{7.58}$$

Proceeding the same way with $|\langle e_L^L\rangle|^2$ one finds

$$\begin{aligned} |\langle e_L^L\rangle|^2 = \; & \frac{8G^2}{\pi(2\pi)^d}\sum_{j,k=0}^{d/2}\langle K(|\underline{x}|,j)K(|\underline{x}|,k)\frac{1}{|\underline{x}|^2}(i\omega)^{j+k}\rangle\ \hat{\mathcal{S}}_N^N\hat{\mathcal{S}}_L^{L*} \\ = \; & \frac{8G^2}{\pi(2\pi)^d}\sum_{j,k=0}^{d/2}\langle K(|\underline{x}|,j)K(|\underline{x}|,k)\frac{1}{|\underline{x}|^2}(i\omega)^{j+k}\rangle\ |T_L^L|^2(\frac{2}{2+d})^2 \quad . \end{aligned} \tag{7.59}$$

Evaluating the T terms in eq. (7.59) and (7.58) separately leads to

$$\hat{T}^{SL}\hat{T}^{*}_{SL} = (\hat{T}^{(in)SL} + \hat{T}^{(out)SL})(\hat{T}^{(in)*}_{SL} + \hat{T}^{(out)*}_{SL}) \quad . \tag{7.60}$$

In the notation of eq. (7.49) and (7.50) this is a rather lengthy expression. To simplify this, one sums over all involved states instead of initial and final states separately ($\sum_i + \sum_j$) and uses that every outgoing state contributes one $-$ sign. After defining

$$\eta_I = \begin{cases} +1 & \text{for a particle in the initial state} \quad , \\ -1 & \text{for a particle in the final state} \quad , \end{cases} \tag{7.61}$$

this gives

$$\hat{T}^{MN} = \eta^{M\mu}\eta^{N\nu} \sum_I \frac{P_{(I)\mu}P_{(I)\nu}\eta_I}{kP_{(I)}} \quad . \tag{7.62}$$

In this notation one finds

$$\hat{T}^{SL}\hat{T}^{*}_{SL} = \sum_{I,J} \frac{(P^{\mu}_{(I)}P_{(J)\mu})^2\eta_I\eta_J}{(P_{(I)}k)(P_{(J)}k)} \quad , \tag{7.63}$$

and

$$\hat{T}^{L}_{L}\hat{T}^{S*}_{S} = \sum_{I,J} \frac{P^2_{(I)}\,P^2_{(J)}\eta_I\eta_J}{(P_{(I)}k)(P_{(J)}k)} \quad . \tag{7.64}$$

The last two equations are inserted into eq. (7.58 and 7.56) to derive the energy carried by the induced gravitational radiation

$$\begin{aligned} \frac{dE}{d\Omega d\omega} = \; & \frac{G|\underline{x}^{2+d}|}{2\pi^2(2\pi)^d} \sum_{j,k=0}^{d/2} \langle K(|\underline{x}|,j)K(|\underline{x}|,k)\tfrac{1}{|\underline{x}|^2}(i\omega)^{j+k}\rangle \\ & \sum_{I,J} \tfrac{\eta_I\eta_J}{(P_{(I)}k)(P_{(J)}k)} \left[(P^{\mu}_{(I)}P_{(J)\mu})^2 - \tfrac{1}{2+d}P^2_{(I)}\,P^2_{(J)}\right] \end{aligned} \quad . \tag{7.65}$$

For the cases with even extra dimensions $d = 0, 2, 4, 6$ equation Eq. (7.65) explicitly gives

$$\begin{aligned}
\frac{dE(d=0)}{d\Omega d\omega} &= \frac{G_0}{2\pi^2}\omega^2 \sum_{I,J} \frac{\eta_I \eta_J}{(P_{(I)}k)(P_{(J)}k)} \left[(P^\mu_{(I)} P_{(J)\mu})^2 - \frac{1}{2} P^2_{(I)}\, P^2_{(J)} \right] \\
\frac{dE(d=2)}{d\Omega d\omega} &= \frac{G_2}{8\pi^4} \left(\omega^4 + 2\frac{\omega^3}{|\underline{x}|} + \frac{\omega^2}{|\underline{x}|^2} \right) \\
&\quad \sum_{I,J} \frac{\eta_I \eta_J}{(P_{(I)}k)(P_{(J)}k)} \left[(P^\mu_{(I)} P_{(J)\mu})^2 - \frac{1}{4} P^2_{(I)}\, P^2_{(J)} \right] \\
\frac{dE(d=4)}{d\Omega d\omega} &= \frac{G_4}{32\pi^6} \left(\omega^6 + 6\frac{\omega^5}{|\underline{x}|} + 15\frac{\omega^4}{|\underline{x}|^2} + 18\frac{\omega^3}{|\underline{x}|^3} + 9\frac{\omega^2}{|\underline{x}|^4} \right) \\
&\quad \sum_{I,J} \frac{\eta_I \eta_J}{(P_{(I)}k)(P_{(J)}k)} \left[(P^\mu_{(I)} P_{(J)\mu})^2 - \frac{1}{6} P^2_{(I)}\, P^2_{(J)} \right] \\
\frac{dE(d=6)}{d\Omega d\omega} &= \frac{G_6}{128\pi^8} \left(\omega^8 + 12\frac{\omega^7}{|\underline{x}|} + 66\frac{\omega^6}{|\underline{x}|^2} + 210\frac{\omega^5}{|\underline{x}|^3} + 405\frac{\omega^4}{|\underline{x}|^4} \right. \\
&\quad \left. +450\frac{\omega^3}{|\underline{x}|^5} + 225\frac{\omega^2}{|\underline{x}|^6} \right) \sum_{I,J} \frac{\eta_I \eta_J \left[(P^\mu_{(I)} P_{(J)\mu})^2 - \frac{1}{8} P^2_{(I)}\, P^2_{(J)} \right]}{(P_{(I)}k)(P_{(J)}k)} \quad ,
\end{aligned} \tag{7.66}$$

with G_d being the d-dimensional gravitational constant. In the limit without extra dimensions ($d = 0$), eq. (7.66) agrees with the well known result given by Weinberg [14]. For $d > 0$ one obtains additional contributions: There is always a ω^{d+2} dependence and there are terms with the same mass dimension, but containing a $\omega^{d+2-i}/|\underline{x}|^i$ dependence. For an uncompactified $3 + d$-dimensional space the additional terms vanish for a distant observer and only the ω^{2+d} term survives, in line with [138].

7.2 Matching the obtained cross sections to compactified spaces

The compactification of the d extra dimensions is expected to have two consequences on eq. (7.66).

- The first is the change of the gravitational coupling $G \to G_d = \frac{1}{\bar{M}_D^{2+d}}$.
- The second is the change in the ω dependence of the cross section. To calculate the ω dependence in a compactified space one has to fulfill periodical boundary conditions and use the Greens function given in

eq. (7.26). Unfortunately the integrals in (7.26) only allow direct integration for two extreme regimes ($\omega \to 0$) and ($\omega \to \infty$). Therefore, eq. (7.66) has to be used as an effective model for the intermediate regimes and take $|\underline{x}|$ as the parameter of this model. This parameter is fixed by demanding, that the case without extra dimensions is the long wave length limit ($\omega \to 0$) of the kinematical part of (7.66)

$$\begin{aligned} \lim_{\omega\to 0}\int dV_E\, d\frac{dE(d)}{d\Omega_{3+d}d\omega} &= \frac{dE(d=0)}{d\Omega_3 d\omega} \\ \text{lowest order in}\,\omega^{\mathrm{i}} &\Rightarrow \\ |\underline{x}| &= \begin{cases} 2\pi R & \text{for} \quad d=2 \\ 2\pi R\sqrt{3} & \text{for} \quad d=4 \\ 2\pi R\sqrt[3]{15} & \text{for} \quad d=6\ . \end{cases} \end{aligned} \tag{7.67}$$

Those values for the parameter $|\underline{x}|$ support the intuitive guess that $|\underline{x}|$ has to be of the order of the compactification perimeter.

From those two arguments one finds the radiated energy in models with compactified extra dimensions

$$\begin{aligned} \tfrac{dE(d=0)}{d\Omega d\omega} &= \tfrac{1}{\tilde{M}_P^2}\tfrac{4}{\pi}\omega^2 \sum_{I,J}\tfrac{\eta_I\eta_J}{(P_{(I)}k)(P_{(J)}k)}\left[(P^\mu_{(I)}P_{(J)\mu})^2 - \tfrac{1}{2}P^2_{(I)}\,P^2_{(J)}\right] \\ \tfrac{dE(d=2)}{d\Omega d\omega} &= \tfrac{1}{\tilde{M}_D^4}\tfrac{1}{\pi^3}\left(\omega^4 + 2\tfrac{\omega^3}{|2\pi R|} + \tfrac{\omega^2}{|2\pi R|^2}\right)\sum_{I,J}\tfrac{\eta_I\eta_J}{(P_{(I)}k)(P_{(J)}k)} \\ &\quad \left[(P^\mu_{(I)}P_{(J)\mu})^2 - \tfrac{1}{4}P^2_{(I)}\,P^2_{(J)}\right] \\ \tfrac{dE(d=4)}{d\Omega d\omega} &= \tfrac{1}{\tilde{M}_D^6}\tfrac{1}{4\pi^5}\left(\omega^6 + \tfrac{6\omega^5}{|2\pi R|\sqrt{3}} + \tfrac{5\omega^4}{|2\pi R|^2} + \tfrac{6\omega^3}{|2\pi R|^3\sqrt{3}} + \tfrac{\omega^2}{|2\pi R|^4}\right) \\ &\quad \sum_{I,J}\tfrac{\eta_I\eta_J\left[(P^\mu_{(I)}P_{(J)\mu})^2 - \frac{1}{6}P^2_{(I)}\,P^2_{(J)}\right]}{(P_{(I)}k)(P_{(J)}k)} \\ \tfrac{dE(d=6)}{d\Omega d\omega} &= \tfrac{1}{\tilde{M}_D^8}\tfrac{1}{16\pi^7}\left(\omega^8 + \tfrac{12\omega^7}{|2\pi R|\sqrt[3]{15}} + \tfrac{66\omega^6}{|2\pi R|^2 15^{2/3}} + \tfrac{14\omega^5}{|2\pi R|^3} + \tfrac{41\omega^4}{3|2\pi R|^4\sqrt[3]{15}}\right. \\ &\quad \left. + \tfrac{30\omega^3}{|2\pi R|^5 15^{2/3}} + \tfrac{\omega^2}{|2\pi R|^6}\right)\sum_{I,J}\tfrac{\eta_I\eta_J\left[(P^\mu_{(I)}P_{(J)\mu})^2 - \frac{1}{8}P^2_{(I)}\,P^2_{(J)}\right]}{(P_{(I)}k)(P_{(J)}k)}\quad . \end{aligned} \tag{7.68}$$

7.3 Physical relevance of the obtained cross section

From eq. (7.68) one sees that the radiated energy increases rapidly with ω. Therefore, a cut-off has to be used to estimate the amount of gravitationally radiated energy. In a $2 \to 2$ particle scattering process (radiating gravitational waves) the largest cut-off is reached as soon as the gravitational

radiation takes away the invariant energy $\sqrt{s}/2$ from one of the participants. The strongest suppression of the $1/R$ terms is reached when one takes this extreme value for ω. Limits on the compactification radius down to the μm range (depending on d) have been derived from a large number of physical observations [140, 141, 142, 143]. Thus, under the condition of

$$\omega \gg \frac{1}{2\pi R} \,, \tag{7.69}$$

eq. (7.68) transforms to the result previously obtained by [138]. This shows that the additional terms become important for small $\sqrt{s}$ or very large $\bar{M}_D$. For a particle scattering with invariant energy in the TeV range, $\bar{M}_D$ would have to be > 1000 TeV, for the new terms to be relevant. However, then the whole cross-section is suppressed by a factor $1/\bar{M}_D^{2+d}$ and would be negligible. Summarizing one can say that for quasi-elastic high energetic $N \to N$ particle collisions in models with large extra dimensions the energy loss into gravitational radiation stays as given in [138]:

$$\frac{dE}{d\Omega d\omega} = \frac{4}{\bar{M}_D^{2+d}} \frac{\omega^{2+d}}{\pi(2\pi)^d} \sum_{I,J} \frac{\eta_I \eta_J}{(P_{(I)}k)(P_{(J)}k)} \left[(P^\mu_{(I)} P_{(J)\mu})^2 - \frac{1}{2+d} P^2_{(I)} P^2_{(J)} \right] \quad .(7.70)$$

This result is valid for quasi-elastic $N \to N$ particle scattering with highly relativistic particle velocities so that the interaction can be approximated to be instantaneous. Although the discussed terms are negligible in the standard ADD setup, still they might become important for similar models on negatively curved manifolds [144, 145]. Equation (7.68) is derived from classical general relativity and gives an semi-quantitative estimate for the gravitationally radiated energy. A quantum calculation for example in the ADD model was not performed, but should be considered as the next step to do.

Chapter 8

Gravitational radiation from ultra high energetic cosmic rays

In this chapter the following notation will be used $4+d$ spacetime vectors will be $x = (x_0, \underline{x})$, where the spatial part can be split again into a three-dimensional and a d-dimensional part $\underline{x} = (\boldsymbol{x}, x_\perp)$. The figures in this chapter are taken from [146].

8.1 Gravitational radiation from quasi-elastic scattering with extra dimensions

First estimates to study effects of gravitational energy loss of CRs due to the presence of extra dimensions were explored by [147]. There, the presence of large extra dimensions was incorporated into the well known results from general relativity [14] by a change of the phase space seen by the emitted gravitational wave. The additional phase space factor for the emitted gravitational wave was given by

$$g_d(k_d) = \frac{(k_d R)^d}{d\Gamma(d/2)\pi^{d/2}2^{d-1}} \quad . \tag{8.1}$$

Note that $g_0 = 1$. Where R is the compactification radius of the extra dimensions in the ADD scenario given by [38]:

$$R = M_f^{-\frac{d+2}{d}} M_{\mathrm{Pl}}^{\frac{2}{d}} \quad . \tag{8.2}$$

Here, M_f is the new fundamental scale and M_{Pl} is the four-dimensional Planck mass related to the gravitational constant by $G_{\mathrm{N}} = 1/M_{\mathrm{Pl}}^2$.

This method led to a strong modification of the reconstructed energy spectrum and the authors concluded that the steepening of the CR energy spectrum around $10^{15.5}$ eV (the "knee") might be due to gravitational energy loss.

However, from our present studies (see also [138]) it seems that a calculation of the effects of the gravitational energy loss requires a more elaborate treatment as will be discussed now. The simplified treatment can be improved by direct calculation of the gravitational energy loss in a $N \to M$ scattering process as given by [138, 148]:

$$\frac{dE}{d\Omega_{3+d}dk_0} = \frac{1}{M_f^{2+d}} \frac{k_0^{2+d}}{2(\pi)^2(2\pi)^d} \sum_{I,J} \frac{\eta_I \eta_J \left[(P^\mu_{(I)} P_{(J)\mu})^2 - \frac{1}{2+d} P^2_{(I)}\, P^2_{(J)} \right]}{(P_{(I)}k)(P_{(J)}k)} \quad , \tag{8.3}$$

The $P_{(N)}$ are the momenta of the colliding particles and the factors η_N are defined by

$$\eta_N = \begin{cases} -1 & \text{for initial state particles} \quad . \\ +1 & \text{for final state particles} \quad . \end{cases} \tag{8.4}$$

Thus, in the case of a $2 \to 2$ collision the index N runs from 1 to 4. Before continuing, one has to point out that equation (7.70) follows from classical considerations and is not derived from any form of quantum theory of gravity (e.g. loop quantum gravity, SUGRA or string theory). However, we believe that it can account - at least semi-quantitatively - for the major effects of the gravitational energy loss.

Eqation (7.70) was integrated with the help of the Mathematica package FeynCalc [149, 150]. Difficulties for the $d\Omega_{3+d}$ integration arise from the $P \cdot k$ terms in the numerator. The protons are bound to the brane and the product $P \cdot k$ gives for example for one of the incoming protons:

$$P_1 \cdot k = P_1^0 k_0 - \boldsymbol{p_1 k} - 0 = |\boldsymbol{p}| k_0 \left(\sqrt{1 + \frac{m_p^2}{|\boldsymbol{p}^2|}} - \sqrt{1 - \frac{k_d^2}{k_0^2}} \cos\phi_k \right) \quad . \tag{8.5}$$

For $k_d^2/k_0^2 \approx 0$ and $\phi_k \approx 0$, $P_1 \cdot k$ becomes small and the denominator in eq. (7.70) is only regularized by $m_p^2/|\boldsymbol{p}^2|$, with m_p being the proton mass.

We introduce the Mandelstam variables s, t and u by

$$s = (P_1 + P_2)^2, \quad t = (P_1 - P_3)^2, \quad u = (P_1 - P_4)^2 \quad . \tag{8.6}$$

It is convenient to perform a coordinate transformation to rewrite eq. (7.70) in terms of spherical coordinates in three-dimensional space and the d extra-dimensional coordinates separately:

$$\frac{dE}{dk_0 d\Omega_{3+d}} = \frac{k^{d+2} dE}{dk^{3+d}} = \frac{k^{d+2} dE}{dk^d dk^3} = \frac{(\boldsymbol{k}^2 + k_d^2)^{(d+2)/2} dE}{\boldsymbol{k}^2 d\boldsymbol{k} d\Omega_3 |k_d|^{d-1} dk_d d\Omega_d} \quad . \tag{8.7}$$

Solving this for the new integration variables yields

$$\frac{dE}{d\boldsymbol{k}d\Omega_3 dk_d d\Omega_d} = \frac{dE}{dk_0 d\Omega_{3+d}} \frac{\boldsymbol{k}^2 k_d^{d-1}}{(\boldsymbol{k}^2 + k_d^2)^{(d+2)/2}} \quad . \tag{8.8}$$

The first term on the right side can be approximated by eq. (7.70) as soon as the wavelength of the gravitational wave is smaller than the compactification radius R of the extra dimensions and the gravitational wave can propagate freely into the bulk. Rephrased as a condition for $|k|$ this constrained becomes

$$|k| > M_f \left(\frac{M_f^2}{M_{\rm Pl}^2}\right)^{\frac{1}{d}} \quad . \tag{8.9}$$

But this bound on $|k|$ is not relevant for the energy loss discussion, because the major contribution to the radiated energy comes from the high energy (i.e. large $|k|$) part. To calculate the energy loss due to the gravitational wave emission one has to perform the $d\Omega_3 = \sin\phi_{kz} d\phi_k d\phi_{kz}$, the $d\Omega_d$, the $d\boldsymbol{k}$ and the dk_d integrals. However, the rather steep t dependence of the elastic proton-proton cross section allows us to simplify these integrals, because the physically relevant processes are dominated by small $|t| < m_p^2$ contributions, with m_p being the mass of the proton. Thus, one can expand eq. (7.70) for small $|t|$. This gives for the part $\sum_{I,J} \ldots$ in eq. (7.70) containing the sums over external momenta

$$\begin{aligned}
\sum_{I,J} \ldots \;=\; & -8t \Big\{ (k_0^2 - k_d^2)^3 (4m_p^2 - s) s^4 \cos(\phi_k)^6 \\
& + k_0^2 (k_0^2 - k_d^2) s (4m_p^2 + s) \cos(\phi_k)^2 \left[k_d^2 s (-8m_p^4 - 4m_p^2 s + s^2) \right. \\
& - 4k_0^2 (32m_p^6 - 14m_p^4 s - 3m_p^2 s^2 + s^3) \\
& + \left. (k_0^2 - k_d^2) s (-8m_p^4 - 4m_p^2 s + s^2) \cos(2\phi_k) \right] \\
& - 0.5 \Big[(k_0^2 - k_d^2)^2 s^2 \cos(\phi_k)^4 \left(k_d^2 s (8m_p^4 - 4m_p^2 s + s^2) \right. \\
& + k_0^2 (-128m_p^6 + 88m_p^4 s + 12m_p^2 s^2 - 7s^3) \\
& + \left. (k_0^2 - k_d^2) s (8m_p^4 - 4m_p^2 s + s^2) \cos(2\phi_k) \right) \Big] \\
& - 0.5 \Big[k_0^4 (4m_p^2 + s)^2 \left(k_d^2 s (8m_p^4 - 4m_p^2 s + s^2) \right. \\
& + k_0^2 (-128m_p^6 + 24m_p^4 s + 12m_p^2 s^2 - 3s^3) \\
& + \left. (k_0^2 - k_d^2) s (8m_p^4 - 4m_p^2 s + s^2) \cos(2\phi_k) \right) \Big] \Big\} \\
& / \quad \left\{ k_0^8 \left(-4{m_p}^2 + s\right) \left[4m_p^2 + s + \left(-1 + \tfrac{k_d^2}{k_0^2} \right) s \cos(\phi_k)^2 \right]^4 \right\} .
\end{aligned} \tag{8.10}$$

For $k_d \approx 0$ the radiation does not propagate into the extra dimensions and eq. (8.10) reduces to the well known classical limit. From eq. (8.10) one can see that for $k_d^2/k_0^2 s \geq 4m_p^2$ the regularising part in the denominator is not

m_p^2/s any more and a Taylor expansion of eq. (8.10) around $m_p^2/s = 0$ is allowed. This expansion has a large validity region for ultra high energy collisions because it just demands that

$$\frac{\sqrt{s}}{2} > k_d^2 > \boldsymbol{k}^2 \frac{4m_p^2}{s} \quad . \tag{8.11}$$

This approximation also fulfils the condition in eq. (8.9). After performing the integration $d\phi_{kz}$, this series gives

$$\frac{dE}{dk_d d\boldsymbol{k} d\phi_k d\Omega_d} = \frac{t}{(2\pi)^{d+1} M_f^{d+2}} \frac{2k_d^{d-1}\boldsymbol{k}^2 \left[(k_0^2 - k_d^2)\cos(2\phi_k) - k_0^2\right]}{\left[k_0^2 + (k_d^2 - k_0^2)\cos(\phi_k)\right]^2} \quad . \tag{8.12}$$

Next the ϕ_k integration has to be performed,

$$\frac{dE}{dk_d d\boldsymbol{k} d\Omega_d} = \frac{t}{(2\pi)^d M_f^{d+2}} \frac{k_d^{d-2}\boldsymbol{k}^2(2k_d^2 + 3\boldsymbol{k}^2)}{(k_d^2 + \boldsymbol{k}^2)^2} \quad . \tag{8.13}$$

The integration over the d-dimensional unit sphere Ω_d gives a factor $2\pi^{d/2}/\Gamma(d/2)$,

$$\frac{dE}{dk_d d\boldsymbol{k}} = \frac{t}{2^{d-1}\pi^{d/2}\Gamma(d/2) M_f^{d+2}} \frac{k_d^{d-2}\boldsymbol{k}^2(2k_d^2 + 3\boldsymbol{k}^2)}{(k_d^2 + \boldsymbol{k}^2)^2} \quad . \tag{8.14}$$

Next, the k_d and the $|\boldsymbol{k}|$ integration can be performed with respect to the integration limits from $k_d^2 + \boldsymbol{k}^2 < k_{max}$ and eq. (8.11). This calculation can be done explicitly for two, four and six extra dimensions:

$$\begin{aligned} E(t, d=2) &= -k_{max}^3 t \left[5\sqrt{2} - \log(1+\sqrt{2})\right]/(12\pi M_f^4), \\ E(t, d=4) &= -k_{max}^5 t \left[\sqrt{2} - \log(1+\sqrt{2})\right]/(16\pi^2 M_f^6), \\ E(t, d=6) &= -k_{max}^7 t \left[11\sqrt{2} - 13\log(1+\sqrt{2})\right]/(1792\pi^3 M_f^8). \end{aligned} \tag{8.15}$$

Let us now discuss the relation between this result and those obtained in earlier publications:

- In ref. [138] the gravitational wave was assumed to have a momentum vector only in the direction out of the brane, thus the denominator in eq. (7.70) simplifies to $P_I k = E_I^0 k_0$. After integrating over k_0 (which is not strictly correct, because the problem is not spherically symmetric in $3+d$ spatial dimensions any more) the result shows the same t and k_{max} dependence as eq. (8.15). The different factors are due to the simplification in the integration.

- The phase space argument used in ref. [147] leads to the same k_{max} dependence. However, the pre-factors differ and even more striking the result derived in [147] has no t dependence (but s instead). Therefore, this approach leads to drastic overestimation of the gravitational energy loss in high energy cosmic rays, as shown in the following sections.

8.2 Quasi-elastic hadron-nucleus scattering

In order to calculate the energy loss due to gravitational wave emission in air showers at high energies one has to know the elastic scattering cross section $\mathrm{d}\sigma_{\mathrm{elastic}}/\mathrm{d}t$. This is constructed from the hadron-nucleon scattering cross section.

In the impact parameter representation, the profile function is defined as

$$\Gamma(s,b) = \frac{\sigma_{\mathrm{total}}}{2}\frac{1}{2\pi B_{\mathrm{elastic}}}\exp\left(-\frac{b^2}{2B_{\mathrm{elastic}}}\right) \quad , \tag{8.16}$$

where B is the elastic scattering slope and σ_{total} is the total hadron-nucleon cross section. The profile function is related to the amplitude by

$$\Gamma(s,b) = -\frac{i}{8\pi}A(s,b) \quad . \tag{8.17}$$

The profile function eq. (8.16) can be expressed via the eikonal [151] function χ by

$$\Gamma(s,\boldsymbol{b}) = 1 - \exp\left[i\chi(\boldsymbol{b})\right] \quad , \tag{8.18}$$

and is related to the phase shift of the scattered wave.

The Fourier transform relates impact parameter space to momentum space by

$$A(s,t) = \frac{s}{4\pi}\int \mathrm{d}^2\boldsymbol{b}\, A(s,\boldsymbol{b})\exp(-i\boldsymbol{bq}) \quad , \tag{8.19}$$

with $t = -q^2 \approx -\boldsymbol{q}^2$. The amplitude gives the differential elastic cross section:

$$\frac{\mathrm{d}\sigma_{\mathrm{elastic}}}{\mathrm{d}t} = \frac{1}{16\pi s^2}|A(s,t)|^2 = \left.\frac{\mathrm{d}\sigma_{\mathrm{elastic}}}{\mathrm{d}t}\right|_{t=0}\exp(B_{\mathrm{elastic}}t) \quad . \tag{8.20}$$

From the last expression one can define the elastic scattering slope

$$B \equiv \left[\frac{\mathrm{d}}{\mathrm{d}t}\left(\ln\frac{\mathrm{d}\sigma_{\mathrm{elastic}}}{\mathrm{d}t}\right)\right]_{t=0} \quad . \tag{8.21}$$

Inserting eq. (8.19) and (8.20) into eq. (8.21), the scattering slope becomes

$$\begin{aligned} B &= \left.\frac{2\frac{d}{\mathrm{d}t}|\int \mathrm{d}^2\boldsymbol{b}A(s,\boldsymbol{b})\mathrm{e}^{-i\boldsymbol{bq}}|}{|\int \mathrm{d}^2\boldsymbol{b}A(s,\boldsymbol{b})\mathrm{e}^{-i\boldsymbol{bq}}|}\right|_{t=0} \\ &= \left.\frac{2\frac{\mathrm{d}}{-2q\mathrm{d}q}|\int \mathrm{d}^2\boldsymbol{b}A(s,\boldsymbol{b})(1+(-i\boldsymbol{bq})+\frac{1}{2}(-i\boldsymbol{bq})^2-...)|}{|\int \mathrm{d}^2\boldsymbol{b}A(s,\boldsymbol{b})|}\right|_{t=0} \\ &= \frac{|\int \mathrm{d}^2\boldsymbol{b}A(s,\boldsymbol{b})(b^2\cos^2\phi)|}{|\int \mathrm{d}^2\boldsymbol{b}A(s,\boldsymbol{b})|} = \frac{\int \mathrm{d}bb^3\Gamma(s,b)}{2\int \mathrm{d}bb\Gamma(s,b)} \quad , \end{aligned} \tag{8.22}$$

where the exponential has been expanded and only the third term was kept. The first term does not depend on q and the second term in the expansion vanishes due to symmetry.

To obtain the scattering slope of a hadron-nucleus collision, the hadron-nucleon scattering profile function is replaced by

$$\Gamma_{\mathrm{hA}}(s,\boldsymbol{b}) = 1 - \exp\left[-t\sum_{i=1}^{A}\chi_i(s,\boldsymbol{b}_i)\right] = 1 - \left[1-\tilde{T}_A(\boldsymbol{b})\right]^A \tag{8.23}$$

where $\tilde{T}_A$ is obtained from the Glauber-Gribov formalism [152, 153, 154] by convolution of the thickness function with the hadron-nucleon profile,

$$\begin{array}{rcl} \tilde{T}_A(\boldsymbol{b}) & = & \int \mathrm{d}^2\boldsymbol{c}\, T_A(\boldsymbol{b})\Gamma(\boldsymbol{b}-\boldsymbol{c}) \quad , \\ T_A(\boldsymbol{b}) & = & \frac{1}{A}\int \mathrm{d}z\, \rho(z,\boldsymbol{b}). \end{array} \tag{8.24}$$

Using eq. (8.24), the scattering slope for elastic hadron-nucleus collisions eq. (8.22) is calculated as a function of the collision energy. The underlying hadron-nucleon scattering slopes are taken from the SIBYLL model [155, 156]. figure 8.1 depicts the underlying hadron-nucleon slopes (thin lines) and the calculated hadron-nucleus slopes (thick lines). The hadron-nucleon slopes are clearly higher than the hadron-nucleus slopes at the same energy. However, the ratios of the two slopes decreases with increasing energy.

8.3 Gravitational radiation from high energy cosmic rays

After the derivation of the basic equations in the previous sections, we are now ready to calculate the amount of energy that is emitted into gravitational radiation by a high energy proton propagating through the atmosphere.

The differential energy loss is given by

$$\frac{dE}{dx}(s,d) = \frac{\int_0^{\sqrt{s}/2} dt\, \frac{d\sigma^0_{\mathrm{hA}}}{dt} E(t,s,d)}{\lambda \int_0^{\sqrt{s}/2} dt\, \frac{d\sigma^0_{\mathrm{hA}}}{dt}} \quad , \tag{8.25}$$

where λ is the mean free path for elastic scattering of the projectile in units of g/cm^2 and $\mathrm{d}\sigma^0_{\mathrm{hA}}/\mathrm{d}t$ is the differential hadron-nucleus cross section. For cosmic ray calculations it is convenient to calculate the energy loss E in the

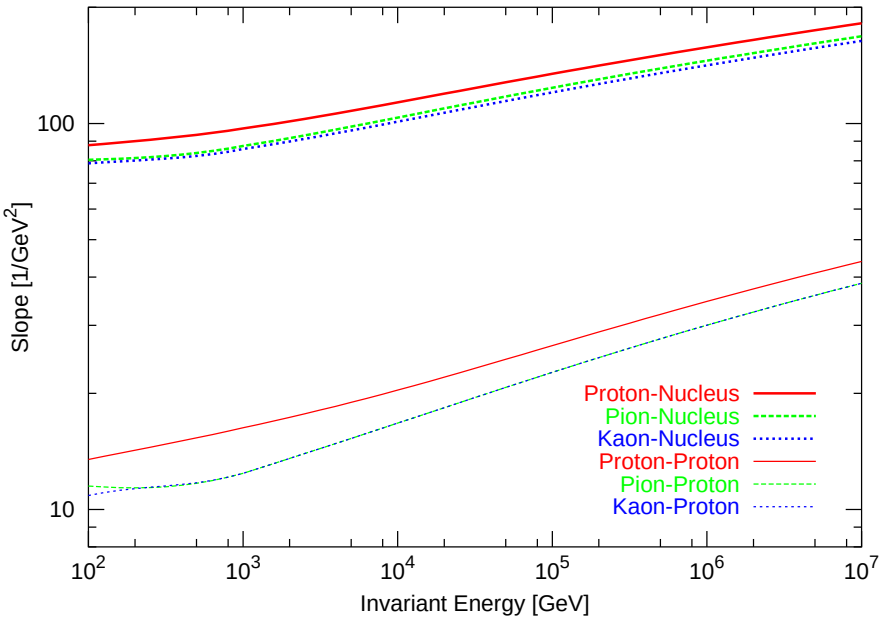

Figure 8.1: The hadron-nucleus slopes (thin lines) and the hadron-nucleon slopes (thick lines) as a function of the collision energy in the center of mass frame. Primary particles are protons (full lines), πs (dashed lines), and Kaons (dotted lines).

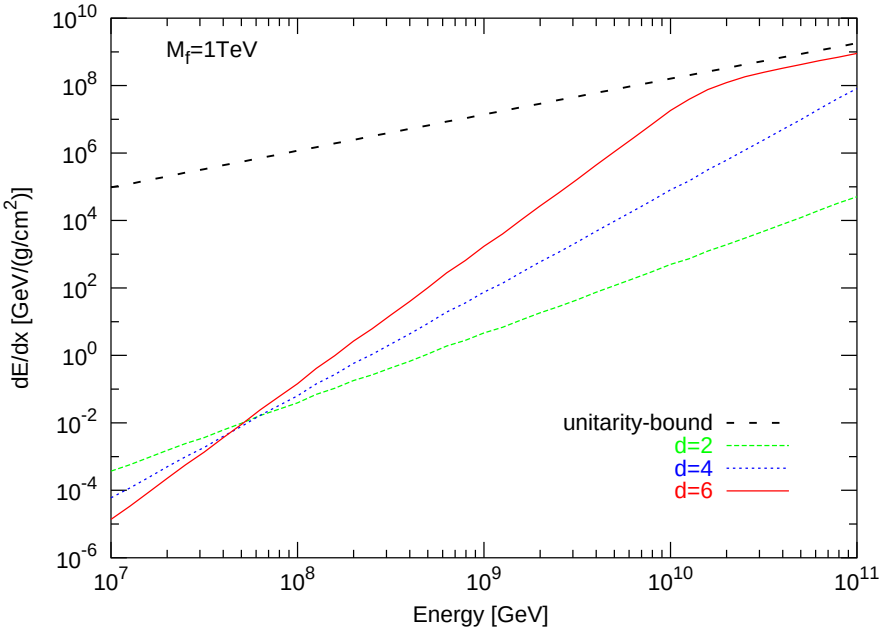

Figure 8.2: Energy loss (in GeV/(g/cm^2)) of a proton propagating through the atmosphere as a function of the lab-frame energy for $M_f = 1$ TeV and $d = 2, 4, 6$.

laboratory frame. The corresponding Lorentz transformations are given in the appendix C.

Figures 8.2 (for $M_f = 1$ TeV) and (8.3) (for $M_f = 2$ TeV) show the differential energy loss of a proton propagating through the atmosphere as a function of the initial energy in the laboratory frame. The short dashed, dotted and full lines give the results for two, four and six extra dimensions, the long dashed lines show the unitarity bounds. For large initial energies, a higher number of extra dimensions leads to an enhancement of the gravitational energy loss. However, with increasing fundamental scale M_f the effect is much weaker as shown in fig. 8.3. Note, that the result is cut-off dependent as $k_{\max}$ is not determined from first principles. For the present study, we have chosen $k_{\max} = \sqrt{s}/2$, which is the maximal value consistent with energy conservation in the picture of a gravitational wave being emitted by one of the outgoing states. The comparison of these results with [147] shows that an approximation of the effects of extra dimension with a simple phase space argument does yield a similar shape for the energy loss as those shown in figs. 8.2 and 8.3. However, the omission of the correct kinematics of the energy loss eq. (8.15) results in a dramatic overestimation of the grav-

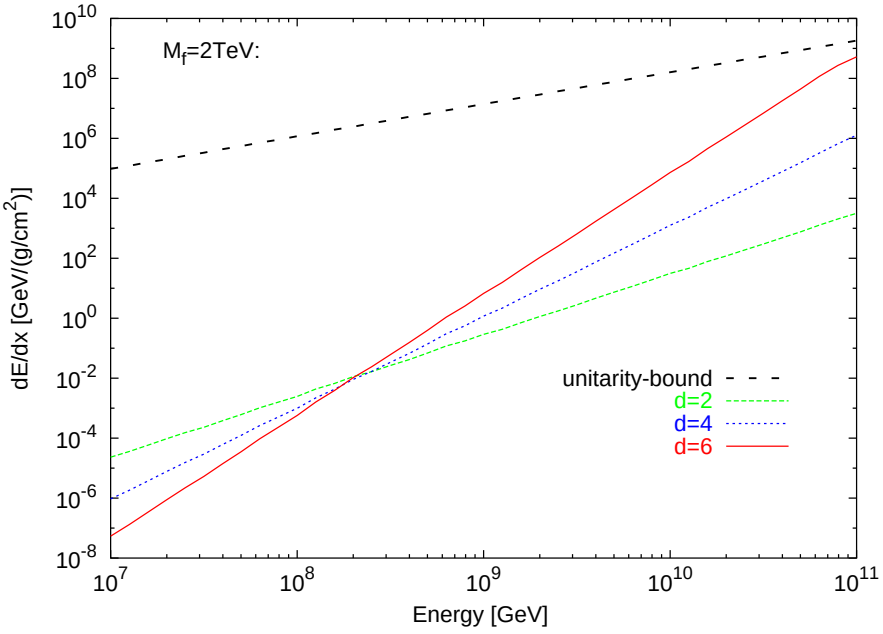

Figure 8.3: Energy loss (in GeV/(g/cm^2)) of a proton propagating through the atmosphere as a function of the lab-frame energy for $M_f = 2$ TeV and $d = 2, 4, 6$.

itational energy loss effect by several orders of magnitude. In addition, the simple extension of the standard formula with a modified phase space factor on the integrated cross sections results in a violation of the unitarity bound.

Even though the energy loss into gravitational waves in our (very optimistic) scenario is much lower than expected from previous approximations, it might still have observable consequences for very high energetic cosmic rays. Therefore, eq. (8.15) and the elastic cross sections were implemented into a complete cosmic ray air shower simulation (SENECA) [157, 158] to study the modifications of the shower properties in detail.

Figure 8.4 gives the relative energy loss as a function of the incident energy E. The calculation is averaged over incident zenith angles dcos(θ) in the range $0° \leq \theta \leq 60°$. The full lines indicate the calculations with six extra dimensions, while the dotted lines show the results for four extra dimensions ($M_f = 1$ TeV is shown by thick lines, $M_f = 2$ TeV is shown by thin lines). For the case of two extra dimensions, deviations from the non-modified shower properties are very small even for the most optimistic cases. However, for four extra dimensions first deviations from the standard calculation become visible at energies higher than $5 \cdot 10^{10}$ GeV. For $d = 6$ the gravitational radiation becomes sizeable and already leads to deviations around $5 \cdot 10^9$ GeV. At the highest energies, the integrated relative energy loss due to gravitational radiation might even exceed 20% of the initial particle energy. In present day experiments, e.g. AUGER, this gravitational energy loss would show up as a decrease in the number of observed secondary particles. The multiplicity of secondary particles $N_{\text{sec}}(E, x)$ is directly observable in fluorescence experiments and is a key observable to estimate the cosmic ray's initial energy. Any non-visible energy emission results in an underestimation of the initial energy in the energy reconstruction procedure. Thus, it has an impact on the interpretation of the measured cosmic ray flux in dependence of the incoming particle energy.

How big is the distortion of the reconstructed flux due to graviton emission quantitatively? Neglecting fluctuations, for a given incoming flux $F = \mathrm{dN/dE}$, the measured flux $F' = \mathrm{dN'/dE'}$ depends on the reconstructed energy $E'(E)$. By identifying the integrated fluxes $N'(E') = N(E)$ one finds

$$F'(E') = \frac{\mathrm{dN'}}{\mathrm{dE'}} = \frac{\mathrm{dN\,(E)}}{\mathrm{dE}} \cdot \frac{\mathrm{dE}}{\mathrm{dE'}} = F(E) \cdot \frac{\mathrm{dE}}{\mathrm{dE'}} \quad . \tag{8.26}$$

For an incoming flux $F = kE^{-3}$ the flux reconstruction is shown in fig. 8.5. In all scenarios ($d \geq 4$) gravitational wave emission might indeed influence the energy reconstruction above $5 \cdot 10^9$ GeV. For ultra high energy cosmic rays even an apparent cut-off seems possible , because the relative

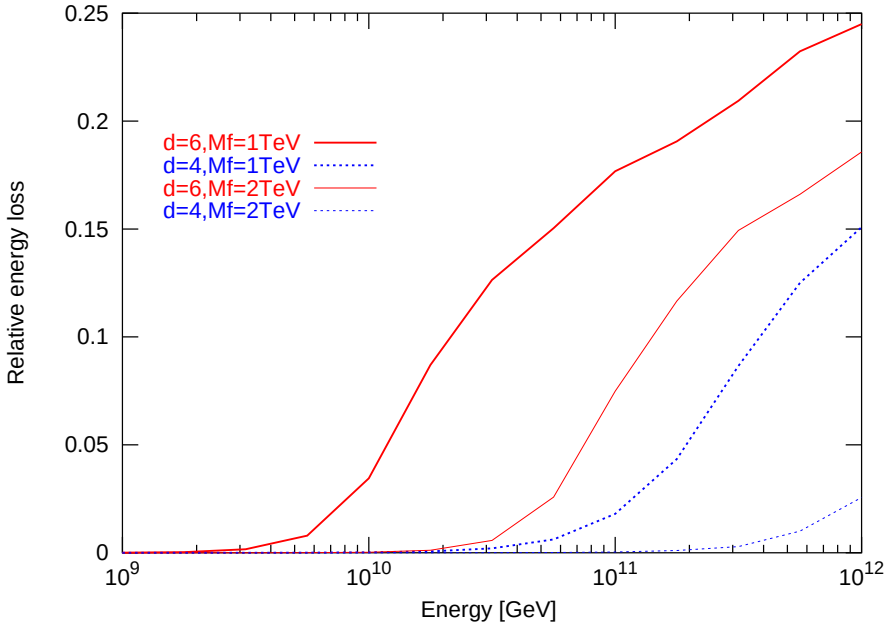

Figure 8.4: Relative energy loss into gravitational radiation as a function of the incident cosmic ray energy E for $d = (4, 6)$ and $M_f = (1,\ 2)$ TeV.

amount of non-visible energy increases strongly with increasing energy. But one has to remember the linear scale on the y-axis, thus the suppression does not mimic the GZK cut-off. Hence, for UHECRs the interpretation of experimental data might have to be modified in scenarios with large extra dimensions.

Presently available data from Hires and AGASA do not allow one to observe the predicted suppression pattern, because even in our most optimistic scenario the flux is reduced only by a factor of 0.5 for the highest energies. However, with the expected high statistics data from the Pierre Auger Observatory a detailed exploration of this phenomenon might be possible.

As a remark, we want to point out that in our calculation, gravitational wave emission does not give new insights into phenomena at lower energies ($E \leq 10^{18}$ eV) and can not be considered as a candidate to explain the famous knee in the cosmic ray spectrum.

The energy loss into gravitational waves is calculated for ultra high energy cosmic rays. In contrast to previous estimates, quasi-elastic particle scattering in the ADD scenario with 4 or 6 extra dimensions has no observable influence on the properties of cosmic ray air showers at incident energies below $5 \cdot 10^{18}$ eV. Thus, the emission of gravitational radiation can not be

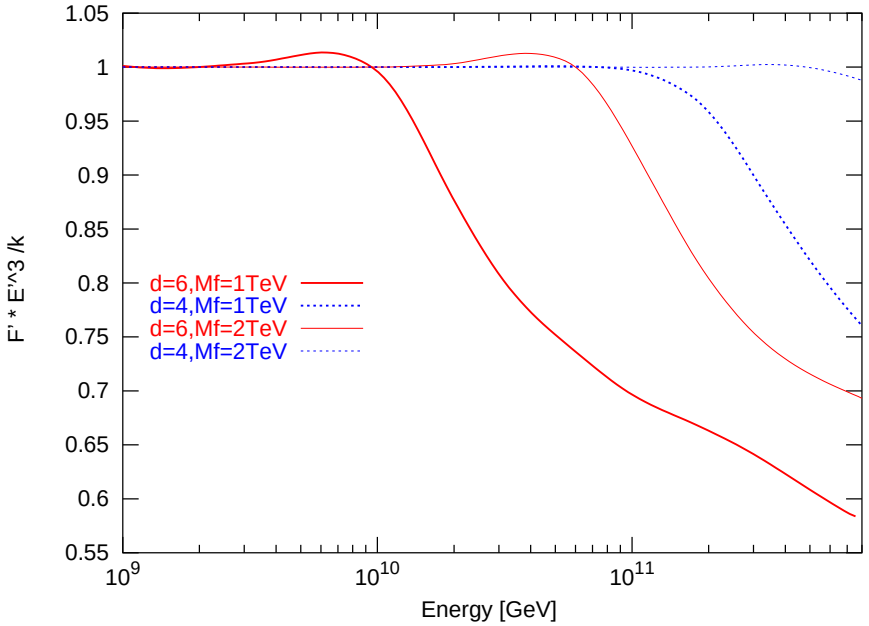

Figure 8.5: Reconstructed flux $F'E'^3/k$ as a function of the incident cosmic ray energy E' for $d = (4, 6)$ and $M_f = (1, 2)$ TeV.

used to explain the steepening of the cosmic ray spectrum at the "knee" ($E \sim 10^{15.5}$ eV). For two large extra dimensions, the studied effects are generally too small to lead to any observable effect.

However, for energies above $5 \cdot 10^{18}$ eV and $M_f \leq 2$ TeV, $d \geq 4$ gravitational energy loss during the air shower evolution can be sizeable. This might result in an underestimation of the reconstructed energy for ultra high energy cosmic rays as studied by Hires, AGASA and the Pierre Auger Observatory.

Chapter 9

Summary and conclusions

After an introduction and problem setting in the first chapter, the chapters two and three sketch the content of the SM and GR. In chapter four the theoretical foundations of models with large extra dimensions are given. The possibility of the production of microscopic black holes in cosmic rays and future particle colliders is discussed.

In the chapters five and six the final fate of such a black hole is discussed and the possible scenario of the formation of a stable black hole remnant (BHR) is introduced. It is argued that BHRs might have a non zero charge. This hypothesis of charged BHRs is tested on the background of BHR production from cosmic rays and the current search for particles with a very small charge to mass ratio. It is found that charged BHRs can not be be excluded from such estimates.

Spectral densities that allow a more realistic simulation of the formation process of such BHRs are suggested and a class of black hole entropy formulas that lead to the desired properties of the spectral densities are discussed. From this, several scenarios for direct detection of BHRs at the LHC are discussed. At the specific example of the ALICE detector it is shown that it might be possible to determine the tracks of charged BHRs, which then would allow to study their properties in more detail. Then further observables such as several p_T distributions, and multiplicity distributions are studied with numerical models for the decay process of BHs and BHRs production. It is found that the signatures for BHs with a final decay are clearly distinguishable from those for the formation of stable BHRs. In one example it is illustrated how neutral BHRs should be detectable by the analysis of missing transversal momentum in hadronic jet events.

In chapter seven the differential cross section for the emission of gravita-

tional waves from elastic particle scattering in models with extra dimensions is derived. Based on that derivation, a simple and intuitive way on how these cross sections, which are only valid for non compactified extra dimensions, could be generalized to compactified scenarios is suggested. It is found that the modified model predicts modifications from existing cross sections for low energetic gravitational waves, but leads to unaltered cross sections for high energetic gravitational waves.

In chapter eight the total cross section for high energetic scattering processes is calculated. The energy loss due to these cross sections is applied to a numerical simulation of UHECRs. The outcome of this is that the reconstructed flux of the highest energetic cosmic rays might be up to a factor of 1.5 bigger than the flux reconstructed from standard models. In contrast to previous estimates, quasi-elastic particle scattering in the ADD scenario with 4 or 6 extra dimensions has no observable influence on the properties of cosmic ray air showers at incident energies below $5 \cdot 10^{18}$ eV. Thus, the emission of gravitational radiation can not be used to explain the steepening of the cosmic ray spectrum at the "knee" ($E \sim 10^{15.5}$ eV). For two large extra dimensions, the studied effects are generally too small to lead to any observable effect. However, for energies above $5 \cdot 10^{18}$ eV and $M_f \leq 2$ TeV, $d \geq 4$ gravitational energy loss during the air shower evolution can be sizeable. This might result in an underestimation of the reconstructed energy for ultra high energy cosmic rays as studied by Hires, AGASA and the Pierre Auger Observatory.

Although this modification is found to be non negligible, it can not account for an explanation of the so called knee in the reconstructed cosmic ray spectrum.

Appendix A

On Riemannian and pseudo-Riemannian geometry

A.1 Riemannian and pseudo-Riemannian metric

In elementary geometry a metric g defines the inner product of two vectors U and V with the components U_i and V_i by $U \cdot V = \sum_{i,j=1}^{m} U_i g_{ij} V_j$. On a general m-dimensional manifold this metric g_p is a (0,2) tensor field defined at each point p of the manifold in the attatched tangent space T_pM. A **Riemannian metric** has to satisfy the conditions

$$\begin{array}{ll} (i) & g_p(U,V) = g_p(V,U) \quad , \\ (ii) & g_p(U,U) \geq 0 \text{ where the equality holds only for } U = 0 \quad , \end{array} \tag{A.1}$$

at each point $p \, \epsilon \, M$. Whereas a **pseudo-Riemannian metric** has to satisfy the conditions

$$\begin{array}{ll} (i) & g_p(U,V) = g_p(V,U) \quad , \\ (ii^*) & \text{if } g_p(U,V) = 0 \text{ for any } U \, \epsilon \, T_pM \text{ then } V = 0 \quad , \end{array} \tag{A.2}$$

at each point $p \, \epsilon \, M$. For a given chart (U, ϕ) in M and the coordinates $\{x^\mu\}$ the metric can be defined as an infinitesimal distansce squared.

$$ds^2 = dx^\mu dx^\nu g(\partial/\partial x^\mu, \partial/\partial x^\nu) = g_{\mu\nu} dx^\mu dx^\nu \quad , \tag{A.3}$$

where $\partial/\partial x^\mu$ (dx^μ) are the unit vectors of the tangent space T_pM (cotangent space T_p^*M). Since $(g_{\mu\nu})$ is a real symmetric matrix it is hermitian and therefore all its eigenvalues are real. The eigenavlues of a Riemannian metric are all positive and the simplest example is the metric of Euclidian

geometry $g_{\mu\nu} = \delta_{\mu\nu} = \text{diag}(1, ..., 1)$ which naturally fulfills the conditions (A.1). As soon as a diagonal matrix has entries of different sign it can not be a Riemannian metric any more as condition (A.1) does not hold. The most famous example for such a metric is the Minkowski metric which fulfills the condition (A.2) which is often defined as $\eta_{\mu\nu} = \text{diag}(1, -1, -1, -1)$. For tangent Minkowski space one can distinguish between three different regions,

$$\begin{array}{ll} (i) & \text{if } g(V,V) > 0 \text{ then V is called timelike,} \\ (ii) & \text{if } g(V,V) = 0 \text{ then V is called lightlike,} \\ (iii) & \text{if } g(V,V) < 0 \text{ then V is called spacelike.} \end{array} \tag{A.4}$$

In relativistic particle physics (and therefore also in the SM) one assumes two points in spacetime, that differ by a spacelike vector, to be causally disconnected.

A.2 Induced metric

For a n-dimensional Riemannian manifold N with the metric g_N and a m-dimensional submanifold M one can define an embedding function $f : M \rightarrow M^{'} \epsilon N$. This embedding induces the submanifold structure of M in N. The inverse pullback map (if it exists) $f^* : M^{'} \rightarrow M$ induces a natural metric on M $g_M = f^* g_N$. The components of this induced metric are given by

$$g_{M\mu\nu}(x) = g_{N\alpha\beta}(\frac{\partial x}{\partial f^*})^\alpha_\mu (\frac{\partial x}{\partial f^*})^\beta_\nu = g_{N\alpha\beta} \frac{\partial f^\alpha}{\partial x^\mu} \frac{\partial f^\beta}{\partial x^\nu}. \tag{A.5}$$

As shown in the figure A.2 one can see the S^2 sphere as a two-dimensional submanifold of the tree-dimensional euclidian space. For this example it is instructive to choose polar coordinates $(\theta,\ \phi)$ in M and euclidian coordinates $(x,\ y,\ z)$ in N. In those coordinates, the emedding function f reads

$$f : (\theta,\ \phi) \rightarrow (\text{sin}\theta\text{cos}\phi, \text{sin}\theta\text{sin}\phi, \text{cos}\theta). \tag{A.6}$$

With equation (A.5) one finds the induced metric on M

$$\begin{array}{rl} g_{\mu\nu} dx^\mu dx^\nu & = \delta_{\alpha\beta} \frac{\partial f^\alpha}{\partial x^\mu} \frac{\partial f^\beta}{\partial x^\nu} dx^\mu dx^\nu \\ & = d\theta d\theta + \text{sin}^2 \text{d}\phi \text{d}\phi. \end{array} \tag{A.7}$$

A.3 Affine connections

The mathematical formulation of equation (3.5) is called affine connection.

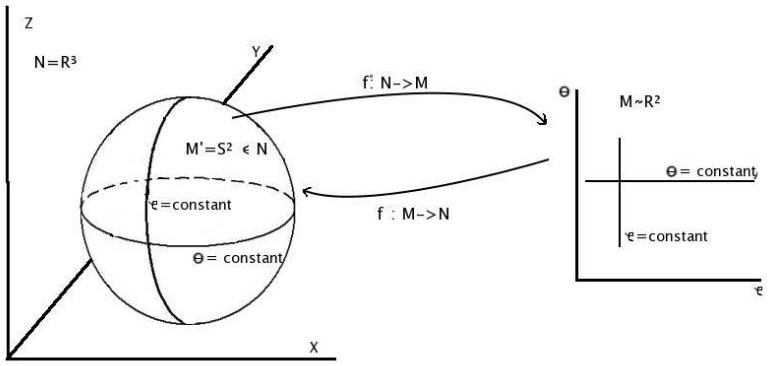

Figure A.1: The embedding function $f : M \to N$ for the example of $M = \Re^3$ and $N = S^2$.

An **affine connection** ∇ is a map $\nabla : TM \times TM \to TM$, which satisfies the following conditions:

$$\begin{aligned} \nabla_X(Y+Z) &= \nabla_X Y + \nabla_X Z \quad , \\ \nabla_{X+Y} Z &= \nabla_X Z + \nabla_Y Z \quad , \\ \nabla_{fX} Y &= f \nabla_X Y \quad , \\ \nabla_X(fY) &= X[f]\, Y + f \nabla_X Y \quad , \end{aligned} \tag{A.8}$$

where f is a differentiable function $f : M \to \Re$ and $X,\ Y$ are $\epsilon\ TM$. It is easy to check that the previous definition for covariant derivative (3.5) meets those conditions. It allows also to find the covariant derivative of the coordinate basis $\{e_\mu\} = \{\partial/\partial x^\mu\}$ in T_pM

$$\nabla_\nu e_\mu = \Gamma^\lambda_{\mu\nu} e_\lambda \quad . \tag{A.9}$$

A.4 Transformation properties

Introduce two different charts $(V,\ \psi)$ and $(U,\ \phi)$ of M such that $U \cap V \neq 0$. Let $\{e_\mu\} = \{\partial/\partial x^\mu\}$ be the basis that is induced by ψ and $\{f_\mu\} = \{\partial/\partial y^\mu\}$ be the basis that is induced by ϕ. According to eq. (3.7) in both coordinate systems a definition for the connection coefficients is given, which is denoted as

$$\nabla_{e_\mu} e_\nu = \Gamma^\lambda_{\mu\nu} e_\lambda \text{ and } \nabla_{f_\alpha} f_\beta = \tilde{\Gamma}^\lambda_{\alpha\beta} f_\lambda \ . \tag{A.10}$$

Now it is desirable to express $\tilde{\Gamma}$ in terms of Γ, which then will explain how the connections transform under the change of one coordinate system to the

other. Therefore, one uses $f_\alpha = (\partial x^\lambda / y^\alpha) e_\lambda$ and $\nabla_{f_\alpha} = \frac{\partial x^\gamma}{\partial y^\alpha} e_\gamma$ to find for the left hand side of the second equation (A.10)

$$\begin{aligned} \nabla_{f_\alpha} f_\beta &= \nabla_{f_\alpha} \left(\frac{\partial x^\lambda}{\partial y^\beta} e_\lambda \right) = \frac{\partial^2 x^\lambda}{\partial y^\beta \partial y^\alpha} e_\lambda + \frac{\partial x^\lambda}{\partial y^\beta} \frac{\partial x^\gamma}{\partial y^\alpha} \nabla_\gamma e_\lambda \\ &= \left(\frac{\partial^2 x^\lambda}{\partial y^\beta \partial y^\alpha} + \frac{\partial x^\tau}{\partial y^\beta} \Gamma^\lambda_{\ \tau\gamma} \right) \left(\frac{\partial y^\nu}{\partial x^\lambda} \right) f_\nu \quad . \end{aligned} \tag{A.11}$$

Since this has to agree with the right hand side of eq. (A.10) one finds

$$\begin{aligned} \tilde{\Gamma}^\nu_{\ \alpha\beta} &= \left(\frac{\partial^2 x^\lambda}{\partial y^\beta \partial y^\alpha} + \frac{\partial x^\tau}{\partial y^\beta} \frac{\partial x^\gamma}{\partial y^\alpha} \Gamma^\lambda_{\ \tau\gamma} \right) \left(\frac{\partial y^\nu}{\partial x^\lambda} \right) \\ &= \frac{\partial^2 x^\lambda}{\partial y^\beta \partial y^\alpha} \frac{\partial y^\nu}{\partial x^\lambda} + \frac{\partial x^\tau}{\partial y^\beta} \frac{\partial x^\gamma}{\partial y^\alpha} \frac{\partial y^\nu}{\partial x^\lambda} \Gamma^\lambda_{\ \tau\gamma} \quad . \end{aligned} \tag{A.12}$$

Now the transformational behavior of the connections is known but this still does not determine yet the actual form of Γ. If for example an arbitrary tensor is added $\tilde{t}^\nu_{\ \alpha\beta} = \frac{\partial x^\tau}{\partial y^\beta} \frac{\partial x^\gamma}{\partial y^\alpha} \frac{\partial y^\nu}{\partial x^\lambda} t^\lambda_{\ \tau\gamma}$ to a connection $\Gamma^\nu_{\ \alpha\beta}$, the resulting object $\bar{\Gamma}^\nu_{\ \alpha\beta} = \Gamma^\nu_{\ \alpha\beta} + t^\nu_{\ \alpha\beta}$ transforms according to eq. (A.12) as well:

$$\begin{aligned} \tilde{\bar{\Gamma}}^\nu_{\ \alpha\beta} &= \frac{\partial^2 x^\lambda}{\partial y^\beta \partial y^\alpha} \frac{\partial y^\nu}{\partial x^\lambda} + \frac{\partial x^\tau}{\partial y^\beta} \frac{\partial x^\gamma}{\partial y^\alpha} \frac{\partial y^\nu}{\partial x^\lambda} \Gamma^\lambda_{\ \tau\gamma} + \frac{\partial x^\tau}{\partial y^\beta} \frac{\partial x^\gamma}{\partial y^\alpha} \frac{\partial y^\nu}{\partial x^\lambda} t^\lambda_{\ \tau\gamma} \\ &= \tilde{\Gamma}^\nu_{\ \alpha\beta} + \tilde{t}^\nu_{\ \alpha\beta} \quad . \end{aligned} \tag{A.13}$$

In a very similar way one can show that the difference of two different connections transforms like a tensor

$$\widetilde{(\Gamma^\nu_{\ \alpha\beta} - \bar{\Gamma}^\nu_{\ \alpha\beta})} = \frac{\partial x^\tau}{\partial y^\beta} \frac{\partial x^\gamma}{\partial y^\alpha} \frac{\partial y^\nu}{\partial x^\lambda} \left(\Gamma^\lambda_{\ \tau\gamma} - \bar{\Gamma}^\lambda_{\ \tau\gamma} \right) \tag{A.14}$$

and that $\nabla_X Y$ is indeed a vector in any coordinate system

$$\tilde{X}^\alpha (\tilde{\partial}_\alpha \tilde{Y}^\gamma + \tilde{\Gamma}^\gamma_{\ \alpha\beta} \tilde{Y}^\beta) f_\beta = X^\alpha (\partial_\alpha Y^\gamma + \Gamma^\gamma_{\ \alpha\beta} Y^\beta) e_\beta \quad . \tag{A.15}$$

From eq. (A.13) one can prove the **fundamental theorem of (pseudo-) Riemannian geometry**: On a (pseudo-) Riemannian manifold (M, g) there exists a unique symmetric connection which is compatible with the metric g. This connection is called the **Levi-Civita connection** .

Proof: From eq. (A.13) one knows that one can add to any connection $\Gamma^\alpha_{\ \mu\nu}$ an arbitrary tensor $t^\alpha_{\ \mu\nu}$ and the result is still a connection. So one is free to add exactly the negative of the contorsion, leaving just the symmetric part (Christoffel symbols) of the connection. As this connection is exactly determined by the metric $\Gamma^\kappa_{\ \alpha\beta} = \frac{1}{2} g^{\kappa\lambda} (\partial_\alpha g_{\beta\kappa} + \partial_\beta g_{\alpha\kappa} - \partial_\lambda g_{\alpha\beta})$ and obviously symmetric, the theorem is proven.

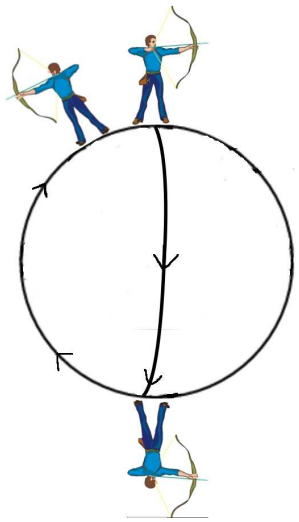

Figure A.2: An archer who is parallel transported along a closed path will eventually shoot in the wrong direction after its journey.

A.5 Curvature and the Riemann tensor

An tangent vector which is parallel transported along a closed path in a curved manifold will not necessarily be the same at the beginning and the end of its journey. This is illustrated in figure A.2, where the shooting direction (which stands for the tangent vector) of the archer who is parallel transported from the north-pole to the south-pole and back on a different meridian.

Apart from the graphic background of the curvature as suggested by the figures A.2 and 3.1 and used for the definition (3.39) one can give an equivalent mathematical definition, based on covariant derivatives which defines the Riemann tensor R as an object which maps $R:\ TM\otimes TM\otimes TM\to TM$ and is defined as

$$R(X,Y,Z)=\nabla_X\nabla_Y Z-\nabla_Y\nabla_X Z-\nabla_{[X,Y]}Z \quad . \tag{A.16}$$

As one can see from

$$\begin{aligned} R(fX,gY,hZ) &= f\nabla_X(g\nabla_Y(hZ))-g\nabla_Y(f\nabla_X(hZ))-\nabla_{[fX,gY]}(hZ)\\ &= f\nabla_X(g\nabla_Y(hZ))-g\nabla_Y(f\nabla_X(hZ))-fX\,[g]\,\nabla_Y(hZ)\\ &\quad +gY\,[f]\,\nabla_X(hZ)-\nabla_{[X,Y]}(hZ)\\ &= fg\nabla_X(Y\,[h]\,Z+h\nabla_Y Z)-gf\nabla_Y(X\,[h]\,Z+h\nabla_X Z)\\ &\quad -fg\,[Z,Y]\,[h]\,Z-fgh\nabla_{[X,Y]}Z\\ &= fghR(X,Y,Z) \end{aligned} \tag{A.17}$$

where f, g and h are real functions on M, R is a multilinear object in every single of its entries and therefore obeys a basic tensor property. When evaluating the Riemann tensor according to definition (A.16) for the unit vectors $e_\mu,\ e_\nu,\ e_\lambda$, the result is an objects with three indices which obviously can not be $R^\kappa_{\lambda\mu\nu}$ yet. Here one has to remember that $R(X,Y,Z)$ itself is a tangent vector and its covariant component can be projected out by forming the scalar product

$$\begin{aligned}\tilde{R}^\kappa_{\lambda\mu\nu} &=< dx^\kappa,\ R(e_\mu,\ e_\nu,\ e_\lambda) >=< dx^\kappa, \nabla_\mu\nabla_\nu e_\lambda - \nabla_\nu\nabla_\mu e_\lambda > \\ &=< dx^\kappa, \nabla_\mu(\Gamma^\eta_{\ \nu\lambda} e_\eta) - \nabla_\nu(\Gamma^\eta_{\ \mu\lambda} e_\eta) > \\ &=< dx^\kappa, (\nabla_\mu\Gamma^\eta_{\ \nu\lambda})e_\eta + \Gamma^\eta_{\ \nu\lambda}\Gamma^\xi_{\ \mu\eta} e_\xi - (\nabla_\nu\Gamma^\eta_{\ \mu\lambda})e_\eta > -\Gamma^\eta_{\ \mu\lambda}\Gamma^\xi_{\ \nu\eta} e_\xi > \\ &= \partial_\mu\Gamma^\kappa_{\ \nu\lambda} - \partial_\nu\Gamma^\kappa_{\ \mu\lambda} + \Gamma^\eta_{\ \nu\lambda}\Gamma^\kappa_{\ \mu\eta} - \Gamma^\eta_{\ \mu\lambda}\Gamma^\kappa_{\ \nu\eta} \\ &= R^\kappa_{\lambda\mu\nu} \quad ,\end{aligned} \tag{A.18}$$

giving exactly back the definition (3.39). Pulling down the covariant index of R gives a tensor with soley contravariant indices $R_{\lambda\mu\nu\kappa} = g_{\lambda\rho}R^{rho}_{\mu\nu\kappa}$ which obeyes several algebraic properties:

- Symmetry:
$$R_{\lambda\mu\nu\kappa} = R_{\nu\kappa\lambda\mu} \quad , \tag{A.19}$$
- Antisymmetry:
$$R_{\lambda\mu\nu\kappa} = -R_{\mu\lambda\nu\kappa} = -R_{\lambda\mu\kappa\nu} \quad , \tag{A.20}$$
- Cyclicity:
$$R_{\lambda\mu\nu\kappa} = R_{\mu\nu\kappa\lambda} \quad . \tag{A.21}$$

In addition to those algebraic identities, the curvature tensor obeys differential identities. It is most convenient to prove those differential identities at at one single point, where one can choose locally flat coordinates (with $\Gamma^\mu_{\alpha\beta} = 0$ but $\partial_\tau\Gamma^\mu_{\alpha\beta}$ does not need to be 0). In such a coordinate system at the point p the covariant derivative of the Riemann tensor $\nabla_\eta R_{\lambda\mu\nu\kappa}$ is

$$\nabla_\eta R_{\lambda\mu\nu\kappa} = \frac{1}{2}\partial_\eta(\partial_\kappa\partial_\mu g_{\lambda\nu} - \partial_\kappa\partial_\lambda g_{\mu\nu}) - \partial_\nu\partial_\mu g_{\lambda\kappa} + \partial_\lambda\partial_\nu g_{\kappa\mu} \quad . \tag{A.22}$$

Cyclic permutation of eq. (A.22) in the indices ν, κ and η gives the **Bianchi identities** of general relativity

$$\nabla_\eta R_{\lambda\mu\nu\kappa} + \nabla_\kappa R_{\lambda\mu\eta\nu} + \nabla_\nu R_{\lambda\mu\kappa\eta} = 0 \quad . \tag{A.23}$$

Eq. (A.23) is generally covariant and therefore a coordinate transformation would affect all three terms in eq. (A.23) in the same way and as the zero

does not change, the whole equation holds in the new coordinates as well. As this argument can be made for any point p on M, equation (A.23) holds in general.

Contracting the first and the third index of $R_{\lambda\mu\nu\kappa}$ gives the so called **Ricci tensor**

$$R_{\mu\kappa} = g^{\lambda\nu} R_{\lambda\mu\nu\kappa} \quad , \tag{A.24}$$

which according to eq. (A.19) is symmetric in its two indices

$$R_{\mu\kappa} = R_{\kappa\mu} \quad . \tag{A.25}$$

The same contraction can be done for the Riemann tensors in eq. (A.23) by multiplying with $g^{\lambda\nu}$ and summing over both indices

$$\nabla_\eta R_{\mu\kappa} - \nabla_\kappa R_{\mu\eta} + \nabla_\nu R^\nu_{\ \mu\kappa\eta} = 0 \quad , \tag{A.26}$$

where $\nabla g = 0$ and eq. (A.20) have been used. Another contraction of the indices μ and κ gives with $R = R^\mu_\mu$

$$\begin{aligned} \nabla_\mu (2R^\mu_\eta - \delta^\mu_\eta R) &= 0 \quad , \\ &\text{or} \\ \nabla_\mu (2R^{\mu\nu} - \tfrac{1}{2} g^{\mu\nu} R) &= 0 \quad . \end{aligned} \tag{A.27}$$

As this equation reminds strongly of the conservation law for the energy momentum thensor $\nabla_\mu (T^{\mu\nu}) = 0$ it can be seen as a strong hint, that it makes sense to formulate Einstein's equations (3.1) the way they are formulated.

Appendix B

Calculations in curved spacetime

B.1 Newtonian limit

Driven by the idea that a gravitationally free falling particle is just propagating along the shortest possible path through a curved spacetime, one recalls the Riemannian definition for such a path

$$\frac{\mathrm{d}^2\mathrm{x}^\mu}{\mathrm{d}\tau^2} + \Gamma^\mu_{\nu\beta}\frac{\mathrm{dx}^\nu(\mathrm{c(t)})}{\mathrm{d}\tau}\frac{\mathrm{dx}^\beta(\mathrm{c(t)})}{\mathrm{d}\tau} = 0 \quad , \tag{B.1}$$

as known from eq. (3.13). In the limit of a very slow particle, we may neglect all terms proportional to $dx/d\tau$ and write this as

$$\frac{\mathrm{d}^2\mathrm{x}^\mu}{\mathrm{d}\tau^2} + \Gamma^\mu_{00}\left(\frac{\mathrm{dt}}{\mathrm{d}\tau}\right)^2 = 0 \quad . \tag{B.2}$$

All time derivatives of g are supposed to vanish and therefore the relevant components of the metric connections are

$$\Gamma^\mu_{00} = -\frac{1}{2}g^{\mu\nu}\partial_\nu g_{00} \quad . \tag{B.3}$$

For a weak field one may also assume that the metric g is not very different from the flat Minkowski metric and expand g in

$$g_{\mu\nu}(X) = \eta_{\mu\nu} + h_{\mu\nu}(x) \;\text{ with }\; |h_{\mu\nu}(x)| \ll 1 \quad . \tag{B.4}$$

In first order in h eq. (B.3) is

$$\Gamma^\mu_{00} = -\frac{1}{2}\eta^{\mu\nu}\partial_\nu h_{00} \quad . \tag{B.5}$$

Using this affine connection the equations of motion give

$$\begin{array}{ll} \frac{d^2x^0}{d\tau^2} & = 0 \quad , \\ \frac{d^2x^i}{d\tau^2} & = \frac{1}{2}\left(\frac{dx^0}{d\tau}\right)^2 \partial_i h_{00} \quad . \end{array} \tag{B.6}$$

The first of those equations reveals that $dt/d\tau$ is a constant and can therefore be inverted (excluding the $= 0$ case) which makes the second equation

$$\frac{d^2x^i}{(dx^0)^2} = \frac{1}{2}\partial^i h_{00} \quad . \tag{B.7}$$

This result has to be compared to Newtons equations of motion which are

$$\frac{d^2x^i}{(dx^0)^2} = \frac{1}{2}\partial^i \phi \text{ with } \phi = -\frac{GM}{r} \quad , \tag{B.8}$$

where ϕ is the well known Newton potential. Comparison of the equations (B.7) and (B.8) allows the conclusion that

$$h_{00} = -2\phi + \text{constant}_k. \tag{B.9}$$

The condition that for zero mass M the flat Minkowski metric has to be reproduced gives $\text{constant}_k = 0$. So finally, in the limit of a static weak gravitational field the metric g has to be

$$g_{\mu\nu} = \begin{pmatrix} 1-2\phi & 0 & 0 & 0 \\ 0 & -1 & 0 & 0 \\ 0 & 0 & -1 & 0 \\ 0 & 0 & 0 & -1 \end{pmatrix} \quad . \tag{B.10}$$

B.2 Spacetime structure

For the quantization procedure of fields in curved spacetime (see subsection 3.4.1) one needs to define a hyper surfaces Σ which are the analogon to the equal time section in flat Minkowski spacetime. This is done by defining Σ_t as the orthogonal to the time direction t. In a general spacetime one can define the "lapse" N as the part of an infinitesimal step which is orthogonal to Σ_t and the "shift" N^i as the part of such a step which is in Σ_t. By knowing the total metric $g_{\mu\nu}$ and Σ_t one can calculate the induced metric $g^{(3)}_{ij}$ on Σ_t. The total metric can then be expressed in terms of the induced metric, the "shift" and the "lapse"

$$\mathrm{ds}^2 = \mathrm{g}_{\mu\nu}\mathrm{dx}^\nu\mathrm{dx}^\mu = \mathrm{N}^2\mathrm{dt}^2 - \mathrm{g}^{(3)}_{\mathrm{ij}}(\mathrm{dx}^\mathrm{i} + \mathrm{N}^\mathrm{i}\mathrm{dt})(\mathrm{dx}^\mathrm{i} + \mathrm{N}^\mathrm{i}\mathrm{dt}) \quad . \tag{B.11}$$

Now that the spacetime is split up in hyper surfaces, it makes sense to distinguish between two different kinds of curvature:

- Intrinsic curvature is the curvature that can be noticed by a life form that is living on the slice Σ_t by calculating the Ricci tensor for the induced metric $R_{ij}(g^{(3)})$.
- Extrinsic curvature is the part of the total curvature $R_{\mu\nu}$ which can only be noticed when one knows about the additional orthogonal direction.

Apart from understanding the composition of spacetime it is also useful to study its asymptotic behavior. For the example of a $(1+1)$-dimensional Minkowski space the line element is

$$\mathrm{ds}^2 = \eta_{\mu\nu}\mathrm{dx}^\nu \mathrm{dx}^\mu = \mathrm{dt}^2 - \mathrm{dx}^2 \quad . \tag{B.12}$$

To see the asymptotic behavior at the far out regions, one can rescale the metric tensor

$$g'_{\mu\nu} = \Omega(x)\eta_{\mu\nu} \quad . \tag{B.13}$$

This transformation is called **conformal transformation** and the metric $g'_{\mu\nu}$ is called a conformal metric to $eta_{\mu\nu}$. A such coordinate transformation is

$$\begin{aligned} t + x &= \tan(\tfrac{\psi+\xi}{2}) \\ t - x &= \tan(\tfrac{\psi-\xi}{2}) \end{aligned} \quad , \tag{B.14}$$

where ψ and ξ are the new coordinates which just run from $-\pi$ to π instead of from $-\infty$ to ∞. By applying the chain rule it turns out that the line element is still diagonal in ψ and ξ and that both entries of the diagonal metric are scaled by the same factor

$$\mathrm{ds}^2 = \mathrm{dt}^2 - \mathrm{dx}^2 = \frac{1}{4}\frac{1}{\cos^2(\psi+\xi/2)\cos^2(\psi-\xi/2)}(\mathrm{d}\psi^2 - \mathrm{d}\xi^2) \quad , \tag{B.15}$$

confirming that (B.14) is a conformal transformation. Now it is possible to plot the entire infinitely extended Minkowsi spacetime, on one finite piece of paper by going to the coordinates ψ and ξ as it is shown in (B.1). Diagrams with the above described properties are called **Penrose diagrams**.

B.3 Dirac equation in curved spacetime

The Dirac equation can be generalized to curved spactime. Therefore, as the Dirac matrices are only know in flat Minkowski γ^m space one has to introduce a position dependent coordinate transformation e^μ_m that locally transforms from the coordinates in curved spacetime (indicated greek indices μ) to the coordinates in locally flat spacetime (indicated by latin indices m)

$$\eta_{mn} = e^\mu_m e^\nu_n g_{\mu\nu} \quad , \tag{B.16}$$

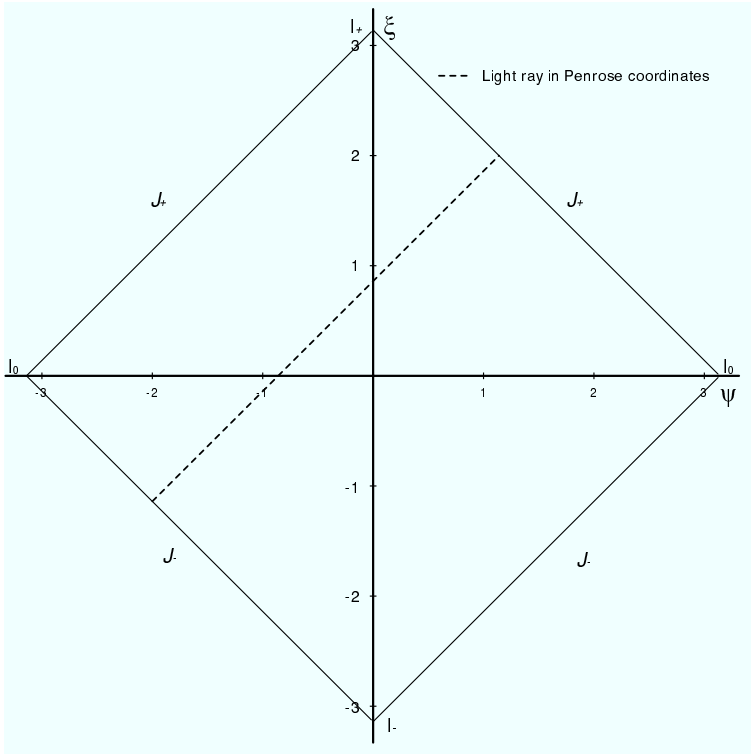

Figure B.1: Two-dimensional Minkowski space in the conformal coordinates ψ and ξ. The infinites are: I_+ as endpoint for time-like curves, I_- as starting point of time-like curves, I_0 as endpoint for space-like curves, $\mathcal{I}_+$ as endpoint for light-like curves and $\mathcal{I}_-$ as starting point for light-like curves. The dashed line depicts the trace of a light beam.

where η_{mn} denotes the flat Minkowski metric. The fields e^{μ}_{m} are called vierbein fields which fulfill the relations

$$e^{\mu}_{m}e^{n}_{\mu} = \delta^{n}_{m} \quad \text{and} \quad e^{\mu}_{m}e^{m}_{\nu} = \delta^{\mu}_{\nu} \quad . \tag{B.17}$$

As the vierbein fields are space dependent, the derivative in flat space ∂_m is expressed by the derivative in curved space ∂_μ, by the vierbein fields e^{n}_{μ} and by the so called spinor connection ω_μ:

$$\partial_m = e^{\mu}_{m}(\partial_\mu + i\omega_\mu). \tag{B.18}$$

The spinor connection again is determined by local Lorentz invariance to

$$\omega_\mu(x) = \frac{1}{2}e^{m}_{\nu}e^{n}_{\lambda}\Gamma^{\nu}{}_{\mu}{}^{\lambda}\Sigma_{mn} \quad , \tag{B.19}$$

where $\Gamma^{\nu}{}_{\mu}{}^{\lambda}$ is the normal Christoffel symbol and Σ_{mn} are the generators of the Lorentz group satisfying

$$\Sigma_{mn} = \frac{i}{4}\left[\gamma_m, \gamma_n\right] \quad \text{and} \quad \left[\Sigma_{mn}, \Sigma_{op}\right] = \eta_{mo}\Sigma_{np} - \eta_{mp}\Sigma_{no} - \eta_{no}\Sigma_{mp} + \eta_{np}\Sigma_{mo} \quad . \tag{B.20}$$

The Lagrangian for a fermionic field in curved spacetime reads then

$$\mathcal{L} = \bar{\psi}(i\gamma^{l}e^{\mu}_{l}(\partial_\mu + \frac{i}{2}e^{m}_{\nu}e^{n}_{\lambda}\Gamma^{\nu}{}_{\mu}{}^{\lambda}\Sigma_{mn}) - m)\psi \quad . \tag{B.21}$$

B.4 Bogolubov coefficients between Minkowski and Rindler coordinates

For calculating the Bogolubov coefficients

$$\begin{aligned} {}^{I}\beta_{\omega\bar{\omega}} &= (u_\omega, {}^{I}v^{*}_{\bar{\omega}}) \\ &= -i\int \mathrm{d}\Sigma^{-g}\sqrt{n}^{\mu}\left[(\partial_\mu {}^{\mathrm{I}}\mathrm{v}_{\bar{\omega}})\mathrm{u}_\omega - (\partial_\mu \mathrm{u}_\omega){}^{\mathrm{I}}\mathrm{v}_{\bar{\omega}}\right] \quad , \end{aligned} \tag{B.22}$$

in the Rindler setup of section (3.4.2), one chooses the space-like hyper surface ($\bar{t} = 0$). One further takes advantage of the conformal invariance of the Klein Gordon equation, by rescaling the metric $g_{\mu\nu} \to e^{-g\bar{x}}g_{\mu\nu}$. In those rescaled coordinates the determinant of the metric is unity and one finds

$${}^{I}\beta_{\omega\bar{\omega}} = \frac{1}{4\pi}\int \mathrm{d}\bar{x}e^{i\bar{k}\bar{x}}e^{ik(e^{g\bar{x}}/g)}\left(-\sqrt{\frac{\bar{\omega}}{\omega}} - i\sqrt{\frac{\omega}{\bar{\omega}}}e^{g\bar{x}}\right) \quad . \tag{B.23}$$

After the substitution $s := e^{g\bar{x}}/g$ this goes into

$$ {}^{I}\beta_{\omega\bar{\omega}} = \frac{1}{4\pi}\int_0^\infty \mathrm{d}\bar{x} e^{iks}(gs)^{i\bar{k}/g}\left(-\sqrt{\frac{\bar{\omega}}{\omega}}(gs)^{-1}+\sqrt{\frac{\omega}{\bar{\omega}}}\right) \quad . \tag{B.24} $$

By using $\Gamma(z) = \int_0^\infty t^{z-1}e^{-t}\mathrm{d}t$ and $\Gamma(z+1) = z\Gamma(z)$ the complex continued integrals give

$$ {}^{I}\beta_{\omega\bar{\omega}} = \frac{1}{4\pi g}\Gamma(i\bar{k}/g)\left(\frac{k}{g}\right)^{-i\bar{k}/g} e^{\pi\bar{k}/(2g)}\left(\sqrt{\frac{\bar{\omega}}{\omega}}+\frac{\bar{k}}{k}\sqrt{\frac{\omega}{\bar{\omega}}}\right) \quad . \tag{B.25} $$

For $\bar{\omega} = \bar{k}$ and $\omega = k$ this simplifies to the result (3.93)

$$ {}^{I}\beta_{\omega\bar{\omega}} = \frac{-i}{2\pi g}\sqrt{\frac{\bar{\omega}}{\omega}}e^{\frac{-\bar{\omega}\pi}{2g}}\Gamma(\frac{-i\bar{\omega}}{g})\left(\frac{\omega}{g}\right)^{i\bar{\omega}/g} \quad . \tag{B.26} $$

Appendix C

Energy loss in the lab system

Equation (8.15) provides the gravitationally radiated energy in the centre of mass frame of the reaction. To transform the kinematic variables to the laboratory frame with a target proton at rest one has to apply the Lorentz transformation matrix

$$\Lambda = \begin{pmatrix} \mathrm{Cosh}(\eta) & \mathrm{Sinh}(\eta) \\ \mathrm{Sinh}(\eta) & \mathrm{Cosh}(\eta) \end{pmatrix} = \begin{pmatrix} \frac{\sqrt{s}}{2m_p} & \frac{\sqrt{s-16m_p^2}}{2m_p} \\ \frac{\sqrt{s-16m_p^2}}{2m_p} & \frac{\sqrt{s}}{2m_p} \end{pmatrix} \quad , \tag{C.1}$$

which acts on the t(time) and the z (i.e. longitudinal) component of the $4+d$-dimensional vector. All the other (transverse) components remain unchanged. Eq. (8.15) gives the energy E and momentum $\underline{k}$ of the gravitational radiation emitted from one of the interacting particles (p_1, p_2). For different momentum directions $\underline{k}/|\underline{k}|$ the Lorentz transformation eq. (C.1) gives different energy losses in the lab-frame. To avoid this complication one has to use a mean value of the left over four momentum $\overline{p'}$ of the scattering particles. If the energy is radiated away from particle i one defines $p_i' = p_i - k$. Averaging over these cases yields

$$\overline{p'} = \sum_i^N \frac{p_i' + \sum_{l\neq i}^N p_l}{N} \quad . \tag{C.2}$$

Using the symmetry of a $2 \to 2$ scattering in the centre of mass system it is found that

$$\overline{p'}_{\mathrm{CM}} = \left(\sqrt{s} - k_0, 0, 0, 0, \dots\right) \quad . \tag{C.3}$$

Because $\overline{p'}_{\mathrm{CM}}$ has no z component, the mean left over energy in the laboratory system becomes

$$\overline{p'}_{\mathrm{lab}} = \Lambda \cdot \overline{p'}_{\mathrm{CM}} = \left(\frac{\sqrt{s}}{2m_p}(\sqrt{s} - k_0), 0, 0...\right) \quad . \tag{C.4}$$

From eq. (C.4) the mean energy loss in the lab system is obtained as

$$\overline{E}^{\rm loss}_{\rm lab} = \frac{s}{2m_p} - \overline{p'}_{0\,\rm lab} = \frac{\sqrt{s}}{2m_p} E^{\rm loss}_{\rm CM} \quad . \tag{C.5}$$

Bibliography

[1] Michael E. Peskin and Schroeder Daniel V. An introduction to quantum field theory. *Westview Press*, 09, 1995.

[2] Lewis H. Ryder. Quantum field theory. *Cambridge University Press*, 2nd edition, 1996.

[3] Vernon D. Barger et al. Neutrino oscillation parameters from minos, icarus and opera combined. *Phys. Rev.*, D65:053016, 2002, hep-ph/0110393.

[4] S. Fukuda et al. Determination of solar neutrino oscillation parameters using 1496 days of super-kamiokande-i data. *Phys. Lett.*, B539:179–187, 2002, hep-ex/0205075.

[5] T. Araki et al. Measurement of neutrino oscillation with kamland: Evidence of spectral distortion. *Phys. Rev. Lett.*, 94:081801, 2005, hep-ex/0406035.

[6] S. F. King. Neutrino mass models. *Rept. Prog. Phys.*, 67:107–158, 2004, hep-ph/0310204.

[7] G. Arnison et al. Experimental observation of isolated large transverse energy electrons with associated missing energy at s**(1/2) = 540-gev. *Phys. Lett.*, B122:103–116, 1983.

[8] G. Arnison et al. Further evidence for charged intermediate vector bosons at the sps collider. *Phys. Lett.*, B129:273, 1983.

[9] W. M. Yao et al. Review of particle physics. *J. Phys.*, G33:1–1232, 2006.

[10] Lincoln Wolfenstein. Parametrization of the kobayashi-maskawa matrix. *Phys. Rev. Lett.*, 51:1945, 1983.

[11] Gerard 't Hooft. Computation of the quantum effects due to a four-dimensional pseudoparticle. *Phys. Rev.*, D14:3432–3450, 1976.

[12] I. S. Altarev et al. Search for an electric dipole moment of the neutron. *JETP Lett.*, 44:460–465, 1986.

[13] R. D. Peccei. The strong cp problem and axions. 2006, hep-ph/0607268.

[14] S. Weinberg. Gravitation and cosmology. *ISBN 0-471-92567-5*, 1972.

[15] C. Misner, K Thorne, and J. Wheeler. Gravitation. *ISBN 0-7167-0344-0*, 1973.

[16] Schwarzschild Karl. On the gravitational field of a pointmass according to einstein's theory (german). *Sitzungsber. Preuss. Akad. Wiss. Berlin (Math. Phys.)*, 1:189–196, 1916.

[17] N. D. Birrell and D. C. W. Davies. Quantum fields in curved space. *Cambridge university press*, 1982.

[18] G. Ellis S. Hawking. The large scale structure of space-time. *Cambridge University Press*, 1973.

[19] W. G. Unruh. Notes on black hole evaporation. *Phys. Rev.*, D14:870, 1976.

[20] S. Hawking. Black hole explosions? *Nature*, 248:30, 1974.

[21] S. Hawking. *Commun. Math. Phys.*, 43:199–220, 1975.

[22] S. Hawking. Black holes and thermodynamics. *Phys. Rev.*, D13:191–197, 1976.

[23] Kaluza Theodor. On the problem of unity in physics. *Sitzungsber. Preuss. Akad. Wiss. Berlin (Math. Phys.)*, K1:966–972, 1921.

[24] Thomas Appelquist and Alan Chodos. Quantum effects in kaluza-klein theories. *Phys. Rev. Lett.*, 50:141, 1983.

[25] M. J. Duff. Modern kaluza-klein theories. Lectures given at Kaluza-Klein Workshop, Chalk River, Canada, Aug 11-16, 1983.

[26] M. J. Duff. Kaluza-klein theory in perspective. 1994, hep-th/9410046.

[27] R. Kerner, L. Nikolova, and V. Rizov. A two level kaluza-klein theory. *Lett. Math. Phys.*, 14:333–341, 1987.

[28] Oskar Klein. *Z. Phys.*, 37:895, 1926.

[29] Oskar Klein. *Arkiv. Mat. Astron. Fys. B*, 34A, 1946.

[30] Edward Witten. Fermion quantum numbers in kaluza-klein theory. *APPELQUIST, T. (ED.) ET AL.*, pages 438–511, 1983.

[31] Edward Witten. Search for a realistic kaluza-klein theory. *Nucl. Phys.*, B186:412, 1981.

[32] Riccardo D'Auria, Sergio Ferrara, and Silvia Vaula. N = 4 gauged supergravity and a iib orientifold with fluxes. *New J. Phys.*, 4:71, 2002, hep-th/0206241.

[33] Ignatios Antoniadis. A possible new dimension at a few tev. *Phys. Lett.*, B246:377–384, 1990.

[34] Nima Arkani-Hamed, Savas Dimopoulos, and G. R. Dvali. Phenomenology, astrophysics and cosmology of theories with sub-millimeter dimensions and tev scale quantum gravity. *Phys. Rev.*, D59:086004, 1999, hep-ph/9807344.

[35] Gian F. Giudice, Riccardo Rattazzi, and James D. Wells. Quantum gravity and extra dimensions at high-energy colliders. *Nucl. Phys.*, B544:3–38, 1999, hep-ph/9811291.

[36] Tao Han, Joseph D. Lykken, and Ren-Jie Zhang. On kaluza-klein states from large extra dimensions. *Phys. Rev.*, D59:105006, 1999, hep-ph/9811350.

[37] Robert C. Myers and M. J. Perry. Black holes in higher dimensional space-times. *Ann. Phys.*, 172:304, 1986.

[38] Nima Arkani-Hamed, Savas Dimopoulos, and G. R. Dvali. The hierarchy problem and new dimensions at a millimeter. *Phys. Lett.*, B429:263–272, 1998, hep-ph/9803315.

[39] Kip Thorne. Nonsphericla gravitational collapse: A short review. *In *J R Klauder, Magic Without Magic*, San Francisco*, pages 231–258, 1972.

[40] Tom Banks and Willy Fischler. A model for high energy scattering in quantum gravity. 1999, hep-th/9906038.

[41] Steven B. Giddings and Scott D. Thomas. High energy colliders as black hole factories: The end of short distance physics. *Phys. Rev.*, D65:056010, 2002, hep-ph/0106219.

[42] Douglas M. Eardley and Steven B. Giddings. Classical black hole production in high-energy collisions. *Phys. Rev.*, D66:044011, 2002, gr-qc/0201034.

[43] Aichelburg P. C. and Sexl R. U. On the gravitational field of a massless particle. *Gen. Rel. Grav*, 2:303, 1971.

[44] M. B. Voloshin. More remarks on suppression of large black hole production in particle collisions. *Phys. Lett.*, B524:376–382, 2002, hep-ph/0111099.

[45] G. W. Gibbons and S. W. Hawking. Action integrals and partition functions in quantum gravity. *Phys. Rev.*, D15:2752–2756, 1977.

[46] Steven B. Giddings and Vyacheslav S. Rychkov. Black holes from colliding wavepackets. *Phys. Rev.*, D70:104026, 2004, hep-th/0409131.

[47] Lisa Randall and Raman Sundrum. An alternative to compactification. *Phys. Rev. Lett.*, 83:4690–4693, 1999, hep-th/9906064.

[48] Walter D. Goldberger and Mark B. Wise. Modulus stabilization with bulk fields. *Phys. Rev. Lett.*, 83:4922–4925, 1999, hep-ph/9907447.

[49] Walter D. Goldberger and Mark B. Wise. Bulk fields in the randall-sundrum compactification scenario. *Phys. Rev.*, D60:107505, 1999, hep-ph/9907218.

[50] Jaume Garriga and Takahiro Tanaka. Gravity in the brane-world. *Phys. Rev. Lett.*, 84:2778–2781, 2000, hep-th/9911055.

[51] Steven B. Giddings, Emanuel Katz, and Lisa Randall. Linearized gravity in brane backgrounds. *JHEP*, 03:023, 2000, hep-th/0002091.

[52] I. D. Novikov and V. P. Frolov. Black hole physics. *Kluver Academic Publishers*, 1998.

[53] S. Hawking. The unpredictability of quantum gravity. *Commun. Math. Phys.*, 87:395, 1982.

[54] Don N. Page. Is black hole evaporation predictable? *Phys. Rev. Lett.*, 44:301, 1980.

[55] Gerard 't Hooft. On the quantum structure of a black hole. *Nucl. Phys.*, B256:727, 1985.

[56] Erik P. Verlinde and Herman L. Verlinde. A unitary s matrix and 2-d black hole formation and evaporation. *Nucl. Phys.*, B406:43–58, 1993, hep-th/9302022.

[57] Leonard Susskind, Larus Thorlacius, and John Uglum. The stretched horizon and black hole complementarity. *Phys. Rev.*, D48:3743–3761, 1993, hep-th/9306069.

[58] Don N. Page. Information in black hole radiation. *Phys. Rev. Lett.*, 71:3743–3746, 1993, hep-th/9306083.

[59] Aleksandar Mikovic. Hawking radiation and back reaction in a unitary theory of 2-d quantum gravity. *Phys. Lett.*, B355:85–91, 1995, hep-th/9407104.

[60] Y. Aharonov, A. Casher, and S. Nussinov. The unitarity puzzle and planck mass stable particles. *Phys. Lett.*, B191:51, 1987.

[61] Tom Banks, A. Dabholkar, Michael R. Douglas, and M. O'Loughlin. Are horned particles the climax of hawking evaporation? *Phys. Rev.*, D45:3607–3616, 1992, hep-th/9201061.

[62] Tom Banks and M. O'Loughlin. Classical and quantum production of cornucopions at energies below 10**18-gev. *Phys. Rev.*, D47:540–553, 1993, hep-th/9206055.

[63] Tom Banks, M. O'Loughlin, and Andrew Strominger. Black hole remnants and the information puzzle. *Phys. Rev.*, D47:4476–4482, 1993, hep-th/9211030.

[64] Steven B. Giddings. Black holes and massive remnants. *Phys. Rev.*, D46:1347–1352, 1992, hep-th/9203059.

[65] Tom Banks. Horned particles as the endpoint of hawking evaporation. *Gen. Rel. Grav.*, 25:1213–1218, 1993.

[66] Steven B. Giddings. Comments on information loss and remnants. *Phys. Rev.*, D49:4078–4088, 1994, hep-th/9310101.

[67] Steven B. Giddings. Constraints on black hole remnants. *Phys. Rev.*, D49:947–957, 1994, hep-th/9304027.

[68] M. D. Maia. Information storage in black holes. *Int. J. Mod. Phys.*, D14:2251–2256, 2005, gr-qc/0505119.

[69] Viqar Husain and Oliver Winkler. How red is a quantum black hole? *Int. J. Mod. Phys.*, D14:2233–2238, 2005, gr-qc/0505153.

[70] M. A. Markov. Proc. 2nd seminar in quantum gravity. *M. A. Markov and P. C. West, Plenum, New York*, 1984.

[71] Y. B. Zel'dovich. Proc. 2nd seminar in quantum gravity. *M. A. Markov and P. C. West, Plenum, New York*, 1984.

[72] Ronald J. Adler, Pisin Chen, and David I. Santiago. The generalized uncertainty principle and black hole remnants. *Gen. Rel. Grav.*, 33:2101–2108, 2001, gr-qc/0106080.

[73] John D. Barrow, Edmund J. Copeland, and Andrew R. Liddle. The cosmology of black hole relics. *Phys. Rev.*, D46:645–657, 1992.

[74] Brian Whitt. Spherically symmetric solutions of general second order gravity. *Phys. Rev.*, D38:3000, 1988.

[75] Robert C. Myers and Jonathan Z. Simon. Black hole thermodynamics in lovelock gravity. *Phys. Rev.*, D38:2434–2444, 1988.

[76] Jr. Callan, Curtis G., Robert C. Myers, and M. J. Perry. Black holes in string theory. *Nucl. Phys.*, B311:673, 1989.

[77] S. Alexeyev, A. Barrau, G. Boudoul, O. Khovanskaya, and M. Sazhin. Black hole relics in string gravity: Last stages of hawking evaporation. *Class. Quant. Grav.*, 19:4431–4444, 2002, gr-qc/0201069.

[78] S. Alexeyev, N. Popov, A. Barrau, and J. Grain. New black hole solutions in the string gravity with noncompact extra dimensions and their experimental search. i. *ECONF*, C041213:1202, 2004.

[79] Thomas G. Rizzo. Collider production of tev scale black holes and higher- curvature gravity. *JHEP*, 06:079, 2005, hep-ph/0503163.

[80] Mark J. Bowick, Steven B. Giddings, Jeffrey A. Harvey, Gary T. Horowitz, and Andrew Strominger. Axionic black holes and a bohm-aharonov effect for strings. *Phys. Rev. Lett.*, 61:2823, 1988.

[81] Sidney R. Coleman, John Preskill, and Frank Wilczek. Quantum hair on black holes. *Nucl. Phys.*, B378:175–246, 1992, hep-th/9201059.

[82] Ki-Myeong Lee, V. P. Nair, and Erick J. Weinberg. A classical instability of reissner-nordstrom solutions and the fate of magnetically charged black holes. *Phys. Rev. Lett.*, 68:1100–1103, 1992, hep-th/9111045.

[83] Ki-Myeong Lee, V. P. Nair, and Erick J. Weinberg. Black holes in magnetic monopoles. *Phys. Rev.*, D45:2751–2761, 1992, hep-th/9112008.

[84] G. W. Gibbons and Kei-ichi Maeda. Black holes and membranes in higher dimensional theories with dilaton fields. *Nucl. Phys.*, B298:741, 1988.

[85] Takashi Torii and Kei-ichi Maeda. Black holes with nonabelian hair and their thermodynamical properties. *Phys. Rev.*, D48:1643–1651, 1993.

[86] A. Bonanno and M. Reuter. Spacetime structure of an evaporating black hole in quantum gravity. *Phys. Rev.*, D73:083005, 2006, hep-th/0602159.

[87] Sabine Hossenfelder, Marcus Bleicher, Stefan Hofmann, Horst Stoecker, and Ashutosh V. Kotwal. Black hole relics in large extra dimensions. *Phys. Lett.*, B566:233–239, 2003, hep-ph/0302247.

[88] Roberto Casadio and Benjamin Harms. Can black holes and naked singularities be detected in accelerators? *Int. J. Mod. Phys.*, A17:4635–4646, 2002, hep-th/0110255.

[89] S. D. Majumdar. A class of exact solutions of einstein's field equations. *Phys. Rev.*, 72:390–398, 1947.

[90] D. Korotkin and H. Nicolai. A periodic analog of the schwarzschild solution. 1994, gr-qc/9403029.

[91] Andrei V. Frolov and Valeri P. Frolov. Black holes in a compactified spacetime. *Phys. Rev.*, D67:124025, 2003, hep-th/0302085.

[92] Troels Harmark and Niels A. Obers. Phase structure of black holes and strings on cylinders. *Nucl. Phys.*, B684:183–208, 2004, hep-th/0309230.

[93] Troels Harmark, Kristjan R. Kristjansson, Niels A. Obers, and Peter B. Ronne. Three-charge black holes on a circle. 2006, hep-th/0606246.

[94] Dan Gorbonos and Barak Kol. Matched asymptotic expansion for caged black holes: Regularization of the post-newtonian order. *Class. Quant. Grav.*, 22:3935–3960, 2005, hep-th/0505009.

[95] Piet Hut and Martin J. Rees. How stable is our vacuum? 1983. Print-83-0042 (IAS,PRINCETON).

[96] W. Busza, R. L. Jaffe, J. Sandweiss, and Frank Wilczek. Review of speculative 'disaster scenarios' at rhic. *Rev. Mod. Phys.*, 72:1125–1140, 2000, hep-ph/9910333.

[97] A. Ringwald and H. Tu. Collider versus cosmic ray sensitivity to black hole production. *Phys. Lett.*, B525:135–142, 2002, hep-ph/0111042.

[98] M. Kowalski, A. Ringwald, and H. Tu. Black holes at neutrino telescopes. *Phys. Lett.*, B529:1–9, 2002, hep-ph/0201139.

[99] P. F. Smith et al. A search for anomalous hydrogen in enriched d-2 o, using a time-of-flight spectrometer. *Nucl. Phys.*, B206:333–348, 1982.

[100] Z. T. Lu et al. Searches for stable strangelets in ordinary matter: Overview and a recent example. *Nucl. Phys.*, A754:361–368, 2005, nucl-ex/0402015.

[101] Roberto Casadio and Benjamin Harms. Black hole evaporation and large extra dimensions. *Phys. Lett.*, B487:209–214, 2000, hep-th/0004004.

[102] Roberto Casadio and Benjamin Harms. Black hole evaporation and compact extra dimensions. *Phys. Rev.*, D64:024016, 2001, hep-th/0101154.

[103] Per Kraus and Frank Wilczek. Selfinteraction correction to black hole radiance. *Nucl. Phys.*, B433:403–420, 1995, gr-qc/9408003.

[104] Per Kraus and Frank Wilczek. Effect of selfinteraction on charged black hole radiance. *Nucl. Phys.*, B437:231–242, 1995, hep-th/9411219.

[105] Esko Keski-Vakkuri and Per Kraus. Microcanonical d-branes and back reaction. *Nucl. Phys.*, B491:249–262, 1997, hep-th/9610045.

[106] S. Massar. The semiclassical back reaction to black hole evaporation. *Phys. Rev.*, D52:5857–5864, 1995, /9411039.

[107] S. Massar and R. Parentani. How the change in horizon area drives black hole evaporation. *Nucl. Phys.*, B575:333–356, 2000, /9903027.

[108] Ted Jacobson, Gungwon Kang, and Robert C. Myers. On black hole entropy. *Phys. Rev.*, D49:6587–6598, 1994, gr-qc/9312023.

[109] Ted Jacobson and Renaud Parentani. Horizon entropy. *Found. Phys.*, 33:323–348, 2003, /0302099.

[110] Maulik K. Parikh and Frank Wilczek. Hawking radiation as tunneling. *Phys. Rev. Lett.*, 85:5042–5045, 2000, /9907001.

[111] A. J. M. Medved and Elias C. Vagenas. On hawking radiation as tunneling with back-reaction. *Mod. Phys. Lett.*, A20:2449–2454, 2005, gr-qc/0504113.

[112] Michele Arzano. Information leak through the quantum horizon. *Mod. Phys. Lett.*, A21:41–48, 2006, hep-th/0504188.

[113] Gian Luigi Alberghi, Roberto Casadio, and Alessandro Tronconi. Quantum gravity effects in black holes at the lhc. 2006, hep-ph/0611009.

[114] Benjamin Koch, Marcus Bleicher, and Sabine Hossenfelder. Black hole remnants at the lhc. *JHEP*, 10:053, 2005, hep-ph/0507138.

[115] Torbjorn Sjostrand, Leif Lonnblad, and Stephen Mrenna. Pythia 6.2: Physics and manual. 2001, hep-ph/0108264.

[116] C. M. Harris, P. Richardson, and B. R. Webber. Charybdis: A black hole event generator. *JHEP*, 08:033, 2003, hep-ph/0307305.

[117] Luis Anchordoqui and Haim Goldberg. Black hole chromosphere at the lhc. *Phys. Rev.*, D67:064010, 2003, hep-ph/0209337.

[118] King-man Cheung. Black hole production and large extra dimensions. *Phys. Rev. Lett.*, 88:221602, 2002, hep-ph/0110163.

[119] Kingman Cheung. Black hole, string ball, and p-brane production at hadronic supercolliders. *Phys. Rev.*, D66:036007, 2002, hep-ph/0205033.

[120] Marcus Bleicher, Stefan Hofmann, Sabine Hossenfelder, and Horst Stocker. Black hole production in large extra dimensions at the tevatron: A chance to observe a first glimpse of tev scale gravity. *Phys. Lett.*, 548:73–76, 2002, hep-ph/0112186.

[121] Marco Cavaglia, Saurya Das, and Roy Maartens. Will we observe black holes at lhc? *Class. Quant. Grav.*, 20:L205–L212, 2003, hep-ph/0305223.

[122] Marco Cavaglia and Saurya Das. How classical are tev-scale black holes? *Class. Quant. Grav.*, 21:4511–4522, 2004, hep-th/0404050.

[123] S. Hossenfelder. Suppressed black hole production from minimal length. *Phys. Lett.*, B598:92–98, 2004, hep-th/0404232.

[124] Irina Mocioiu, Yasushi Nara, and Ina Sarcevic. Hadrons as signature of black hole production at the lhc. *Phys. Lett.*, B557:87–93, 2003, hep-ph/0301073.

[125] Andreas Ringwald. Production of black holes in tev-scale gravity. *Fortschr. Phys.*, 51:830–835, 2003, hep-ph/0212342.

[126] Andrew Chamblin and Gouranga C. Nayak. Black hole production at lhc: String balls and black holes from p p and lead lead collisions. *Phys. Rev.*, D66:091901, 2002, hep-ph/0206060.

[127] Junichi Tanaka, Taiki Yamamura, Shoji Asai, and Junichi Kanzaki. Study of black holes with the atlas detector at the lhc. *Eur. Phys. J.*, C41:19–33, 2005, hep-ph/0411095.

[128] C. M. Harris et al. Exploring higher dimensional black holes at the large hadron collider. *JHEP*, 05:053, 2005, hep-ph/0411022.

[129] B Koch. Black holes and the possible detection of black hole remnants at the lhc. 2006, Proceedings Lake Louise.

[130] Thomas J. Humanic, Benjamin Koch, and Horst Stoecker. Signatures for black hole production from hadronic observables at the large hadron collider. 2006, hep-ph/0607097.

[131] Gerald Gabrielse et al. Cooling and slowing of trapped anti-protons below 100-mev. *Phys. Rev. Lett.*, 63:1360–1363, 1989.

[132] A. Arvanitaki, S. Dimopoulos, A. Pierce, S. Rajendran, and Jay G. Wacker. Stopping gluinos. 2005, hep-ph/0506242.

[133] Sabine Hossenfelder, Benjamin Koch, and Marcus Bleicher. Trapping black hole remnants. 2005, hep-ph/0507140.

[134] Stefan Hofmann et al. Suppression of high-p(t) jets as a signal for large extra dimensions and new estimates of lifetimes for meta stable micro black holes: From the early universe to future colliders. 2001, hep-ph/0111052.

[135] S. Hofmann et al. Tevatron - probing tev-scale gravity today. *J. Phys.*, G28:1657–1665, 2002.

[136] S. Hassani. Mathematical physics. *Springer-Verlag, New York*, 1972.

[137] D. V. Galtsov. Radiation reaction in various dimensions. *Phys. Rev.*, D66:025016, 2002, hep-th/0112110.

[138] Vitor Cardoso, Oscar J. C. Dias, and Jose P. S. Lemos. Gravitational radiation in d-dimensional spacetimes. *Phys. Rev.*, D67:064026, 2003, hep-th/0212168.

[139] Joseph D. Lykken. Weak scale superstrings. *Phys. Rev.*, D54:3693–3697, 1996, hep-th/9603133.

[140] Luis Anchordoqui, Thomas Paul, Stephen Reucroft, and John Swain. Ultrahigh energy cosmic rays: The state of the art before the auger observatory. *Int. J. Mod. Phys.*, A18:2229–2366, 2003, hep-ph/0206072.

[141] Steen Hannestad and Georg G. Raffelt. Stringent neutron-star limits on large extra dimensions. *Phys. Rev. Lett.*, 88:071301, 2002, hep-ph/0110067.

[142] J. D. Barrow. Observational limits on the time evolution of extra spatial dimensions. *Phys. Rev.*, D35:1805–1810, 1987.

[143] S. Hossenfelder et al. Collider signatures in the planck regime. *Phys. Lett.*, B575:85–99, 2003, hep-th/0305262.

[144] Glenn D. Starkman, Dejan Stojkovic, and Mark Trodden. Large extra dimensions and cosmological problems. *Phys. Rev.*, D63:103511, 2001, hep-th/0012226.

[145] Glenn D. Starkman, Dejan Stojkovic, and Mark Trodden. Homogeneity, flatness and 'large' extra dimensions. *Phys. Rev. Lett.*, 87:231303, 2001, hep-th/0106143.

[146] Ben Koch, Hans-Joachim Drescher, and Marcus Bleicher. Gravitational radiation from ultra high energy cosmic rays in models with large extra dimensions. *Astropart. Phys.*, 25:291–297, 2006, astro-ph/0602164.

[147] D. Kazanas and A. Nicolaidis. Cosmic rays and large extra dimensions. *Gen. Rel. Grav.*, 35:1117–1123, 2003, hep-ph/0109247.

[148] B. Koch and M. Bleicher. Gravitational radiation from elastic particle scattering in models with extra dimensions. 2005, hep-th/0512353.

[149] R. Mertig, M. Bohm, and A. Denner. Feyn calc: Computer algebraic calculation of feynman amplitudes. *Comput. Phys. Commun.*, 64:345–359, 1991.

[150] S. Wolfram. The mathematica book. *Cambridge University Press*, 1996.

[151] Maurice Levy and Joseph Sucher. Eikonal approximation in quantum field theory. *Phys. Rev.*, 186:1656–1670, 1969.

[152] V. N. Gribov. Glauber corrections and the interaction between high-energy hadrons and nuclei. *Sov. Phys. JETP*, 29:483–487, 1969.

[153] R. J. Glauber and G. Matthiae. High-energy scattering of protons by nuclei. *Nucl. Phys.*, B21:135–157, 1970.

[154] R. J. Glauber. High-energy collision theory. 1987. In *Lo, S.Y. (ed.): Geometrical pictures in hadronic collisions*, 83-182. (see Book Index).

[155] R. S. Fletcher, T. K. Gaisser, Paolo Lipari, and Todor Stanev. Sibyll: An event generator for simulation of high-energy cosmic ray cascades. *Phys. Rev.*, D50:5710–5731, 1994.

[156] R. Engel, T. K. Gaisser, T. Stanev, and P. Lipari. Air shower calculations with the new version of sibyll. Prepared for 26th International Cosmic Ray Conference (ICRC 99), Salt Lake City, Utah, 17-25 Aug 1999.

[157] G. Bossard et al. Cosmic ray air shower characteristics in the framework of the parton-based gribov-regge model nexus. *Phys. Rev.*, D63:054030, 2001, hep-ph/0009119.

[158] Hans-Joachim Drescher and Glennys R. Farrar. Air shower simulations in a hybrid approach using cascade equations. *Phys. Rev.*, D67:116001, 2003, astro-ph/0212018.

Acknowledgments

First of all, I want to thank my parents, and my family for the invaluable help they have provided me throughout the past 3(0) years.
I want to thank Ina for motivating, comforting, and proof reading.
I'm grateful to my supervisors Marcus Bleicher, and Horst Stoecker for their help and advise.
For physical discussions, criticism, or proof reading I further want to thank Sabine Hossenfelder, Sascha Vogel, Stefan Strüber, and Stefan Scherer. The informal meetings "on everything - leading to nowhere" with Jorge Noronha, Ulrich Harbach, and Miklos Gyulassi have been inspiring and great fun. Hannah Petersen deserves respect for staying in the same office with me during the past months. For their collaboration I'm obliged to Hajo Drescher, Tom Humanic, Martin Kober, Oliver Brein, and Vowi Flotte. Thanks also to Adrian Dumitru for an interesting lecture series.

This work was supported by ITP-Frankfurt and the Frankfurt International Graduate School of science (FIGSS).